Annex A – MTU/KRC FINAL REPORT: NG-NRMM CDT

Note: This Annex appears in its original format.

Next Generation NATO Reference Mobility Model Cooperative Demonstration of Technology

Contract W56HZV-14-C-0286

Assured Mobility and Maneuver Support

Work Directive MTU-AMS - 025

By

Scott Bradley, PE, Russ Alger, Geoff Gwaltney, and Thomas Page

From the Keweenaw Research Center at Michigan Technological University

And, Ryan Williams

From the Great Lakes Research Center at Michigan Technological University

Michigan Technological University

Houghton, MI 49931

January 2019

NOTICES

This report is not to be construed as an official Department of the Army position.

Mention of any trade names or manufacturers in this report shall not be construed as an official endorsement or approval of such products or companies by the U.S. Government.

REPORT DOCUMENTATION PAGE

Form Approved
OMB No. 074-0188

1. AGENCY USE ONLY (Leave blank)	2. REPORT DATE	3. REPORT TYPE AND DATES COVERED
	January 2019	Final: December 2017 thru January 2019

4. TITLE AND SUBTITLE
Next Generation NATO Rerference Mobility Model Cooperative Demonstration of Technology

5. FUNDING NUMBERS
Contract No. W56HZV-14-C-0286
MTU-AMMS-025

6. AUTHOR(S)
SCOTT BRADLEY

7. PERFORMING ORGANIZATION NAME(S) AND ADDRESS(ES)

KEWEENAW RESEARCH CENTER
MICHIGAN TECHNOLOGICAL UNIV.
1400 TOWNSEND DR.
HOUGHTON MI 49931-1295

8. PERFORMING ORGANIZATION REPORT NUMBER

9. SPONSORING / MONITORING AGENCY NAME(S) AND ADDRESS(ES)

COMMANDER
U.S. ARMY TANK-AUTOMOTIVE & ARMAMENTS COMMAND
ATTN:AMSTA-TR-R BUILDING 215 MS159

10. SPONSORING / MONITORING AGENCY REPORT NUMBER

11. SUPPLEMENTARY NOTES

12a. DISTRIBUTION / AVAILABILITY STATEMENT

DISTRIBUTION A. APPROVED FOR PUBLIC RELEASE:
DISTRIBUTION UNLIMITED. OPSEC #: 2336

12b. DISTRIBUTION CODE

13. ABSTRACT ***(Maximum 200 Words)***

14. SUBJECT TERMS
Mobility, NRMM, NATO, Testing, Geospatial, Terramechanics

15. NUMBER OF PAGES
XX

16. PRICE CODE

17. SECURITY CLASSIFICATION OF REPORT	18. SECURITY CLASSIFICATION OF THIS PAGE	19. SECURITY CLASSIFICATION OF ABSTRACT	20. LIMITATION OF ABSTRACT
Unclassified	**Unclassified**	**Unclassified**	**Unrestricted**

TABLE OF CONTENTS

LIST OF FIGURES

LIST OF TABLES

Table Page

Executive Summary

The NATO Reference Mobility Model (NRMM) is a modeling and simulation tool developed to predict military ground vehicles' mobility capabilities. It was developed by the U.S. Army Tank Automotive Research, Development, and Engineering Center (TARDEC) and Engineer Research and development Center (ERD) in the 1970s and last updated in the 1990s. The NRMM is based on many years of Army testing data, but that data does not encompass the past 30 years of vehicle mobility advancements. An update to the model was necessary to accurately predict the performance of modern military vehicles.

The objective of this project to update the simulation tool was to establish a state of the art for ground vehicle mobility modeling. Dubbed Next Generation NRMM (NG-NRMM) Cooperative Demonstration of Technology (CDT), the effort established the NRMM's current mobility prediction capabilities and identified gaps where current simulation technology failed to produce accurate mobility predictions. For their part, researchers at Michigan Technological University's (MTU) Keweenaw Research Center (KRC) were tasked to collect live reference data for a specific terrain and vehicle combination. Collection and dissemination of the large dataset was also considered a large part of the technology demonstration. The combined terrain and vehicle dataset was then used by a team of software developers to provide predictions of the live vehicle performance. The final stage of the project was a gathering hosted at the KRC facility where the participating software vendors presented their mobility predictions and related mobility technology and test procedures were demonstrated on the KRC test course.

Chapter 1 – NG-NRMM CDT Virtual and Physical Demonstration Plan

1.1 Phase 1

1.1.1 Tasks

Phase 1 of the project first involved the collection of vehicle specifications, surrogate terrain information, and previous test data. Once this was acquired, software developers conducted 3-dimensional high-resolution physics-based simulations of the FED-A vehicle performing many of the planned physical tests. The model of the FED-A was subjected to each physical test and specific test results on were provided. Software developers were asked to show capacity to conduct simulations of all tests and to calibrate their methodologies to a subset of the live tests. The results of this phase were delivered to TARDEC for approval to move to Phase 2 of the demonstration.

1.1.2 Overall Goal

The main goal of Phase 1 was to develop and run vehicle terrain interaction (VTI) models for each of the live events using surrogate terrain information. This phase allowed the NG-NRMM team time to initiate simulation development prior to compilation of the full terrain data set and completion of all testing. It also provided insight to potential issues that became apparent once simulations were run and a chance to adjust Phase 2 activities to address and resolve these issues.

1.2 Phase 2

1.2.1 Tasks

In Phase 2 of the project, the full terrain data set for the KRC test site was released. This data was provided to the various software developers and used to modify mobility prediction models for the actual KRC terrain. The Phase 2 effort then continued simulations in support of further comparing live test results. First, the predictive capacity of each methodology was again compared to the subset of tests used in Phase 1. At this time, simulations were allowed to be refined to more closely match the live performance of the FED-A. Once calibration was deemed complete, each software developer was requested to predict the vehicle behavior for all vehicle tests.

1.2.2 Overall Goal

The overall goal of Phase 2 was to conduct a staged validation and verification against the full set of vehicle tests in order to access each methodology's capacity to accurately predict vehicle behavior.

Chapter 2 – NG-NRMM CDT Geospatial Data Preparation

The NG-NRMM CDT geospatial data set was assembled and provided by Michigan Technological University (MTU) through the collaboration of two research departments within the University; the Great Lakes Research Center (GLRC) and the Keweenaw Research Center (KRC).

2.1 Terrain Data Set

2.1.1 Source and Condition of Geospatial Data

Geospatial data is data that is referenced to a specific location on earth, and represents the earth's shape and description at that location. It may be used to model human or natural processes.

For the CDT project, geospatial data was collected about the physical environment that would model the interaction of a vehicle moving across the terrain within an area of operations.

This data was organized into several thematic layers including: Elevation, Slope Grade, Slope Aspect, Soil Classification, Soil Moisture, Bulk Density, Depth to Bedrock, Soil Strength (Cone Index), Road Type, Land Cover, Vegetation Size, Vegetation Density, Recognition Distance, and Obstacles.

Often there were pre-existing sources for many of these thematic layers that were easily available, however none of these pre-existing sources had the level of precision, accuracy or timeliness necessary to support complex terramechanics modeling. Additional data collection was necessary to produce higher resolution datasets, and all the geospatial data required some form of processing before it was suitable for use in models. This data organization, production and processing was done using tools within a Geographic Information System, specifically ArcGIS Desktop from ESRI.

Very high resolution elevation data is available for download in 3D mesh and TIN format , and all geospatial data thematic data layers such as land use and soil types are available in GeoTiff and Geodatabase format.

Thematic Layers Organized into a Geodatabase

Each of these thematic data layers, as well as additional reference data such as aerial imagery, were organized inside of a Geodatabase. A Geodatabase is a spatially enabled relational database that supports the comparison and unification of multiple data layers and allows the data to be easily transferred and shared. Geodatabases can hold data in multiple formats including vector data such as road maps, raster data such as photography, tabular data such as soil type attributes and surface models such as topography data in Triangulated Irregular Network (TIN) format.

Pre-existing Coarse-resolution Data Obtained

Readily available pre-existing data sources were identified and procured from publicly accessible websites. These included Elevation data and Land Cover data from the United States Geologic Survey (USGS) and Soil attribute data from the United States Department of Agriculture (USDA).

Elevation data from the USGS managed National Elevation Dataset (NED) has a resolution of ⅓ arc second (approximately 8 meters at our location) and accuracy of +/- 2 Meters at our area of interest. It is produced from diverse source datasets and is continually updated, but has not been updated recently in this project's area of operations.

Land Cover data from the USGS managed National Land Cover Dataset (NLCD) has a resolution of 30 Meters and accuracy of +/- 10m and classifies land cover into 16 broad categories over the area of operations.

Soil attribute data from the United States Department of Agriculture (USDA) Soil Survey Geographic Database (SSURGO) has a varying resolution, with most information being collected at a map scale of 1:12,000. Numerous soil attributes are described and linked to soil map unit polygons that can be overlaid with other thematic layers. While there were several USDA soil types described over the area of operations, this project required the use of Universal Soil Classification System (USCS) soil type codes. There were only two (2) unique USCS codes described in the area of operations: Sand and Peat. This database also did not capture the varied composition of the test courses and structures within the area of operations.

Overall, these data layers were considered 'coarse resolution' and were not precise or accurate enough for use in complex terramechanics models. They could however be used to fill in gaps outside of the areas to be modeled.

High Resolution Data Created using Remote and Direct Sensing Techniques

In order to produce data layers suitable for use in complex terramechanics models, high-resolution geospatial data was collected using remote sensing and direct sensing techniques.

Multi-Season aerial imagery was collected by KRC Staff in the Winter of 2015 and Summer of 2015. Individual images were stitched together into a mosaic of images and georeferenced to their correct location on earth using GIS software and 2015 USDA National Aerial Imagery Program (NAIP) Aerial Imagery as a reference layer. Additionally, three (3) inch resolution aerial photography was collected and georeferenced by the State of Michigan in May of 2018.

This collection of aerial imagery was to create several high-resolution layers including land cover, surface type, road type, surface water depth, vegetation stem size, vegetation density, and recognition distance.

Several direct-sensing techniques were used including Terrestrial Lidar Scanning, Cone Penetrometer testing, and manual soil sampling and classification. Data from these techniques was used to create more high-resolution layers including elevation, slope, aspect, cone index, and custom soil type.

Bevameter readings were also collected for each custom soil type and stored as attributes that could be linked to custom soil type map polygons.

High resolution data was compiled for all areas to be traversed in a model while coarse resolution data was used to fill in areas not to be traversed.

2.1.2 Manipulation

Detailed High-Resolution Data Layer Creation and Transformation

Specialized techniques were used to create high-resolution geospatial data, fill gaps with coarse resolution data, and transform data attributes to meet NRMM Schema definitions and complex model needs.

Figure 2.1.2-1 High Resolution Images of the KRC Test Course

High-Resolution Land Cover was mapped for the entire area of operations using georeferenced Multi-Season Aerial imagery and 3” Aerial imagery. Due to the small area of operations, complex vegetation mixture, and numerous distinct test course features, manual image classification techniques were used. Polygons were drawn around each distinct area of land cover and classified into 1 of 6 general land cover

categories including: Evergreen Forest, Mixed Forest, Grass, Grass with Scrub, Bare Ground, and Open Water.

Additionally, forested areas were subdivided into areas of differing Stem Diameters and Stem Spacing and classified as Large, Medium, and Small diameters and High, Medium, and Low densities. Land cover classifications were translated to match the NRMM MAP11 schema land cover classification codes. A processing script was written to transform stem diameter and stem spacing codes into the MAP11 schema format of spacing of stems in a series of stem diameter attribute fields.

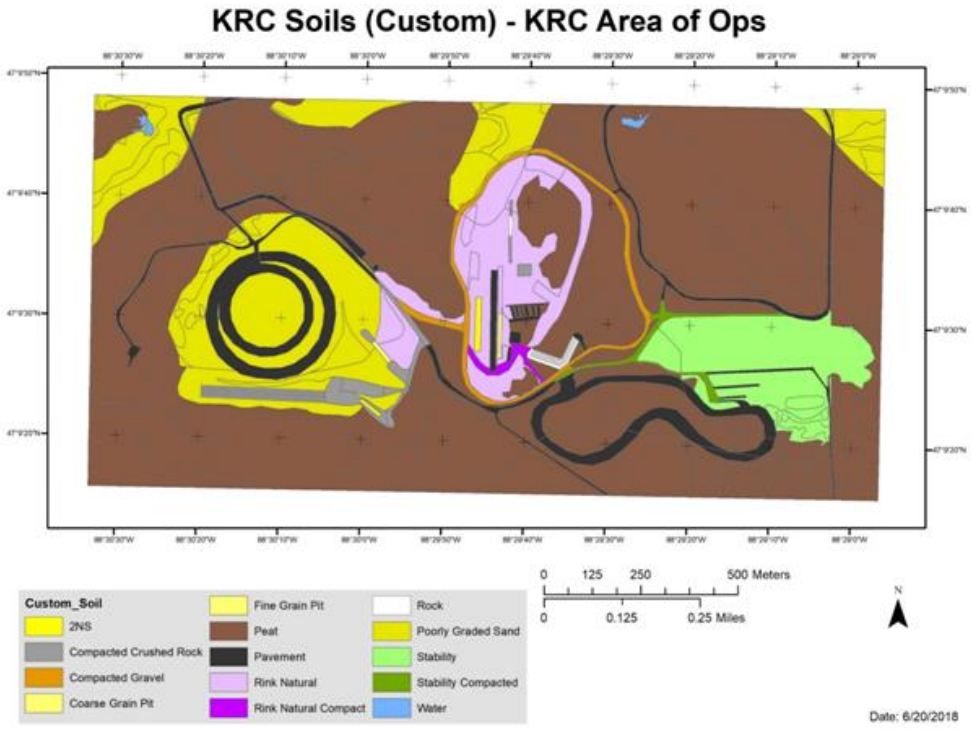

Figure 2.1.2-2 Custom Soil Distribution for the KRC Test Course

High-Resolution Soil data was mapped using field observations, manual soil sampling and analysis, cone penetrometer testing and Bevameter readings. Homogeneous regions within the area to be modeled were identified and mapped using aerial imagery, land cover and field surveys. Soils in each mapped region were sampled, tested and classified by KRC personnel. This intensive field work provided data to produce multiple thematic data layers including Cone Index, Bulk Density, Soil Moisture, Bevameter Readings and Custom Soil Classification codes and names.

This high-resolution soil data was combined with lower-resolution SSURGO data, such that areas within the area to be modeled would contain high-resolution data and areas outside the area to be modeled would contain SSURGO data. This mixed-resolution dataset allowed for a continuous data layer across the entire area of operations with sufficiently high-resolution data where it was necessary.

Bevameter reading data and bulk density data were stored as a tabular dataset and linked to polygons within the Custom Soil Classification layer using the Custom Soil Classification code.

A processing script was written to translate custom soil classification codes to the USCS codes and Integers as defined in the MAP11 schema. Custom soil classification codes, USCS codes and integers were all retained in the final output data.

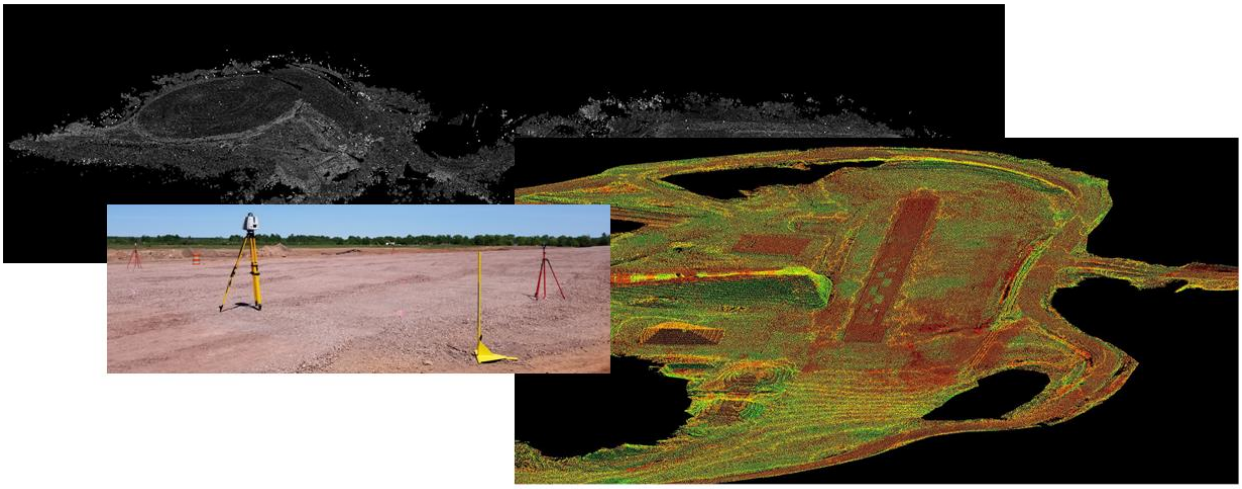

Figure 2.1.2-3 Terrestrial Scanning Tri-Pod and Point Cloud Examples of the KRC Test Course

High-resolution Elevation data was collected at sub-centimeter accuracy through manual elevation mapping using Terrestrial Lidar Scanning techniques. 3D Point clouds were created at individual stations along the 5km path used for the mobility traverse evaluation and other areas of the KRC test course.

The majority of all scans were recorded with the range set to 120m / 270m mode which has a range accuracy of 1.2mm +10ppm recording 1 million points per second. The base data set which made up the original Area of Operation (AO) consisted of 141 individual scans, more were completed as things evolved and "special" scans requested for areas of interest. Due to time constraints the AO was broken up into two registrations. The first registration contained everything around and within Loop 2 which collected data around the start on grades in front of the Terrain Park and also the entrance to the Stability area. The second registration traversed from the end of the stability area to the start of the RMS lanes in the terrain park. These two registrations were later merged to form a complete AO.

Loop 2 Registration (61 scans) Mean Absolute Error = .007ft or .213cm or 2.133mm

Stability Registration (80 scans) Mean Absolute Error = .006ft or .182cm or 1.828mm

This error is calculated from how well each target was registered together to form the combined scan. A target is the black and white checkered disc that is attached to a fixed height survey rod/tripod combo and leveled within 40". A minimum of 2 targets is required to register one scan but many shared 3 or 4 targets. All targets were recorded at the scanner with a known surface height offset and were set on 6" surveyor Magnail survey markers with center drilled heads. A random selection of these survey markers were later checked with the KRC precision GPS staff (2cm horizontal and 4cm vertical accuracy).

Using Leica Cyclone survey software, individual point clouds were stitched together to create larger point clouds. These point clouds were then Georeferenced to survey benchmarks to accurately align them to the surface of the earth. Non-surface features such as vegetation and trees were cleaned from the point cloud to create a surface point cloud. Surface point clouds were then converted to surface elevation models in Triangulated Irregular Network (TIN) format to create a High Resolution Surface Model in TIN format of the areas to be modeled. This cleaning was a multi-pass iterative process where cleaned surface model TINs were reviewed by KRC staff and model developers to identify any residual features needing to be cleaned, editing the point cloud, and re-generating the TIN surfaces.

It should be noted that the entire TIN data set was not smoothed. Only a couple of areas around the SE end of the Terrain park were drastically smoothed due to multiple scans which recorded the evolution of construction of that portion of the test course. These clouds could have been separated but time did not allow for this. Other areas that were "smoothed" or "cleaned" were obtained by removing extraneous vertices that were created from tall grasses or vegetation. The bulk of the TIN data set is extracted from the point cloud so the accuracies should equate to the accuracy limits of the scanner and the registration software. Ultimately, our data accuracy with regards to its position on the globe is limited to the accuracy of the GPS that we are using to Georeference our data set.

The TIN that Cyclone creates is extracted from the point cloud. It is not averaged or fitted so each vertex of a triangle correlates to a point from the point cloud. Mesh resolution isn't a variable that can be controlled in Cyclone so the TIN is created using to algorithm, large point clouds = large triangles. When a TIN was created of the entire AO the resolution was roughly a 1m triangle, this was not enough detail so "hi-resolution" TIN's were created for key course locations and the vehicle path. These "hi-res" TIN's have a resolution of roughly 3in triangles (.076m).

Because TIN and Mesh files of the entire area to be modeled were very large, individual TINs and Meshes were generated for subsections of the course to reduce file sizes to usable levels.

To create a surface model that covered the entire area of operations, the High Resolution Surface Model was combined with lower-resolution NED data, such that areas within the area to be modeled would contain high-resolution elevation values and areas outside the area to be modeled would contain NED elevation values. This process required the high-resolution surface TIN to be converted to TIN Points. Similarly, the low resolution NED Digital Elevation Model (DEM) was converted to a TIN and then to TIN Points. NED TIN Points were removed where high-resolution TIN Points were present. A new mixed-resolution surface model in TIN format was built in ArcGIS Desktop using both the high-resolution TIN Points and the edited NED TIN points. The process of editing NED TIN Points and TIN building was repeated to remove any artificial surface features introduced by the combination process.

This Mixed-Resolution surface model in TIN format was used to create several data layers including Elevation, Slope as Grade and Slope Aspect.

Thematic Layers Combined and Transformed to Meet Schema Guidelines

Output datasets intended for use in modeling environments must adhere to a data schema that defines attribute names, attribute value types, data value domains and ranges and standard default and null values. To facilitate this, a template Geodatabase was created and configured to meet the existing NRMM Map11 Data Schema.

Attributes and polygons from all thematic data layers were combined into a single combined data layer. This combined data layer includes attributes from all the input data layers and polygon geometries representing areas of homogeneous attributes.

Processing scripts were used to map some discrete attribute values to multiple other attribute fields in the MAP11 schema and used by the NRMM Model. Land cover values were used to determine multiple monthly recognition distance values as well as surface cover type values. Cone Index values were used to determine scenario representative cone index values.

Additional processing scripts were also used to set appropriate default and null values that met the MAP11 Schema definition.

After all layers were combined and attributes transformed and filled, geometry boundaries were cleaned using Geodatabase Topology tools in ArcGIS Desktop. Very similar feature boundaries were made coincident to remove small 'sliver' polygons, and features were dissolved to create polygons of homogenous attributes, reducing the number of total polygons.

2.1.3 Data Formats Available

Geospatial Data Output to Multiple Formats and Extents

Several output and Interchange formats were requested to enable data transfer to modeling environments and use in complex terramechanics models and legacy NRMM models.

The NRMM MAP11 format is the newest format for the NRMM model. Attributes from the combined layer were exported using custom built tools to convert polygons into raster format and then into an ASCII file grid of Terrain Units, with associated Terrain Unit attribute table.

The NRMM MAP90 format is a legacy format for the NRMM model. The same tools used to export to MAP11 format were used to export to the MAP90 format, however column headers needed to be manually edited in the MAP90 attribute table to work properly with legacy NRMM models.

Each individual Geodatabase attribute was also exported in GeoTIFF format. GeoTiff is a Raster format similar to a photograph, but with an attribute value in each pixel instead of color in each pixel. This format is commonly used to visualize attribute values such as elevation, slope, aspect and soil type.

Additionally, high-resolution elevation data was output in TIN and Mesh format. High Resolution elevation data could not be retained in NRMM MAP formats without leading to a file too large to use. Similarly, GeoTiff Files of high-resolution elevation data became too large to use.

Triangular Irregular Networks (in TIN or Mesh format) allowed for high resolution elevation data with manageable file sizes.

Because TIN and Mesh files of the entire area to be modeled still proved too large for most models to use, TINs and Meshes were generated for subsections of the course to reduce file sizes to usable levels.

All geospatial data thematic data layers such as land use and soil types are available for downlad in GeoTiff and Geodatabase format, and very high resolution elevation data is available for download in 3D mesh and TIN format for the entire area of operations as well as sub-sections of the area.

Precision map layers provided for uncertainty quantification

Precision map layers were provided to identify where high resolution Lidar elevation data was collected vs coarse resolution NED data. These layers were used in uncertainty quantification performed by UQ team to provide levels of confidence in predictions.

Model Testing and Results Display

Geospatial data was exported in MAP90 format and used to produce speed-made-good prediction files using the Legacy NRMM modeling environment. The ASCII file grid of Terrain Units was converted to a map layer and linked to the attributes of the associated output prediction files using the Terrain Unit ID (NTU) attribute. Thematic maps of speed-made-good and reason-codes were produced and used in data quality assurance testing.

Output from other models and UQ analysis were similarly joined to original Terrain Unit polygons to visualize model outputs. This final testing and output demonstrated how the GIS tools are used throughout this process from beginning to end.

Figure 2.1.2-4 Sample Speed Made Good Map of the KRC Test Course

2.2 Soil Data Set

2.2.1 Geospatial Referencing

In addition to the shape of the earth's surface, we also needed to collect soil data, information that describes the composition of the surface layer. Like elevation, soil data is also available from public sources. Again the data is acquired for the overall area but needs to be processed to fit the exact area of interest and match the target schema. For CDT, general soil data was first obtain from the Natural Resources Conservation Service Web Soil Survey website. This website is the portal to access the Soil Survey Geographic or SSURGO database.

The SSURGO database is an aggregation of state-level soil surveys over the entire United States. This soil database is a multi-level relational database that includes a spatial component as a set of map units. To processes this dataset, the SSURGO data was extracted from flat files to the government-provided database schema and matched to map unit keys. Then the map units were matched to the desired attributes, in this case the soil type and bulk density, and exported to an intermediate dataset. This intermediate dataset was then created by clipping to the correct area of interest, and the field names converted to match the NG-NRMM schema. This intermediate soil dataset was then merged into the geodatabase.

But, like the elevation data, the SSURGO data was not as detailed as was needed. The KRC's test areas are active research areas and the surface composition changes for the different portions of the test course. Readily available soil survey data from the NRCS was also not sufficiently precise or current enough for our software developers to use. NRCS Soils data only provided us with two general soil classifications – Sand and Peat. To improve this, pavement and water were manually added to the source dataset. Then, KRC personnel conducted manual on-the-ground soil sampling to further classified the test course soils into 14 different categories. These classifications were manually mapped and digitized as a thematic map of custom soil types.

2.2.2 Soil Strength Properties

Without minimizing the importance of accurate vehicle and topology models, arguably the most important aspect in mobility assessment is capturing the vehicle-terrain interaction.

While Terramechanics is generally interpreted to cover the full range of issues encountered during off-road operations, the most significant challenge and distinguishing feature of vehicle–terrain interaction models is the soft soil modeling.

This is because soft soil failures are features that most frequently dictate route selection and risk.

At some point every soft soil model requires experiments and empirical data to validate it with the real world. Terramechanics models have accomplished this at three levels:

- at vehicle level
- at running gear level (Simple Terramechanics), and
- at the soil media level (Complex Terramechanics)

NG-NRMM considers terramechanics solutions at the running gear level or below, at the soil media level.

These are termed "simple terramechanics" (ST) and "complex terramechanics" (CT), respectively.

- Being very pragmatic, ST models implement traction and bearing strength models that can be directly measured with instrumented vehicles or pressure plates and shear rings (bevameter).
- With the development of granular materials model solutions, an even more fundamental physics modeling approach has developed over the last decade that promises to reduce the experimental and testing burden further, while offering the potential model almost any conceivable mobility situation. This is the goal of Complex Terramechanics.

This brings us to the experimental data requirements for each of these terramechanics solutions.

- As already mentioned, all models require data, albeit with different levels of complexity and burden.
- Generally this includes terrain geometry, as well as strength characterization models for bearing and tractive strength.
- Terramechanics models require data commensurate with the level of detail and breadth of the study for which they are intended.
    - ST typically require in-situ measurements of soil type, strength, moisture. This is typically done with a so-called bevameter apparatus. More recently, automated data capture was demonstrated and used using the vehicle itself as a sensor.

- CT needs to be calibrated, typically using in-situ or lab experimental data (from typical geomechanics experiments, such as penetrometer, tri-axial, direct shear).

Terramechanics models have been defined as well. These consist of fundamental 3D soil media strength tests such as compressibility, triaxial tests, shear cell and cone penetrometer. The unique power of Complex Terramechanics to utilize in situ test methods such as the cone index and bevameter experiments also gives it the promise of being able to calibrate the more computationally efficient Simple Terramechanics models as well.

In review,

- All current terramechanics solutions rely on experimental data (these are not "first principle" simulations)

- ST: Pressure and slip are used to calculate sinkage and tractive force using (for example) the Bekker-Wong and Janosi-Hanamoto models.

- CT models are those that utilize full 3D soil models capable of accounting for the 3D soil flow/deformation including both elastic and plastic (permanent) deformation under any 3D loading condition of a vehicle surface.

- CT Models must include a calibration phase to identify model parameters that cannot always be directly measured experimentally
    - FEM continuum models: parameters in the underlying constitutive law
    - DEM discrete models: must accommodate for the fact that it is not feasible to simulate particles at their physical size (also they make simplifications in terms of particle shape)
    - Particle size/shape affects the soil model parameters because mechanical properties such as friction, cohesion, and plasticity scale differently with particle size.
- Calibration of CT models can be done using experimental data
    - Field measurements (e.g. bevameter data)
    - Lab tests (e.g. cone penetrometer, direct shear, etc)

2.2.3 Soil Strength Property Collection

The soil collection and analysis plan for the CDT was designed with the intent to fully describe the soils that would be tested to ensure accurate modeling results. To accomplish this, it was decided within the committee that both laboratory and in-situ soils measurements would be included. The intent of this was that standard laboratory tests are well specified and that the engineering properties are documented in ASTM specifications. On the other side, however, was the need to make measurements in the field to supply input data to the models for predictions on the fly.

In a laboratory soil analysis, they will also determine grain size, specific gravity, Proctor compaction, Atterberg limits, direct shear, and triaxial shear.

Terra-Mechanics will provide the data for the soil's exponent of deformation (n), cohesive modulus of deformation (Kc), frictional modulus of deformation (Kphi), soil cohesion (c), soil internal friction angle (phi), and soil shear deformation modulus (K). These will be provided in a lookup table synchronized to the land use or soil type.

For the CDT, a list of "standard" tests was made with input from the committee as well as from some of the modelers. These measurements were made on the soils that were deemed to describe the operational area on the KRC test course.

In general, five different soil regimes are present within the operational area for CDT on the KRC course. These are:

Fine Grained Pit
The fine grained soil is natural to the test course. It was sieved through a 1/8" mesh to remove any coarse particles. It is classified Unified Soil Classification System (USCS) as ML. It is a cohesive soil and is a sandy silt of low plasticity. This soil was chosen since it is highly moisture susceptible. 6% moisture is very stable and 18% moisture has essentially no strength. It is also highly susceptible to freeze taw immobility.

Coarse Grained Pit
The Coarse Grained Pit actually contains a medium sand. It is classified as SP/SM by USCS which is "poorly graded" silty sand. This means that the grains are for the most part the same size. This soil was chosen because it has VERY consistent grain size, and furthermore the grains are very rounded. It is essentially beach sand and has been rounded by glacial water. This results in a soil that is very much like a bucket of tiny marbles and makes it a mobility challenge. This soil gets easier to traverse when it is wet as compared to dry.

2NS Sand – Variable Hill Climb
This sand is also characterized as SP. It is a poorly graded medium sand, but contains a fraction that is closer to coarse sand as compare to the coarse pit. The sand particles are also more angular than the coarse pit resulting in a different mobility scenario. It is in general a little stiffer and slightly easier to traverse. It also exhibits better mobility wet than dry.

Rink Natural Soil
The area around the rink and VDA2 contain a soil type that is classified as SM, or silty sand. It contains a fraction of gravel sized particles also. Since KRC is in a glacial area, our soils are quite mixed up. This soil has some cohesion and is very stable when it is dry. It gets weaker when it gets wet and is susceptible to freeze thaw.

Stability Soil
The area known as "Stability" contains a soil type that is classified as SW/SM, or well graded silty sand. This means that it contains a fractions of clay through medium sand in a gradual amounts. It has more fines including clay than the rink natural. It contains a fraction of gravel sized particles and cobbles also. This soil has some cohesion and is very stable when it is dry. It gets much weaker when it gets wet and is highly susceptible to freeze thaw.

2.2.3.1 Laboratory Data Collection

The list of laboratory tests was:

- Visual – ASTM D2488
- Moisture Content at Time of Sample Collection – ASTM D2216
- Grain Size Analysis: Sieve – ASTM D6913 & Hydrometer - ASTM D7928

- Atterberg Limits – ASTM D4318
- ASTM USCS Classification
- Specific Gravity – ASTM D854 and Relative Density ASTM D4254 and D4253
- Maximum Void ratio (Minimum density/loose state) ASTM D4254
- Minimum Void ratio (Maximum density/Dense state) ASTM D4253
- Standard Proctor – ASTM D698
- Total Organics – ASTM D2974
- Direct Shear – ASTM D3080
- Triaxial Test (drained) – ASTM D7181
- Compressibility in Pressure Cell - ASTM D7181

The laboratory analyses were performed on a schedule that was independent of vehicle testing. Tests were performed in an attempt to blanket the extremes of moisture content and density. Large samples were obtained from each of the 5 different soil areas and taken to the soils laboratory at Michigan Tech. The tests were performed at the start of the CDT project and results of this testing is provided in Appendix A.

In addition to the in-depth laboratory analysis, several different in-situ measurements were made in an attempt to bracket the specific properties needed in the models. These included methods that are commonly used in construction and mobility research as well as the development of a state-of-the-art Bevameter to predict Bekker-Wong parameters of the soils. The list of in-situ measurements was:

- Visual
- Cone Penetrometer
- Rating Cone Index
- CLEGG Hammer
- Standard Moisture Content (moisture samples dried in a soils oven)
- Sand Cone Density
- Nuclear Density
- Moisture content from Nuclear Densometer
- Plate Sinkage (KRC Bevameter)
- Shear annulus (KRC Bevameter)

2.2.3.2 In Situ Measurements

In situ measurements were made when mobility tests were performed. The collection schedule of these measurements varied dependent upon the test as well as the weather. The procedure that was the most time consuming was the Bevameter (Figure 2.2.3.2-1 & 2). It was difficult to get more than 10 full sets (in different locations) with the bevameter in a day. For a single mobility test, it was attempted to get 3 separate sets of plate sinkages and shears within the area being tested. In general, 3 or so sets of Nuclear Densities and moistures, CLEGGS (on hard soils), and moisture tins were also completed for each vehicle test. Cone penetrometer readings were usually made at least 5 times and sometimes 10 per test area and day.

In some instances measurements were made between test days. This was accomplished in an attempt to look at effects of varied moisture content for the day of the CDT when soil measurements wouldn't be made.

Soil Type	Nuc Density	Nuc Moisture	Moisture Tin	Cone Penetrometer	Clegg	Cone Trace	B/W
2NS Sand	5	5	5	20	4	10	10
Coarse Pit	6	6	6	29	5	6	6
Rink Natural	5	5	4	20	2	4	4
Stability	6	6	6	36	3	4	4
Fine Pit	11	11	8	45	14	9	9
Crushed Rock	3	3	0	0	4	----	----
Gravel	1	1	2	3	5	----	----
Total	37	37	31	153	37	33	33

Table 2.2.3.2-1 Inventory of In Situ Soil Strength Measurements Collected

Figure 2.2.3.2-1 KRC Bevameter with Cone Penetrometer Shown in Pressure Sinkage Actuator Location

Figure 2.2.3.2-2 The Four Bevameter Measurement Heads Used During the CDT

For each Bevameter reading a continuous cone penetrometer trace was collected. Figures 2.2.3.2-3 thru 7 show the traces collected grouped by the 5 soil types.

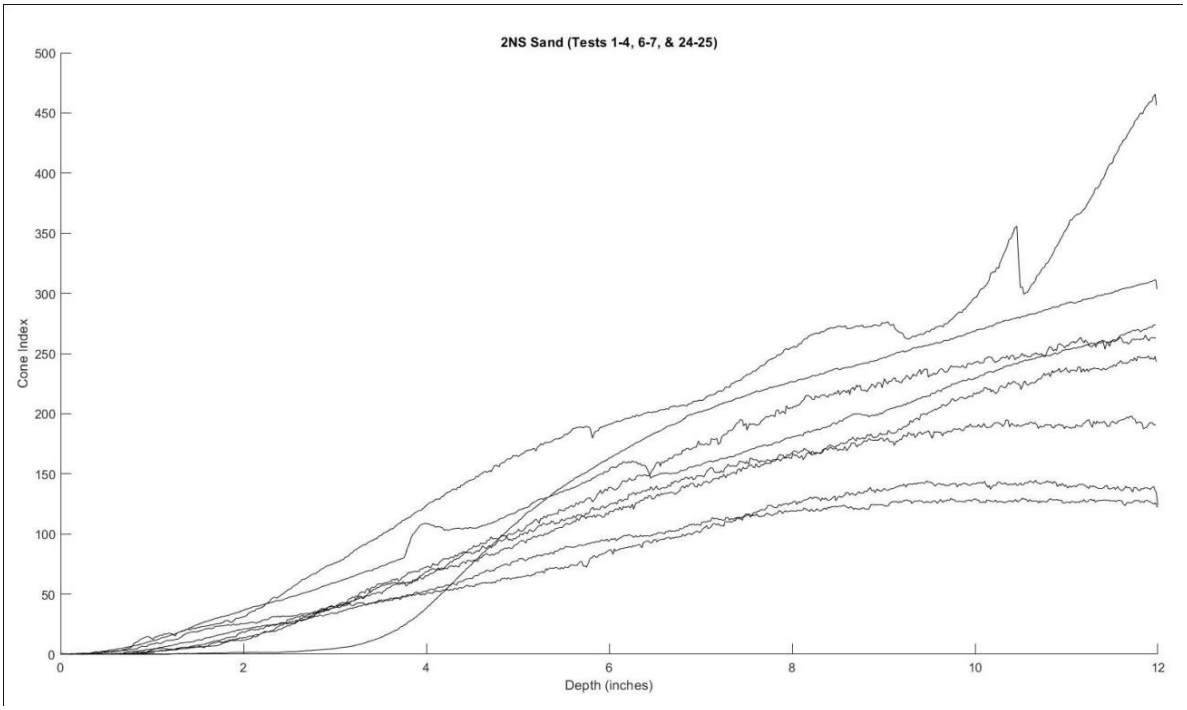

Figure 2.2.3.2-3 Cone Penetrometer Trace Collected (2NS Sand)

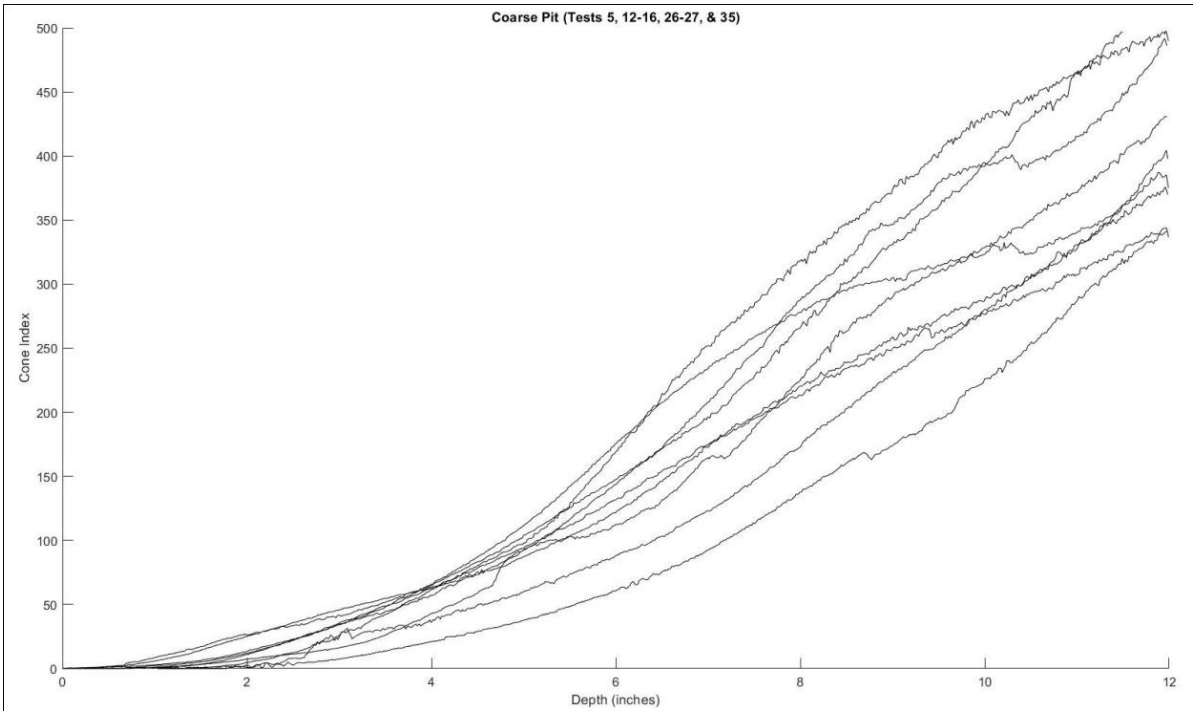

Figure 2.2.3.2-4 Cone Penetrometer Trace Collected (Coarse Grain Sand)

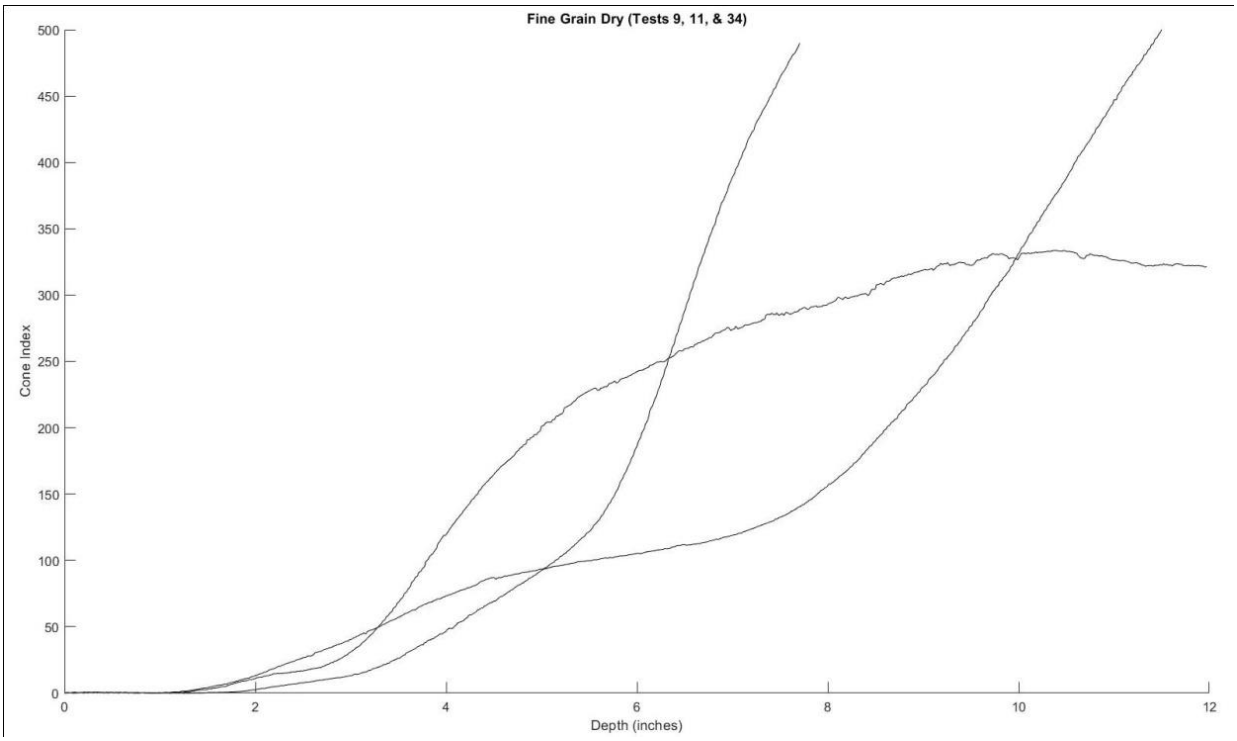

Figure 2.2.3.2-5 Cone Penetrometer Trace Collected (Fine Grain Silt - Dry)

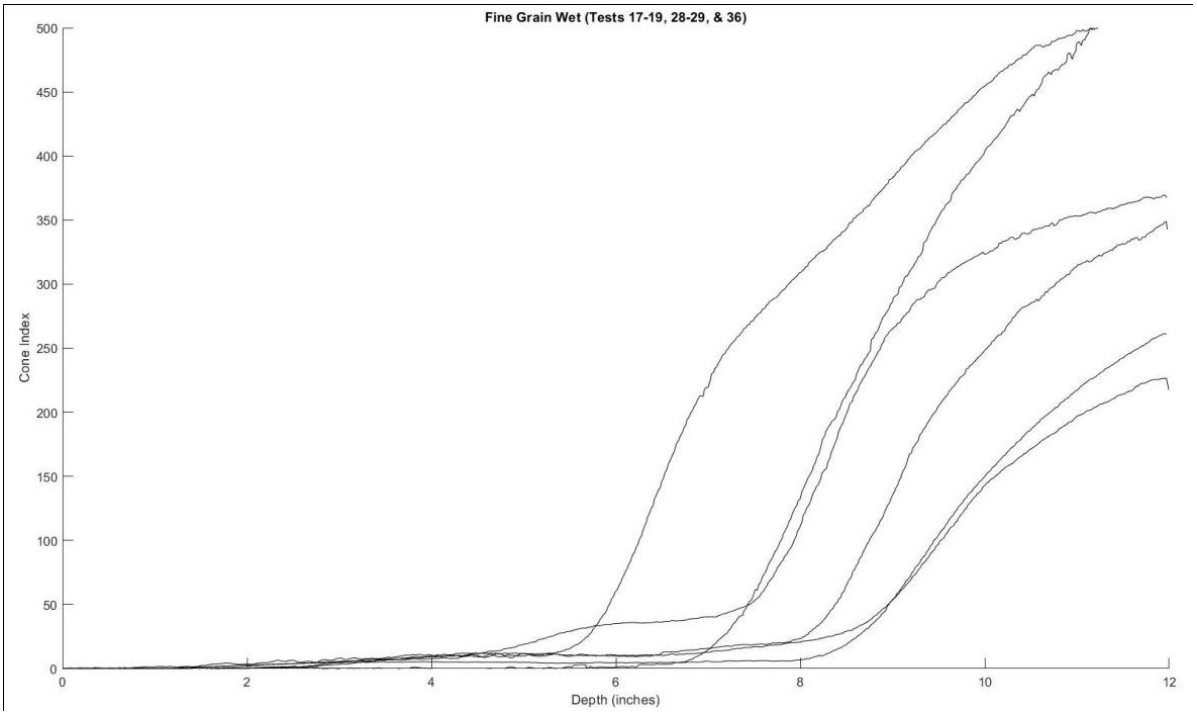

Figure 2.2.3.2-6 Cone Penetrometer Trace Collected (Fine Grain Silt - Wet)

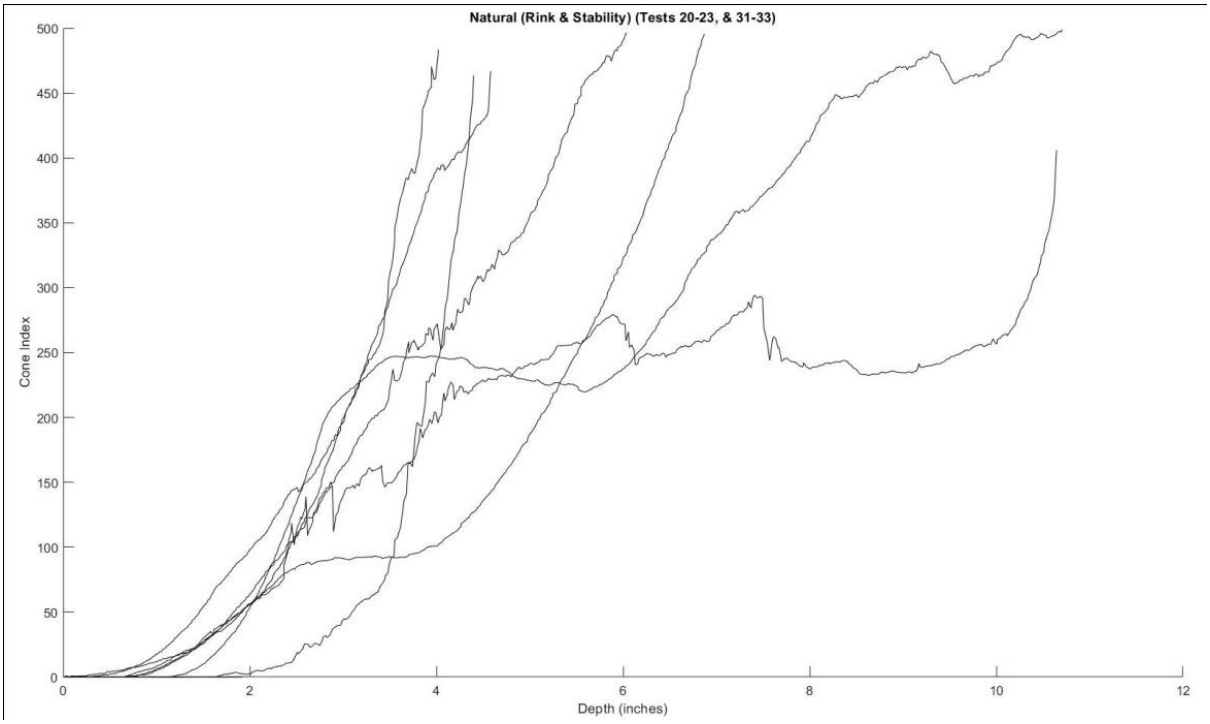

Figure 2.2.3.2-7 Cone Penetrometer Trace Collected (Natural Soil – Stability & Rink)

2.2.3.3 Development of Simple Soil Strength Values

Raw data collected from the bevameter was analyzed using the methods outlined in the text of "Terramechanics and Off-road Vehicle Engineering" by J.Y. Wong (2nd Edition, 2010).

Soil parameters from plate sinkage tests (n, K_c, and K_p) were derived using Wong's weighted least-squares method ($w_r = p^2$) to evaluate experimental data measured in the form of pressure and sinkage of two different sized plates. MATLAB was used to automate the solution of the following equations:

$$n = (\sum p^2 \sum p^2 \ln p \ln z - \sum p^2 \ln p \sum p^2 \ln z) / (\sum p^2 \sum p^2 (\ln z)^2 - (\sum p^2 \ln z)^2)$$

$$\ln k_{eq} = (\sum p^2 \ln p - n \sum p^2 \ln z) / \sum p^2$$

Using data from two different sized plates (b1 and b2), values of k_c and k_p were calculated with the following equations:

$$k_c = (((k_{eq})_{b=b1} - (k_{eq})_{b=b2}) (b_1 b_2)) / (b_2 - b_1)$$

$$k_p = (((keq)_{b=b1} - (keq)_{b=b2}) (b_2)) / (b_2 - b_1)$$

For certain test data, this aforementioned method resulted in negative values for K_c and K_p. To remedy this issue, individual pressure-sinkage curves were curve-fit in MATLAB to

$$p = K_{eq} * z^n$$

using a Levenberg-Marquardt non-linear least-squares approach. This produced optimized values of n and K_{eq} for each pressure sinkage curve of a specific sized plate. The average of the n and K_{eq} pairs were computed and reported as n Avg and K_{eq}.

Terrain response to repetitive loading was approximated by the relationship:

$$k_u = k_o + A_u z_u$$

where k_u represents the terrain stiffness during unloading or reloading and z_u is the corresponding sinkage when unloading begins. The terrain stiffness values (k_u) were extracted from bevameter data by computing the average slope of sequential unloading-reloading cycles. A linear fit was applied to these values and the slope (A_u) and intercept (k_o) were reported.

Soil parameters from shear tests (C, ϕ and K) were derived for both grouser and rubberized ring data sets using a shear stress/shear displacement relationship described by Janosi and Hanamoto as:

$$\tau = \tau_{max}(1 - e^{-j/K}) = (C + \sigma \tan \phi)(1 - e^{-j/K})$$

where τ is the shear stress, C is the cohesion, ϕ is the angle of shear deformation, and K is the shear deformation parameter. MATLAB was used to process the bevameter data (torque and angle) to this model using a least-squares routine (Levenberg-Marquardt) to estimate τ_{max} and K. Linear trend lines were then applied to the shear vs. normal stress relationships for tests run at different vertical loads and the resulting best-fit values of C and ϕ were reported.

The following tables contain an overview of the strength parameters derived for the major soils data groups measured during vehicle testing for CDT.

				Sinkage Plates						Grouser				Rubber Ring			
Date	Test Set	Location	Test Performed	P_{max} (kPa)	n	Kc (kN/m^{n+1})	Kp (kN/m^{n+2})	Au (kN/m^4)	Ko (kN/m^3)	σ_{max} (kPa)	C (kPa)	Phi (deg)	K avg (mm)	σ_{max} (kPa)	C (kPa)	Phi (deg)	K avg (mm)
6/1/2018	Test Set 1	Variable Hill Climb	Variable Hill Climb	825	0.40	8.8	100.8	90523	1317628	34.5	1.23	32.3	23.81	34.5	0.04	26.6	6.44
6/1/2018	Test Set 2	Variable Hill Climb	Variable Hill Climb	825	0.62	7.6	39.2			34.5	1.47	31.7	19.08	34.5	0.00	26.9	11.19
6/5/2018	Test Set 9	Fine grain soil pit (dry)	Drawbar Pull - Dry	825	1.49	-26.6	646.6	93970	3746425	34.5	1.05	37.4	24.16	34.5	0.00	28.6	5.97
6/5/2018	Test Set 10	Fine grain soil pit (dry)	Drawbar Pull - Dry	825	1.82	73.7	-736.0			34.5	1.46	35.9	13.72	34.5	0.00	29.0	9.22
6/5/2018	Test Set 11	Fine grain soil pit (dry)	Drawbar Pull - Dry	NO DATA						34.5	1.93	34.7	20.14	34.5	0.18	27.6	6.31
6/5/2018	Test Set 12	Coarse Pit	Drawbar Pull	825	0.46	6.1	174.1	120421	2309750	34.5	1.56	30.4	18.60	34.5	0.32	26.4	8.88
6/5/2018	Test Set 13	Coarse Pit	Drawbar Pull	825	0.63	4.8	144.8			34.5	1.34	31.8	21.51	34.5	0.06	26.8	11.52
6/5/2018	Test Set 14	Coarse Pit	Drawbar Pull	825	0.81	7.3	46.2			34.5	1.13	31.9	24.56	34.5	0.03	26.8	8.02
6/5/2018	Test Set 17	Fine grain soil pit (wet)	Drawbar Pull - Wet	825	3.57	-0.1	3.5	-89437	1954322	34.5	3.06	37.3	27.53	34.5	0.46	28.7	6.53
6/5/2018	Test Set 18	Fine grain soil pit (wet)	Drawbar Pull - Wet	825	2.97	0.2	-1.5			34.5	4.21	33.0	32.69	34.5	0.40	28.9	7.16
6/5/2018	Test Set 19	Fine grain soil pit (wet)	Drawbar Pull - Wet	NO DATA						34.5	1.99	39.0	30.78	34.5	0.22	29.2	7.25
6/7/2018	Test Set 24	Variable Hill Climb	Traverse	825	0.50	8.3	91.6	?	?	34.5	1.51	31.8	21.75	34.5	0.26	25.3	4.71
6/7/2018	Test Set 25	Variable Hill Climb	Traverse	825	0.59	-1.8	218.3			34.5	1.57	31.1	20.70	34.5	0.42	25.3	6.07
6/7/2018	Test Set 26	Coarse Pit	Traverse	825	0.81	14.0	-70.7	?	?	34.5	1.62	30.7	25.29	34.5	0.22	26.6	9.61
6/7/2018	Test Set 27	Coarse Pit	Traverse	825	0.84	1.3	142.4			34.5	1.73	30.4	22.87	34.5	0.22	26.7	10.51
6/7/2018	Test Set 28	Fine grain soil pit	Traverse	825	3.03	0.0	5.0	?	?	34.5	2.76	37.2	22.51	34.5	0.52	28.8	11.64
6/7/2018	Test Set 29	Fine grain soil pit	Traverse	825	4.01	-0.1	5.0			34.5	2.56	38.6	22.56	34.5	0.24	29.5	6.34
6/7/2018	Test Set 30a	Ice Rink	Traverse	No Test Made						No Test Made				No Test Made			
6/7/2018	Test Set 30	Ice Rink North	Traverse	825	1.69	8.2	94.2	?	?	34.5	4.49	41.5	11.10	34.5	2.458	27.0	5.63
6/7/2018	Test Set 31	Ice Rink North	Traverse	825	1.75	254.8	-2953.7			34.5	4.15	39.8	15.44	34.5	0.000	36.5	6.68
6/7/2018	Test Set 32	Stability	Traverse	825	2.98	10.3	6.2	?	?	34.5	6.23	38.2	10.42	34.5	0.80	35.9	4.89
6/7/2018	Test Set 33	Stability (Saturated+)	Traverse	825	2.15	-20.7	627.6			34.5	6.04	28.5	23.49	34.5	1.05	22.2	7.98

Table 2.2.3.3-1 Bekker-Wong Soil Strength Measurements Collected for the CDT Tests

					Cone Index		Moisture	Bulk Density	Direct Shear				Triaxial			
Date	Test Set	Location	Test Performed	Soil (USCS)	(0-15 cm)	(15-30 cm)	Grav, %	Dry (Kg/m^3)	σ_{max} (kPa)	C (kPa)	C (no-load) (kPa)	Phi (deg)	σ_{max} (kPa)	C (kPa)	Phi (deg)	
6/1/2018	Test Set 1	Variable Hill Climb	Variable Hill Climb	2NS Sand - SP	62	---	2.0	1535	158.6	0	2.9	33.8	140.0	5.5	39.6	
6/1/2018	Test Set 2	Variable Hill Climb	Variable Hill Climb	2NS Sand - SP	59	---	2.8	1663								
6/5/2018	Test Set 9	Fine grain soil pit (dry)	Drawbar Pull - Dry	Fine Grain Pit - ML	127	320+	9.3	1587	158.6	0	2.9	33.8	140.0	4.5	41.8	
6/5/2018	Test Set 10	Fine grain soil pit (dry)	Drawbar Pull - Dry	Fine Grain Pit - ML	161	320+	8.6	1525								
6/5/2018	Test Set 11	Fine grain soil pit (dry)	Drawbar Pull - Dry	Fine Grain Pit - ML	---	---	---	---								
6/5/2018	Test Set 12	Coarse Pit	Drawbar Pull	Coarse Pit - SP/SM	60	258	2.5	1541	158.6	0	3.8	36.5	140.0	3.5	40.6	
6/5/2018	Test Set 13	Coarse Pit	Drawbar Pull	Coarse Pit - SP/SM	85	300+	2.4	1610								
6/5/2018	Test Set 14	Coarse Pit	Drawbar Pull	Coarse Pit - SP/SM	118	320+	7.3	1708								
6/5/2018	Test Set 17	Fine grain soil pit (wet)	Drawbar Pull - Wet	Fine Grain Pit - ML	7	213	14.4	1562	158.6	0	2.9	44.9	140.0	4.5	41.8	
6/5/2018	Test Set 18	Fine grain soil pit (wet)	Drawbar Pull - Wet	Fine Grain Pit - ML												
6/5/2018	Test Set 19	Fine grain soil pit (wet)	Drawbar Pull - Wet	Fine Grain Pit - ML	---	---	---	---								
6/7/2018	Test Set 24	Variable Hill Climb	Traverse	2NS Sand - SP	59	189	3.0	1661	158.6	0	2.9	33.8	140.0	5.5	39.6	
6/7/2018	Test Set 25	Variable Hill Climb	Traverse	2NS Sand - SP	---	---	---	---								
6/7/2018	Test Set 26	Coarse Pit	Traverse	Coarse Pit - SP/SM	89	299	2.3	1605	158.6	0	3.8	36.5	140.0	3.5	40.6	
6/7/2018	Test Set 27	Coarse Pit	Traverse	Coarse Pit - SP/SM	---	---	---	---								
6/7/2018	Test Set 28	Fine grain soil pit	Traverse	Fine Grain Pit - ML	13	253	10.3	1490	158.6	0	2.9	44.9	140.0	4.5	41.8	
6/7/2018	Test Set 29	Fine grain soil pit	Traverse	Fine Grain Pit - ML	32	316	9.1	1490								
6/7/2018	Test Set 30a	Ice Rink	Traverse	Rink Natural (Compact) - SM	320+	320+	4.8	1914	158.6	0	5.2	35.1	140.0	8.3	40.6	
6/7/2018	Test Set 30	Ice Rink North	Traverse	Rink Natural (Grass) - SM	177	247	14.1	1571								
6/7/2018	Test Set 31	Ice Rink North	Traverse	Rink Natural (Grass) - SM	---	---	---	---								
6/7/2018	Test Set 32	Stability	Traverse	Stability - SW/SM	199	308	10.6	1554	158.6	0	4.5	36.5	140.0	12.1	42.6	
6/7/2018	Test Set 33	Stability (Saturated+)	Traverse	Stability (Sat) - SW/SM	200	320+	---	---								

Table 2.2.3.3-2 Additional Measurements Collected at the Bekker-Wong Measurement Sites and the Corresponding Strength Values Obtained from Laboratory Tests for that Soil

2.2.4 Complex Soil Strength and Uncertainty Quantification Properties

Complex Terramechnics Laboratory Soils Testing

The Complex Terramechanics models required a specific cohesion value for the five soil types. In order to derive this cohesion number, a special direct shear test was performed. This test was performed by preloading the direct shear sample in the shear device to the maximum load for the MTU shear ring. This load is 105.8 lb (1037.5 N). The preload was kept on the sample for 60 seconds and then taken off. After removal of the pre-load, an unloaded direct shear test was performed. The shear strength with zero normal load was assumed to be the cohesion for the Complex models. The following table contains the values for this special cohesion number.

Soil	Shear Strength after 60 seconds consolidation under 105.8 lb and sheared under no normal load (psi)	Shear Strength after 60 seconds consolidation under 105.8 lb and sheared under no normal load (kPa)
2NS	0.414	2.9
Coarse Pit	0.544	3.8
Fine Pit	0.424	2.9
Rink Natural	0.754	5.2
Stability	0.657	4.5

Table 2.2.4 Specific Cohesion Values Obtained for Complex Terramechanics Models

The Complex Terramechanics models required a second non-standard soil measurement. In order to calculate the sinkage, the compressibility of the five soil types was used. Compressibility was measured in the lab in a soil pressure cell. This device quantifies the compression of pre-densified soil samples at increasing loads. The values for compressibility for the 5 soils are contained in soils report in Appendix A.

Expanded Uncertainty Soil Groupings

Uncertainty calculations were complicated by the fact that there was only a limited number of B/W measurements made for each deformable soil type during the CDT test period. In an attempt to increase the number of data points available for the calculations, the soils were grouped into "like" soil classes and a second uncertainty analysis was performed on these groups. The 5 CDT soils were grouped into 3 groups as follows:

- "Sands" = 2NS Sand and Coarse Pit
- "Sandy Loams" = Rink Natural and Stability
- "Silt" = Fine Grained Pit

For uncertainty, a 6th deformable soil type, peat, was used for all soils outside the CDT operational area. The B/W parameters for this soil type were derived from readings at KRC and from data found in the literature.

For non-deformable surfaces, there were 3 different types. These were crushed rock, gravel, and pavement. For uncertainty modeling, the crushed rock and gravel were grouped together.

Chapter 3 – Vehicle Data Set

3.1 Discussion

3.1.1 Vehicle Data Set

US army TARDEC's FED Alpha vehicle was used as the surrogate test vehicle for NG-NRMM demonstration effort. The FED ALPHA was part of the Fuel Efficient Ground Vehicle Demonstrator (FED) program by the U.S. Army's Tank Automotive Research, Development and Engineering Center

(TARDEC). Engineering firm Ricardo teamed up with the United States military to create the FED-A as a more fuel-efficient armored personnel carrier.

The vehicle has been undergoing testing at the U.S. Army's Aberdeen Proving Grounds in Maryland.

The FED-A is made of an Alcoa Defense lightweight aluminum structure with armoring and an underbody blast shield. The vehicle features a Cummins I4 engine, a six-speed automatic transmission from Aisin and is fitted with Goodyear 335/65R22.5 G275 Fuel Max low roll resistance tires developed specifically for the FED-A.

The vehicle possesses a commercial off the shelf (COTS) Dana central tire inflation system (CTIS) with 4 settings (E = 15 psi, SS = 25 psi, CC = 40 psi, and HY = 60 psi), a modified COTS adaptive braking system (ABS) and traction control system (TCS), and an active ride height system (Highway = 271 mm clearance, Obstacle = 341 mm clearance). The suspension is a independent unequal length A-arm (SLA) architecture with integrated air-spring-dampers at each corner. The powertrain and driveline consists of

4.5L 200 hpefficiency optimized super & turbocharged Cummins (Modified COTS)

24VDC Kollmorgenintegrated starter-generator (Unique)

6-speed Aisin automatic transmission (COTS)

Full time 4WD T-case (COTS-HMMWV)

Spiral bevel air-locking differentials (Modified COTS)

Non-geared hubs (Unique)

The FED-A selection as a surrogate vehicle for the NG-NRMM CDT was that it was representative of a military vehicle with substantial off road capability that was not fielded and was US Army TARDEC Owned. This meant an appropriately sized and capable vehicle with a database that was essentially open to public dissemination. It had been subjected to some US Army Test & Evaluation Command testing with a published report of this activity and had liberal use of COTS components with some spare part packages available. Ricardo had also developed a multi-body dynamics model in Adams and also had generated a NRMM model.

3.1.2 Vehicle Behavior Data Set

3.1.2.1 Instrumentation Plan

External sensing was applied to the FED-A vehicle to collect the following data:

- Vehicle Position and Pose
- Suspension travel at each wheel location
- Triaxial accelerations at each spindle/hub location
- Driver’s seat triaxial accelerations (seat pad and seat base)
- Passenger’s seat triaxial accelerations (seat pad and seat base)
- Vertical, longitudinal, and lateral accelerations of the vehicle
- Roll, pitch, and yaw rates about the vehicle COG
- Brake Pedal Force
- Vehicle speed over ground
- Steering wheel and Pitman arm angles
- HalfShaft (axle) torques at each wheel location

- Drawbar pull force

Several Controller Area Network (CAN) data streams available on the FED-A were also recorded to collect the following data:

- Accelerator pedal and throttle positions
- Engine RPM and torque
- Wheel speed at each wheel location
- Transmission output speed and gear ratio
- Torque converter status

A common data acquisition system was used to collect both the analog sensor signals and digital data. The system re-sampled and time-synchronized digital data to align with analog sensor data with a common, equidistant time base. This system also has integral anti-alias filtering and simultaneous sampling of all analog input channels.

3.1.2.2 Automotive Testing

The specific maneuvers were performed by the FED-A are shorter tests of individual segments of the course. The vehicle approached the obstacle or special terrain and stop facing it, then drove through the obstacle, stopping again on the other side. In this way, the vehicle's isolated performance on a single piece of homogeneous terrain was measured.

3.1.2.3 Trafficability

3.1.2.4 Mobility Traverse

In addition to the individual maneuvers, the FED-A performed mobility traverses, which involve covering multiple segments in one session without stopping. These traverses were intended to simulate live field use of the vehicle where the driver may encounter multiple different kinds of obstacles without time for stopping or maintenance. They were between 2 and 3.5 km long and will be run in both directions.

3.2 Instrumentation

3.2.1 Data Acquisition Measurement Frontend

A Siemens SCADAS mobile modular data acquisition frontend was used to record both analog signals and digital data streams from sensors and data networks on the FED-A vehicle. All analog signals were filtered (4-pole analog anti-aliasing filter) prior to being digitized by 24-bit sigma-delta ADCs using a sample rate of 1600 Sa/sec/ch. Time-stamped digital data streams from the vehicle CAN bus were re-sampled and synchronized with the analog signals by the SCADAS mobile and assembled in a common data file with a single sample rate. Measurements were stored as time histories in the Siemens Test.Lab format (.ldsf) at the time of acquisition, and were later exported to a common open-source data format (MATLAB .mat) that all users can access.

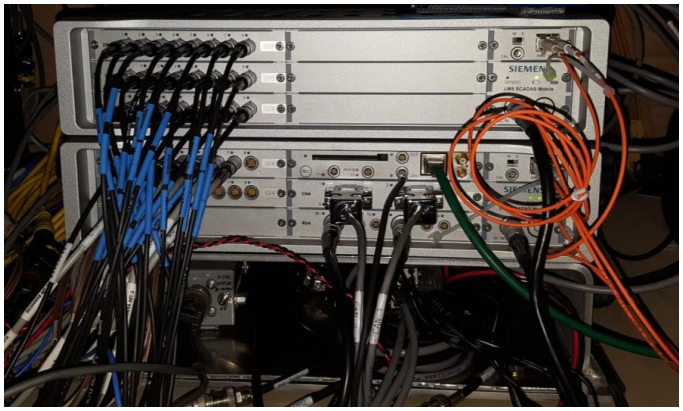

Figure 3.2.1-1: Siemens SCADAS Mobile Data Acquisition Frontend

3.2.2 Basic Movement and Orientation

A Racelogic VBox 3i RTK was used to measure vehicle location, speed, and orientation. The VBox system uses an IMU-compensated dual-antenna GPS/GLONASS receiver, in conjunction with an RTK differential base station, to achieve +/- 2cm positional accuracy in real time at a 100Hz update rate. The VBox antennas were installed on the vehicle roof in a cross-car orientation, with the VBox IMU coincident with the antenna above the driver position.

The VBox logged and output (via CAN) time-stamped digital data including:

Speed over Ground, Velocities, and Positional (Lat/Long/Elevation) Information
IMU accelerations and rotational rates (6-DOF)
Slip, pitch, roll and heading angles
Satellite Time, # and DGPS Correction Status

Figure 3.2.2-1: Racelogic VBox 3i Control Unit

Figure 3.2.2-2: VBox GPS/GLONASS Antennas

3.2.3 Vehicle Acceleration and Rates

A Systron Donner MotionPak (Model MP-GDDDQVVV-100) is an analog output inertial measurement unit used to measure the triaxial accelerations of the vehicle as well as its roll, pitch and yaw rates. The ideal placement for this type of sensor is precisely at the vehicle COG. For the FED-A vehicle, however, the COG is physically located within the power-train structure (transmission) making an ideal installation impossible. As a compromise, the MotionPak was mounted to the transmission tunnel with its sensing axes located at the following vehicle coordinates (defined for high ride height):

Sensor Location	X (in)	Y (in)	Z (in)
MotionPak	0.3	113.5	53.0

Figure 3.2.3-1: Systron Donner MotionPak

Figure 3.2.3-2: Installation of the MotionPak, Near the Vehicle COG

3.2.4 Seating Accelerations

The two principal seating locations are the driver and passenger seats. Accelerations were measured at both the base and the seat pad of those locations for the computation of absorbed power.

A pair of PCB Piezotronics 356B41 seat pad accelerometers were used to measure the accelerations of the principal seating surfaces. These sensors report triaxial accelerations in conformance with ISO 10326-1.

Figure 3.2.4-1: Seat Pad Accelerometer (Driver's Side)

Two PCB Piezotronics T356A15 accelerometers were adhered to the floor to measure the triaxial acceleration of the bases of the principal seats. The rubberized floor covering material was removed at the locations of the accelerometer installations.

Figure 3.2.4-2: Seat Base Accelerometer (Driver's Side)

The seat base accelerometers were located at the following vehicle coordinates (defined for high ride height):

Sensor Location	X (in)	Y (in)	Z (in)
Driver's Seat Base	19.5	108.1	32.2
Passenger's Seat Base	-19.5	109.0	32.2

3.2.5 Steering Wheel Angle

The steering wheel angle was measured using a RLS Renishaw model MR047B040A076B0 radial magnetic encoder ring and a model LM13IC10BCA10F00 reader head. The magnetic encoder ring was attached to a rotating portion of the steering shaft (just below the steering wheel), and the reader head was held stationary by the steering column structure.

Figure 3.2.5-1: Radial Magnetic Encoder Ring and Reader Head Assembly

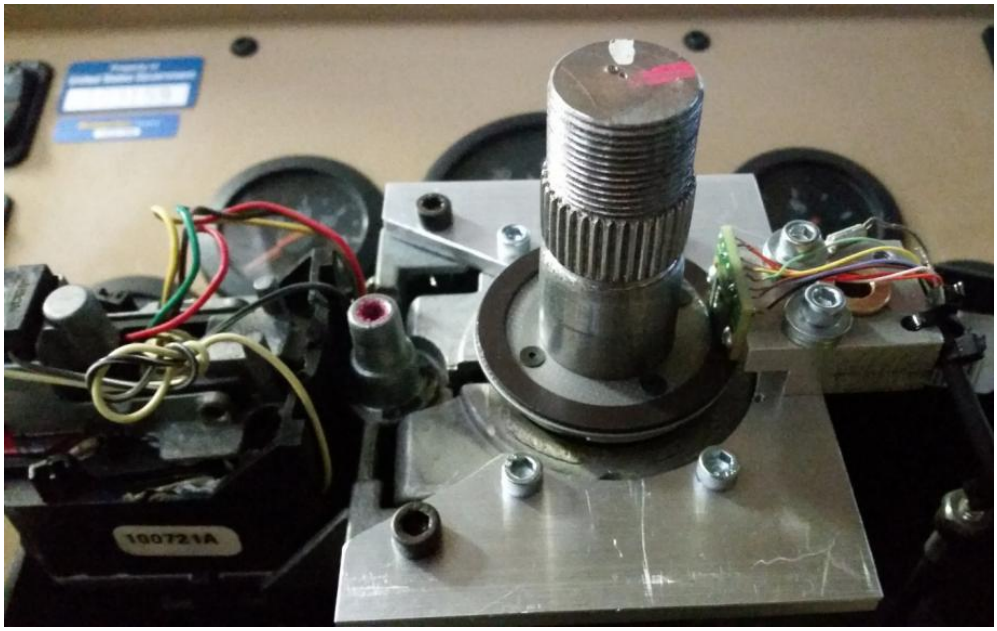

Figure 3.2.5-2: Radial Magnetic Encoder Ring and Reader Head Assembled on Steering Shaft

3.2.6 Pitman Arm Angle

The Pitman arm angle was measured using a Koyo TRD-N5000-RZVWD incremental encoder with a resolution of 5000 pulses/revolution. The encoder was rigidly mounted on a frame-mounted bracket beneath the Pitman arm. The encoder shaft was connected to the Pitman arm pivot using a short steel rod and a zero-backlash misalignment coupling.

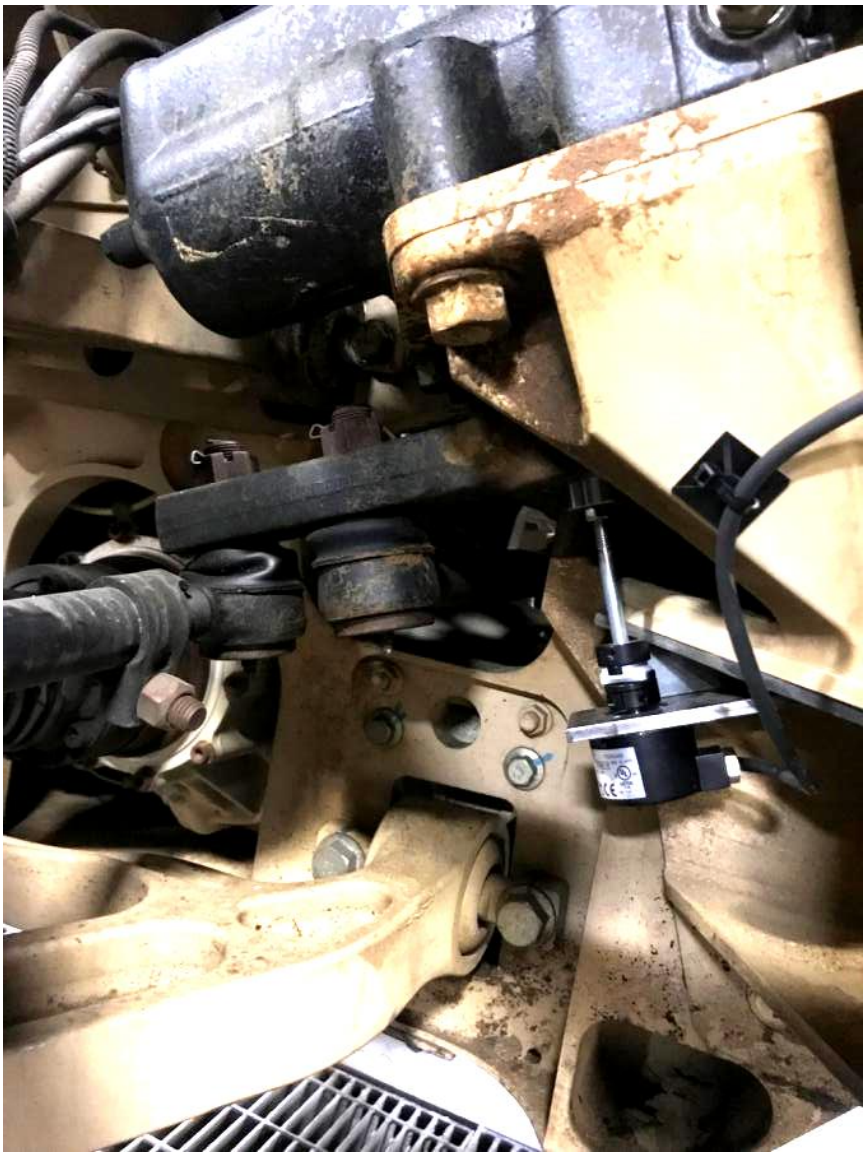

Figure 3.2.6-1: Pitman Arm Angle Encoder Installation

3.2.7 Brake Pedal Force

The force exerted by the driver to the brake pedal was measured using a Futek FSH03184 pedal force sensor. The brake pedal sensor was installed on the pedal using worm-drive clamps.

Figure 3.2.7-1: Brake Pedal Force Sensor

3.2.8 Spindle Accelerations

Four (4) PCB Piezotronics T356A02 accelerometers measured the triaxial acceleration at each of the wheel spindle/hub locations. The T356A02 has linear frequency response between 1 and 5000 Hz and a nominal sensitivity of 100 g's/V.

Figure 3.2.8-1: Spindle/Hub Accelerometer Location

3.2.9 Suspension Travel

The FED-A ride height control system includes Firestone Intelliride 28-3582-0101 sensors to monitor the dynamic suspension displacement at each airspring suspension cartridge. These sensors are mounted on the vehicle chassis and are coupled to the lower A-arms via linkages. The analog outputs from these sensors were recorded by the data acquisition system as a means to report suspension travel at all four vehicle corners during vehicle operation.

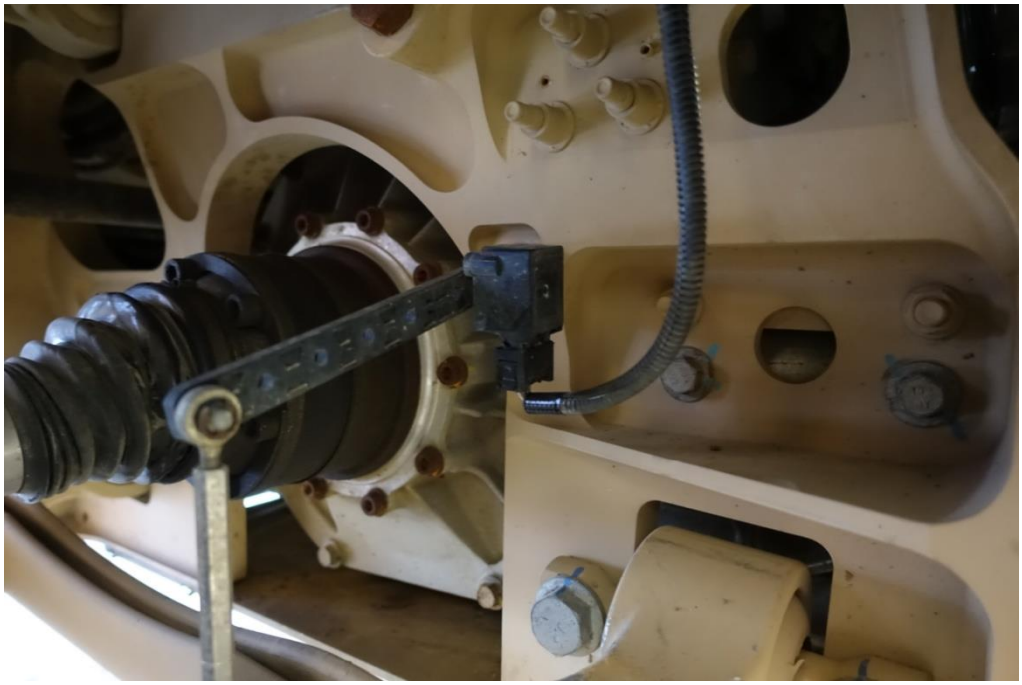

Figure 3.2.9-1: Suspension Travel Sensor

3.2.10 Wheel HalfShaft Torques

In-situ torque measurements were made at all four corners of the vehicle by instrumenting/calibrating the wheel halfshafts and using wireless telemetry to broadcast data back to the data acquisition system. Vishay CEA-06-062UV-350 foil strain gauges were applied to each halfshaft in a full-bridge (torque rosette) configuration. Dynamic strain data was transmitted wirelessly from the rotating shafts during vehicle operations using a Binsfeld Engineering TorqueTrak 10k Telemetry transmitter on each shaft. The receiver units were located in the cab of the FED-A.

Figure 3.2.10-1: Instrumented Half-Shaft with Binsfeld TorqueTrak Telemetry Transmitter

Figure 3.2.10-2: Binsfeld TorqueTrak Telemetry Receivers

3.2.11 Drawbar Force

Drawbar force was measured using a PCB Piezotronics 1381-04A Loadcell. The loadcell was installed with spherical rod-ends and clevises to ensure a pure tensile load during drawbar pulls. A standard military drawbar was installed on the towing lugs at the rear of the FED-A with the loadcell coupling the drawbar to the drawbar load

Figure 3.2.11-1: Drawbar Loadcell

Figure 3.2.11-2: Drawbar and Loadcell Installed on FED-A

3.2.12 Vehicle Controller Area Network (CAN) Data

The FED-A vehicle has two accessible communication networks transporting digital data for operation of the vehicle: J1939 CAN and Aisin.

Both network data streams were logged in their entirety (i.e. all parameters) by the SCADAS data acquisition system. To ease in analysis, a subset of vehicle parameters (tabulated below) were decoded using CAN database files (.dbc) provided by the vehicle manufacturer. Additional parameters can be decoded from the raw data logs using Siemens Test.Lab software.

Vehicle Network Monitoring				
Source	**Parameter**	**Description**	**EU**	**Bus Hz**
J1939	Acc_PedPos	Accelerator Pedal Position	%	20
J1939	Eng_Spd	Engine Speed	rpm	50
J1939	Eng_ActTq	Engine Torque	%	50
J1939	Trans_Output_Speed	Transmission Output Speed	rpm	100
J1939	Trans_Current_Gear	Transmission Gear Range Attained	/	10
J1939	TC_Lockup_Engaged	Torque Converter Lock/Unlock	/	100
J1939	Trans_Gear_Ratio	Transmission Actual Gear Ratio	/	10
Aisin	Whl_Spd_Rear_Left	Wheel Speed- Rear L	rpm	50
Aisin	Whl_Spd_Rear_Right	Wheel Speed- Rear R	rpm	50
Aisin	Whl_Spd_Frnt_Left	Wheel Speed- Front L	rpm	50
Aisin	Whl_Spd_Frnt_Right	Wheel Speed- Front R	rpm	50

Figure 3.2.12-1: Decoded Signals from Vehicle Controller Area Network (CAN) Data

3.3 Automotive Performance Testing

3.3.1 NATO Lane Change

The goal of this test was to determine the dynamic stability of the test item during emergency lane change maneuvering on paved and off-road surfaces. Lane change tests were conducted using TOP 2-2-609 (Steering) and the NATO Allied Vehicle Testing Publication 03-160W (Dynamic Stability) as general guides.

Vehicle tire pressure was adjusted to 60 psi. Lane changes were performed at 20, 30, and 40 MPH on both level paved and gravel roads with a minimum of 5 runs for each speed and road condition. Representative plots of the vehicle path, steering wheel angle, yaw rate, roll angle, and lateral acceleration are shown in figures 3.3.1.1-1 through 3.3.1.1-5 and are taken from the 20 MPH paved lane change tests.

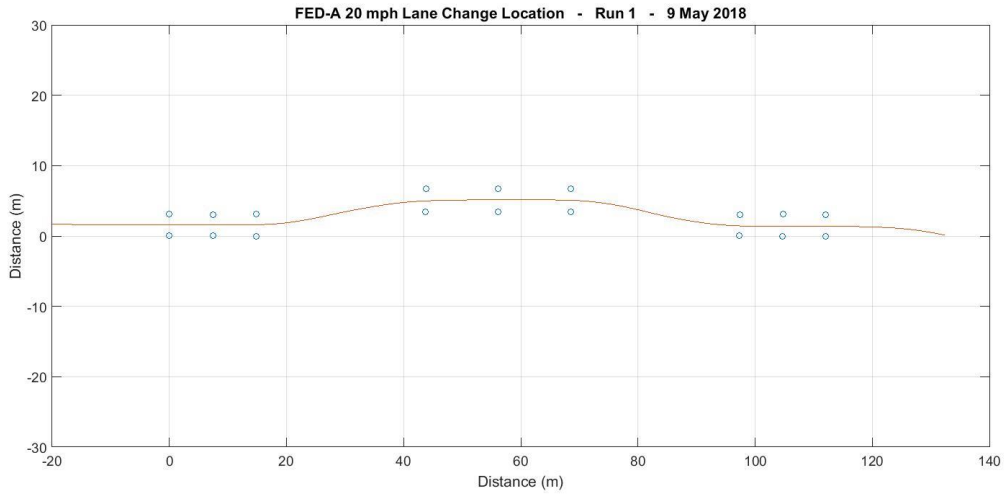

Figure 3.3.1.1-1: Representative lane change path from 20 MPH paved lane change run 1

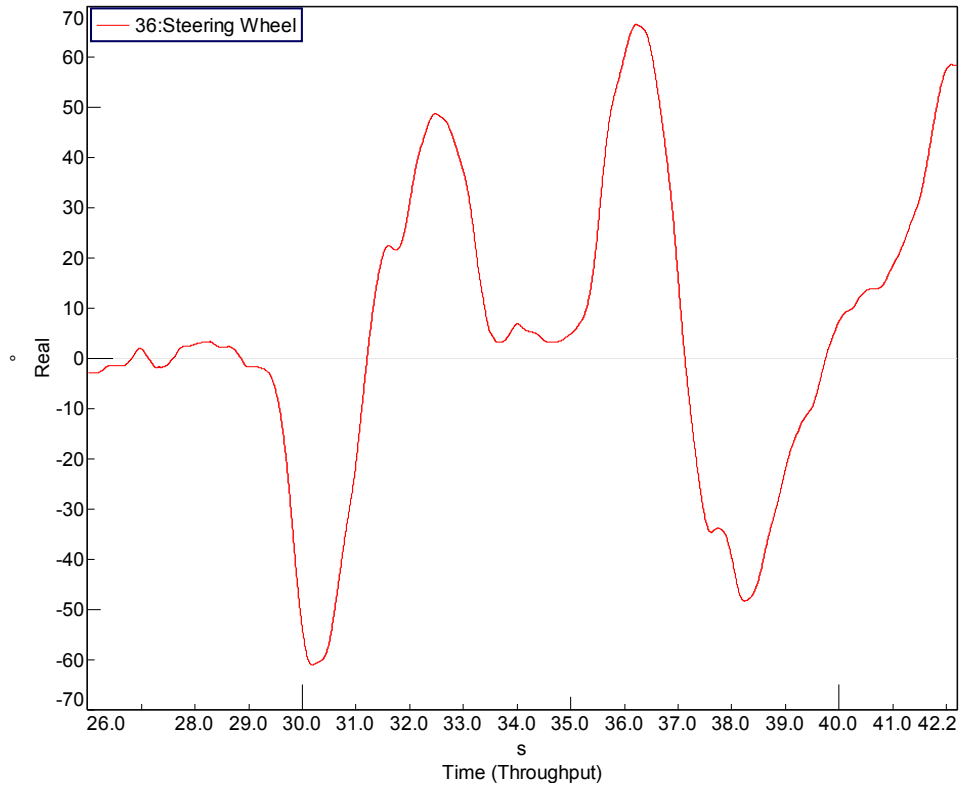

Figure 3.3.1.1-2: Representative steering angle history from 20 MPH paved lane change run 1

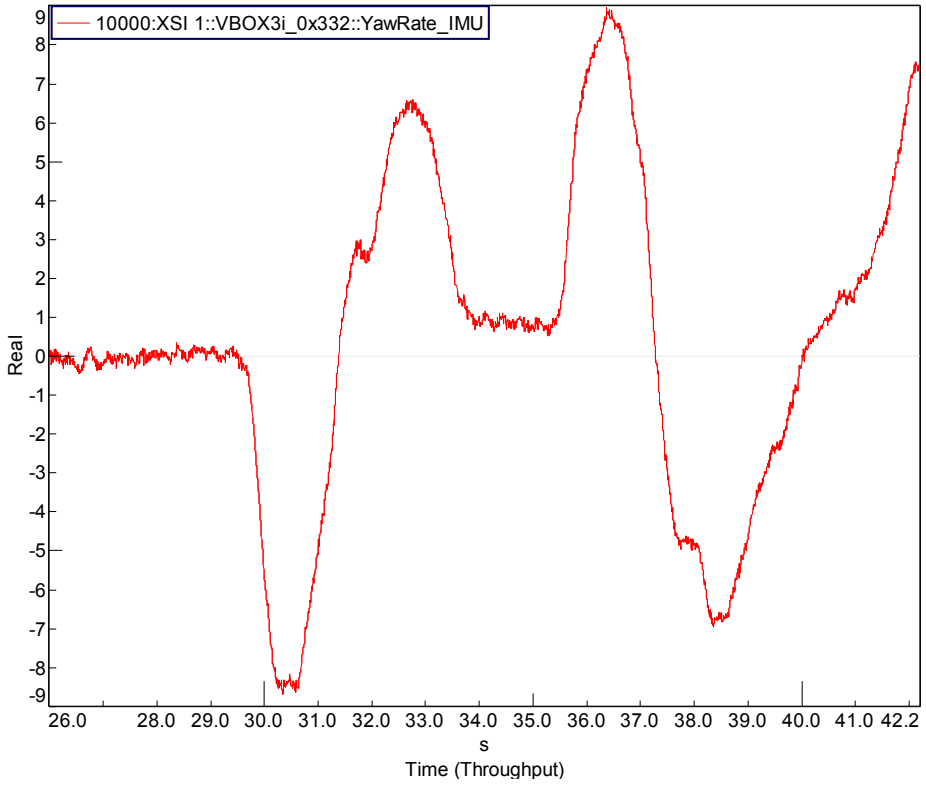

Figure 3.3.1.1-3: Representative yaw rate history from 20 MPH paved lane change run 1

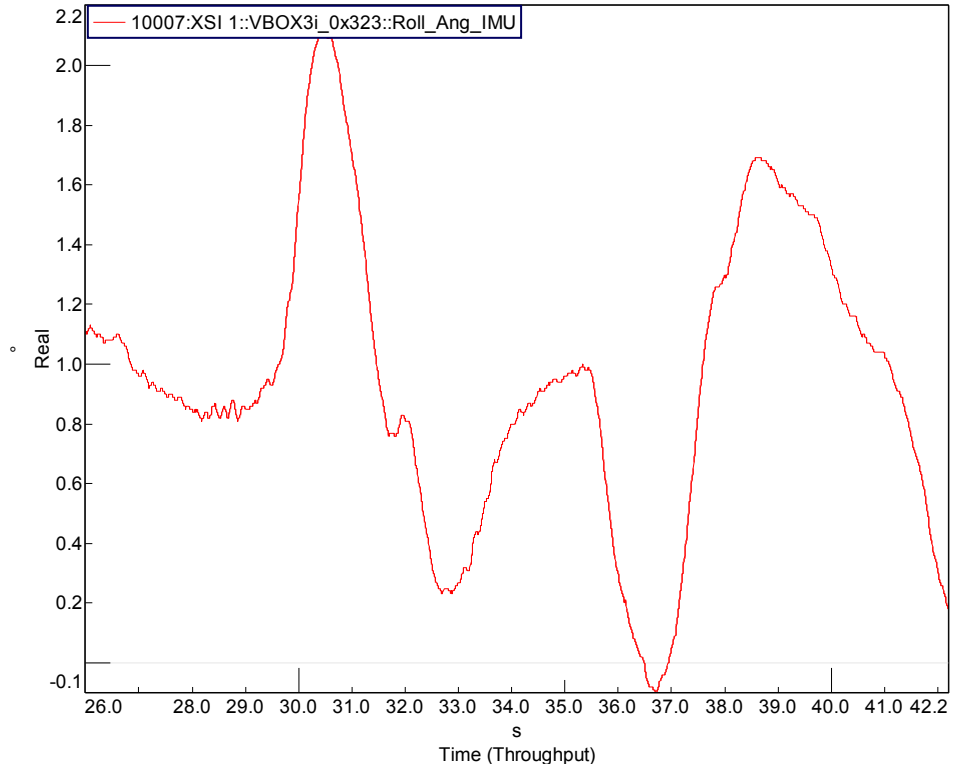

Figure 3.3.1.1-4: Representative roll angle history from 20 MPH paved lane change run 1

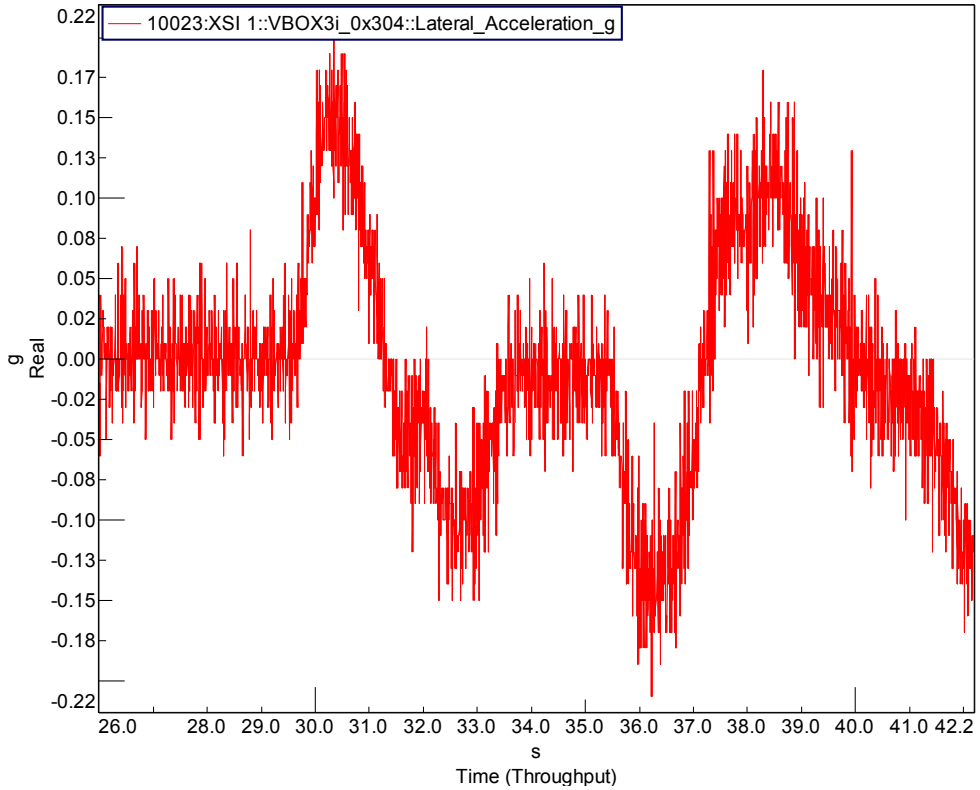

Figure 3.3.1.1-5: Representative lateral acceleration history from 20 MPH paved lane change run 1

3.3.2 Speed and Acceleration

The goal of this test was to determine the operating characteristics of the test item under maximum speed and acceleration conditions on a paved surface. Testing was done in accordance with TOP 2-2-602 (Acceleration; Maximum and Minimum Speeds).

To conduct the test, the vehicle's tires were inflated to 60 psi. The vehicle operator applied maximum throttle to accelerate the vehicle to 70 mph. Data was taken during three runs each in both uphill and downhill directions and averaged to minimize minor grade variations. Representative plots showing the general shapes of the of vehicle speed, accelerator input, vehicle acceleration, transmission gear, engine torque, and engine RPM from the first downward acceleration run are shown in figures 3.3.1.2-1 through 3.3.1.2-5.

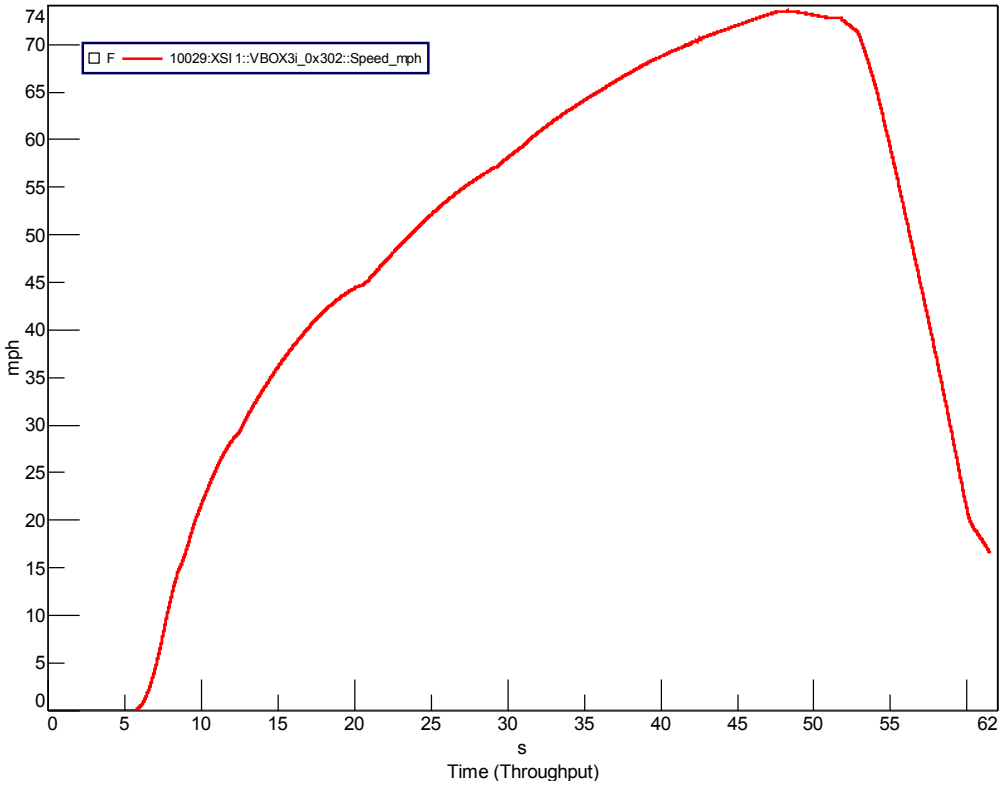

Figure 3.3.1.2-1: Representative plot of vehicle speed from downward acceleration run 1

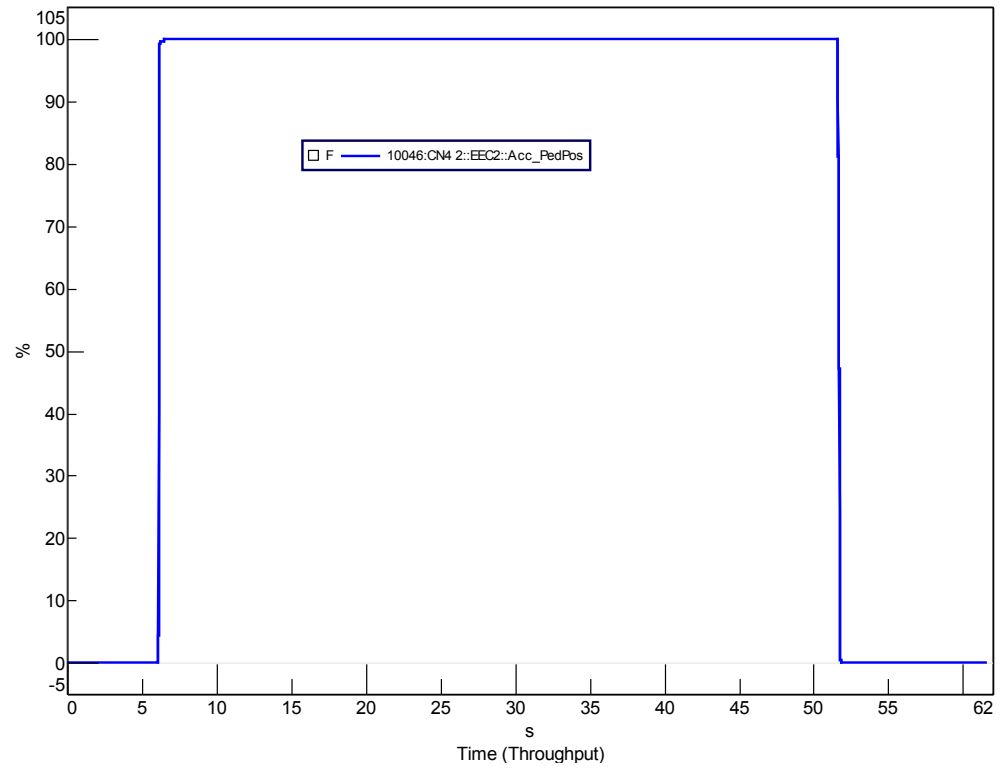

Figure 3.3.1.2-2: Representative plot of accelerator input from downward acceleration run 1

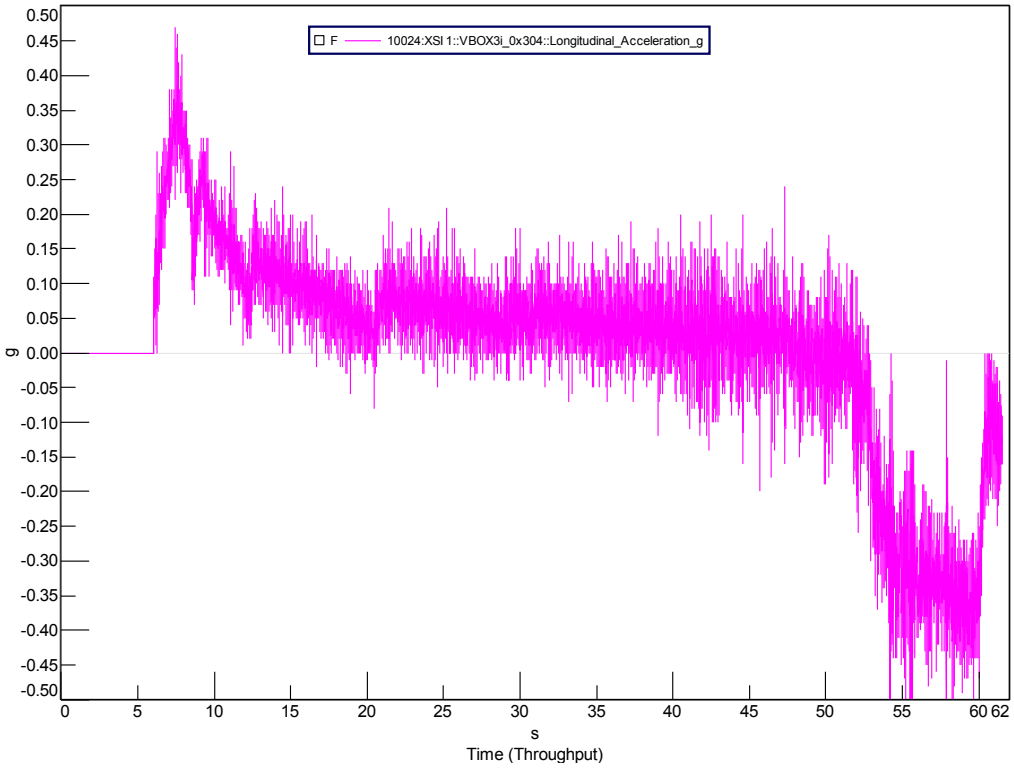

Figure 3.3.1.2-3: Representative plot of vehicle forward acceleration from downward acceleration run 1

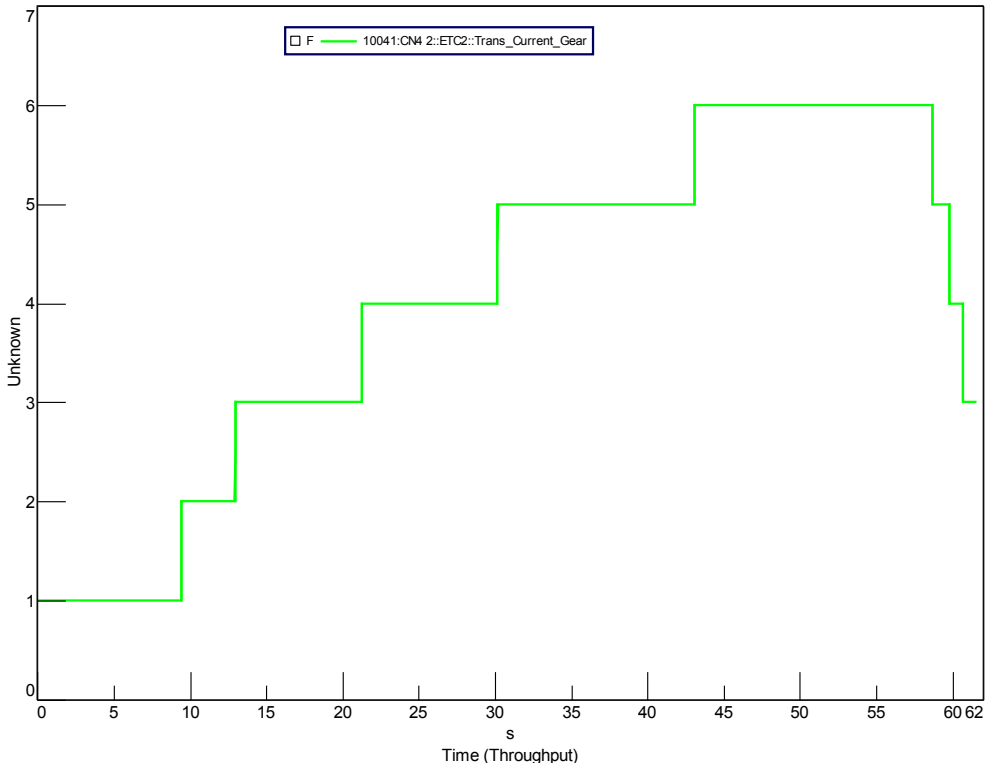

Figure 3.3.1.2-4: Representative plot of vehicle gear from downward acceleration run 1

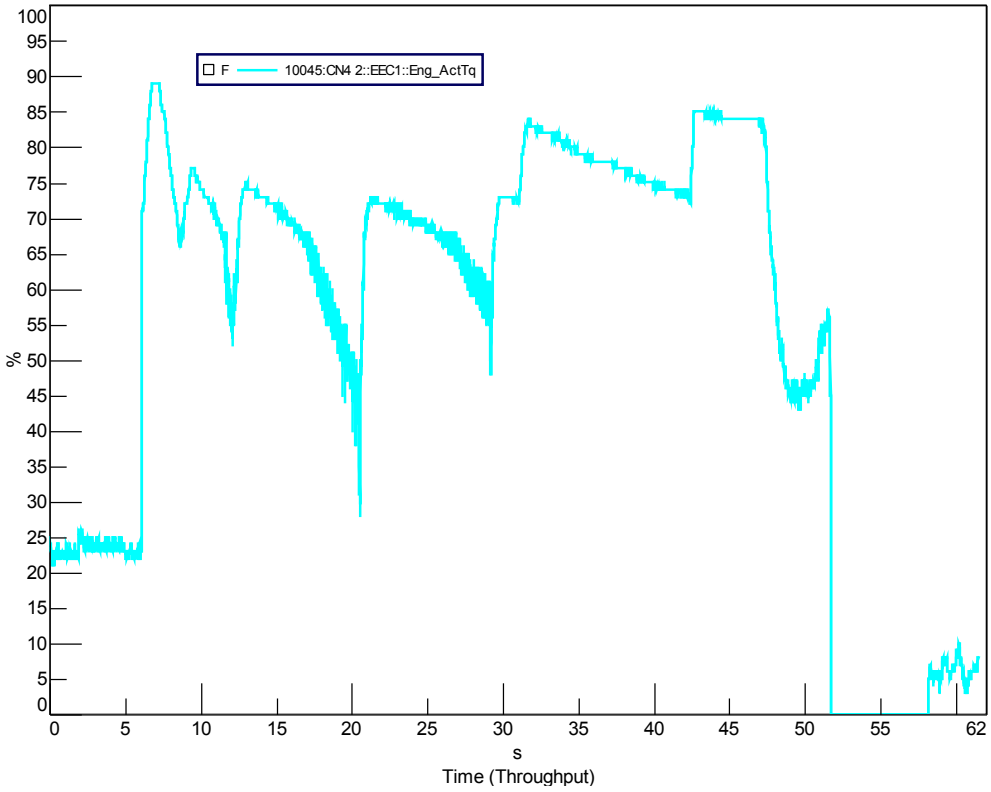

Figure 3.3.1.2-5: Representative vehicle engine torque from downward acceleration run 1

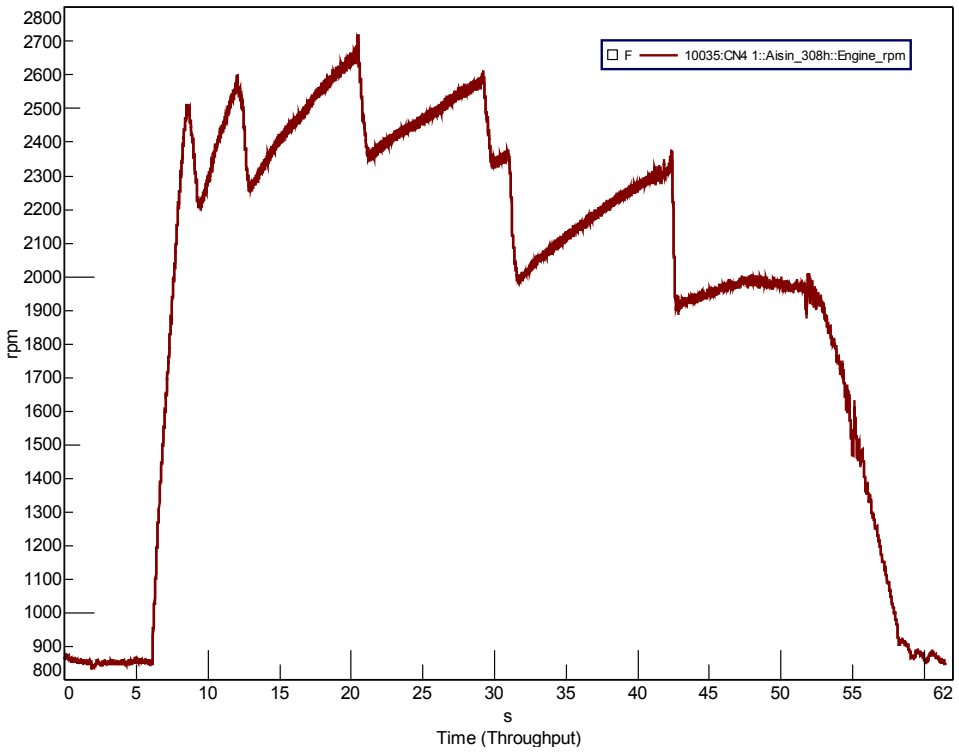

Figure 3.3.1.2-5: Representative vehicle engine RPM from downward acceleration run 1

3.3.3 Braking

The goal of this test was to determine the braking performance of the test item during maximum effort braking. Testing was done using TOP 2-2-608 (Braking, Wheeled Vehicles) and SAE J299 (Stopping Distance Test Procedure) as general guides.

The vehicle's tires were inflated to 60 psi. The braking distance was measured after the brakes were applied when the vehicle was at the target initial speed. Tests were done three times each in both the uphill and downhill directions and at initial speeds of 20 and 40 MPH for a total of twelve tests.

The average corrected stopping distance for 32.2 KPH and 64.4 KPH (20 and 40 MPH) were 7.0 meters and 27.4 meters. IAW SAW J299 was used to correct the stopping distance to account for speed variations. The data recorded is shown in table 3.3.1.3-1, and the SAE corrected stopping distances are shown in figures 3.3.1.3-1 and 3.1.1.3-2.

Stop #	Surface	Travel Direction	Target Speed (KPH)	Speed at brake apply (KPH)	Average Deceleration Rate (m/s^2)	Raw Stopping Distance (m)	SAE Corrected Stopping Distance (m)	Average Corrected Stopping Distance (m)
1	Pavement	Downhill	32.2	33.2	6.6	8.0	7.5	7.0
2	Pavement	Uphill	32.2	31.8	6.7	6.9	7.1	
3	Pavement	Downhill	32.2	32.7	6.8	7.4	7.1	
4	Pavement	Uphill	32.2	33.2	6.8	7.1	6.7	
5	Pavement	Downhill	32.2	32.1	6.6	6.8	6.9	
6	Pavement	Uphill	32.2	29.2	6.7	5.3	6.4	
1	Pavement	Downhill	64.4	63.9	6.9	27.6	28.0	27.4
2	Pavement	Uphill	64.4	63.4	6.9	25.7	26.5	
3	Pavement	Downhill	64.4	65.1	6.8	28.5	27.9	
4	Pavement	Uphill	64.4	65.2	6.8	27.6	26.9	
5	Pavement	Downhill	64.4	64.5	6.7	27.9	27.8	
6	Pavement	Uphill	64.4	64.1	6.6	27.3	27.5	

Table 3.3.1.3-1: Braking data

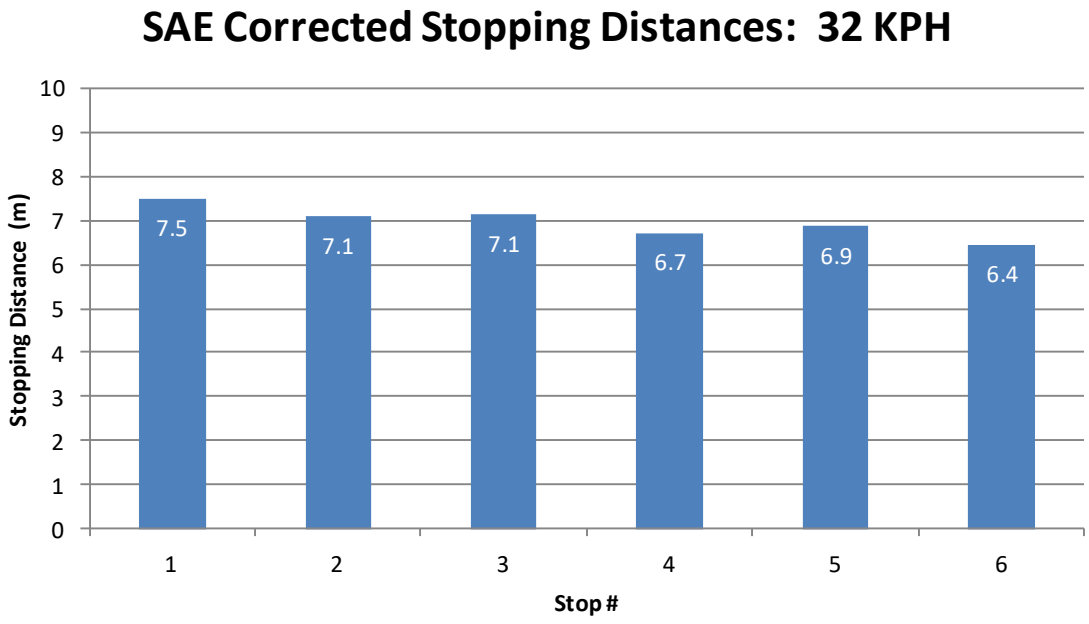

Figure 3.3.1.3-1: SAE corrected stopping distances for 20 MPH tests

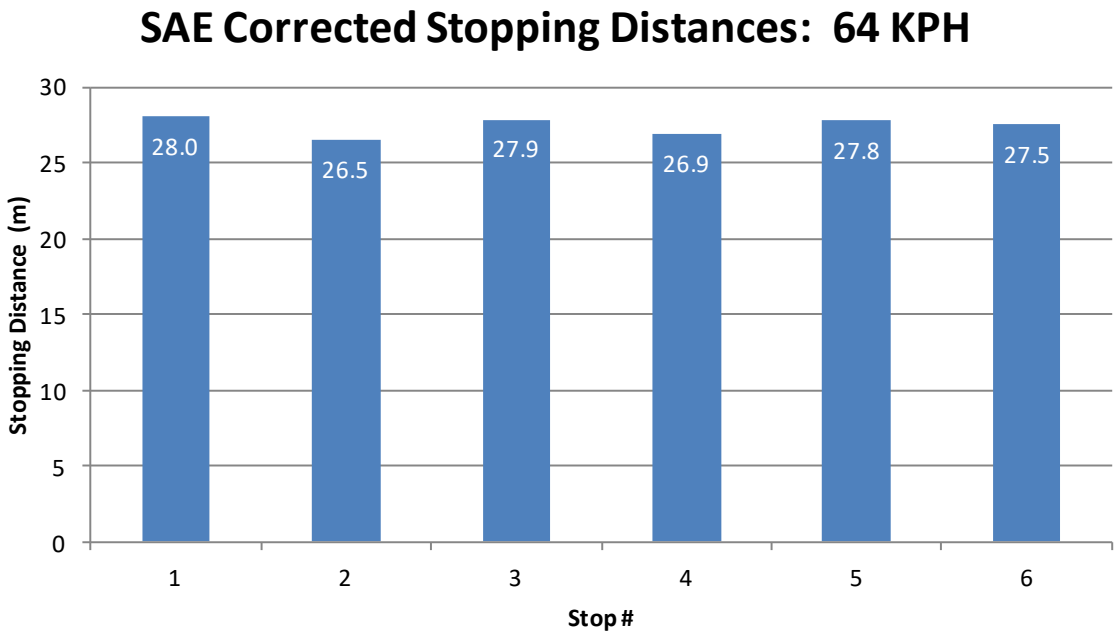

Figure 3.3.1.3-1: SAE corrected stopping distances for 40 MPH tests

3.3.4 Steering and Handling

The goal of these tests was to determine the handling characteristics of the test item during a steady state cornering test and to determine the minimum turning circle diameters of the test item. Testing was done in accordance with TOP 2-2-609 (Steering) and SAE J2181 (Steady State Circular Test Procedures for Trucks and Buses).

Before testing, the vehicle's tires were inflated to 60 psi. To determine the steady-state cornering characteristics, the vehicle was operated at a constant speed around a circular asphalt test track. The vehicle was operated at speeds ranging from 5 MPH to the maximum safely attainable speed.

The minimum wall-to-wall turning diameters were determined by measuring the maximum extent of the radius described by the outermost part of the test vehicle as it makes the tightest turn possible. This test was conducted for both clockwise and counter-clockwise turning.

The average wall-to-wall turning diameters in both clockwise and counter clockwise directions were determined to be about 51 feet. The average turning diameter was calculated from four data sets each. Plots characterizing the vehicles lateral acceleration, wheel angle, roll, yaw at increasing speeds are shown in figures 3.3.1.4-1 through 3.3.1.4-5.

Clockwise			Counter-clockwise		
Measurement	Diameter (ft, in)	Diameter (ft)	Measurement	Diameter (ft, in)	Diameter (ft)
1	50 ft, 11 in	50.9	1	51 ft, 0 in	51.0
2	51 ft, 1 in	51.1	2	50 ft, 10.5 in	50.9
3	51 ft, 1.5 in	51.1	3	50 ft, 7 in	50.6
4	51 ft, 1 in	51.1	4	50 ft, 8 in	50.7
	Avg:	51.1		Avg:	50.8

Table 3.3.1.4-1: Clockwise and counter-clockwise turning diameter data

Front Axle			
Steering Wheel Angle (deg)	Left Wheel Angle (deg)	Right Wheel Angle (deg)	Average Wheel Angle (deg)
0	0	0	0
90	5	5	5
180	10	10	10
270	15	15	15
360	19	20	19.5
450	23	25	24
540	27.5	30	28.75
-90	-4.5	-5	-4.75
-180	-10	-10	-10
-270	-14.5	-14	-14.25
-360	-19	-18	-18.5
-450	-25	-23	-24
-540	-30	-29	-29.5

Table 3.3.1.4-2: Data from turn plates and SW angle sensor

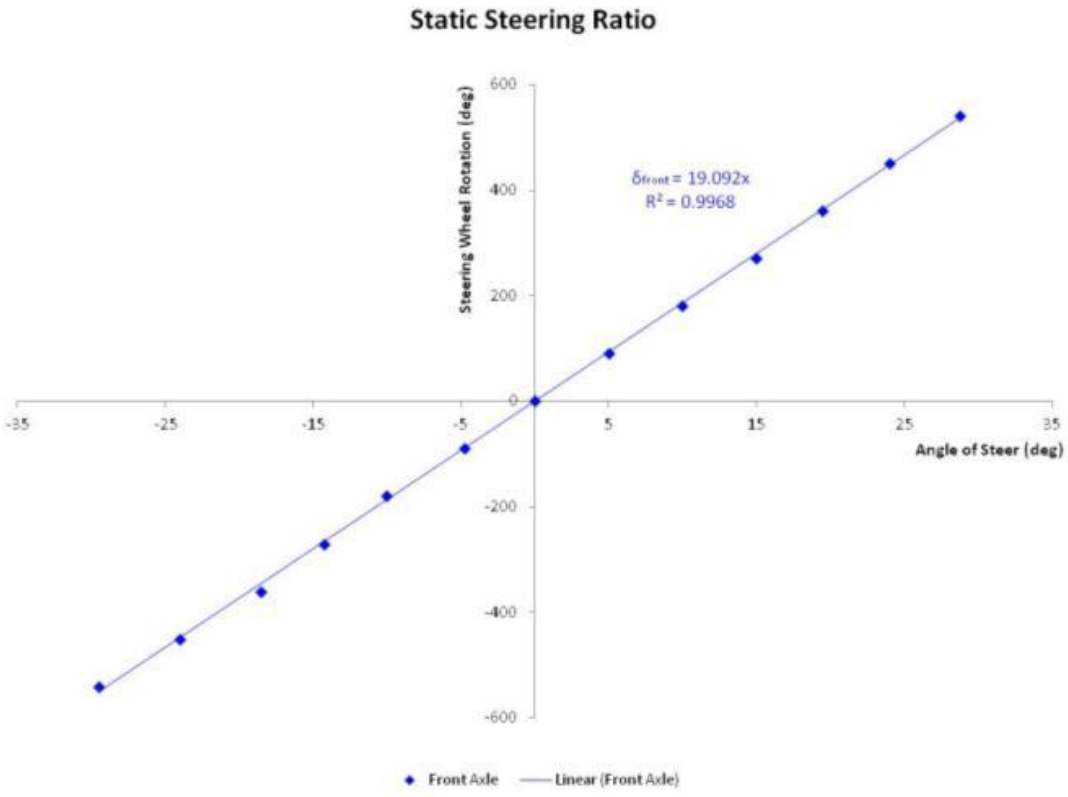

Figure 3.3.1.4-1: Static steering ratio

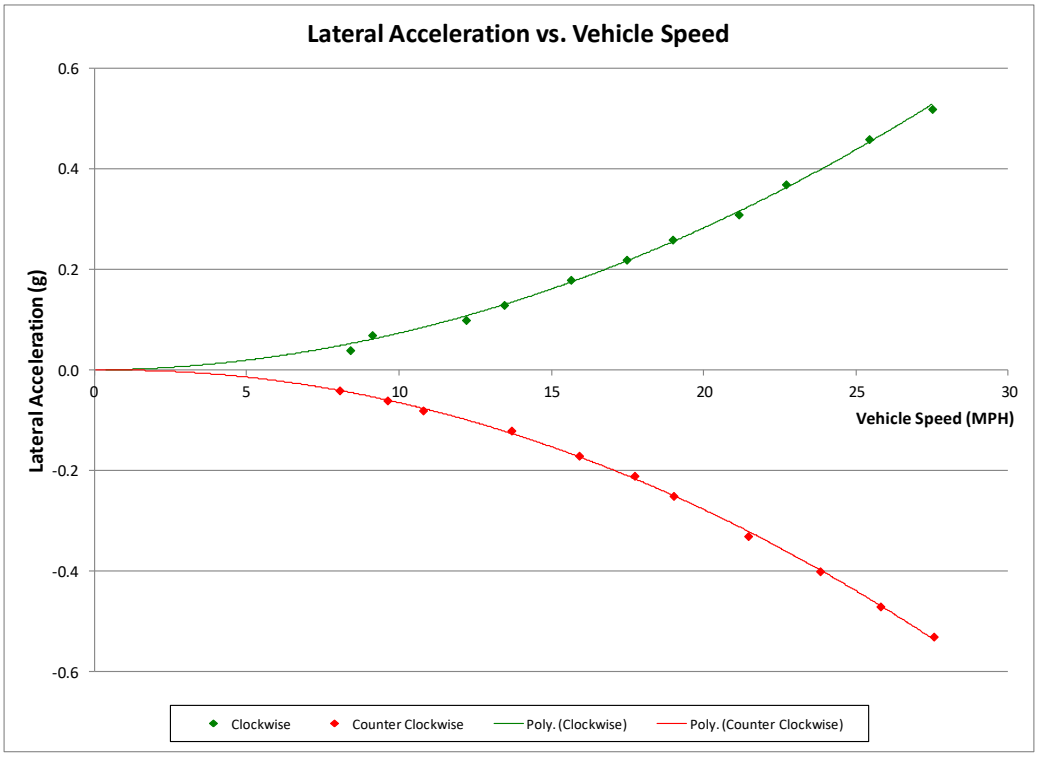

Figure 3.3.1.4-2: Relationship between lateral acceleration and speed of vehicle for steady-state turning

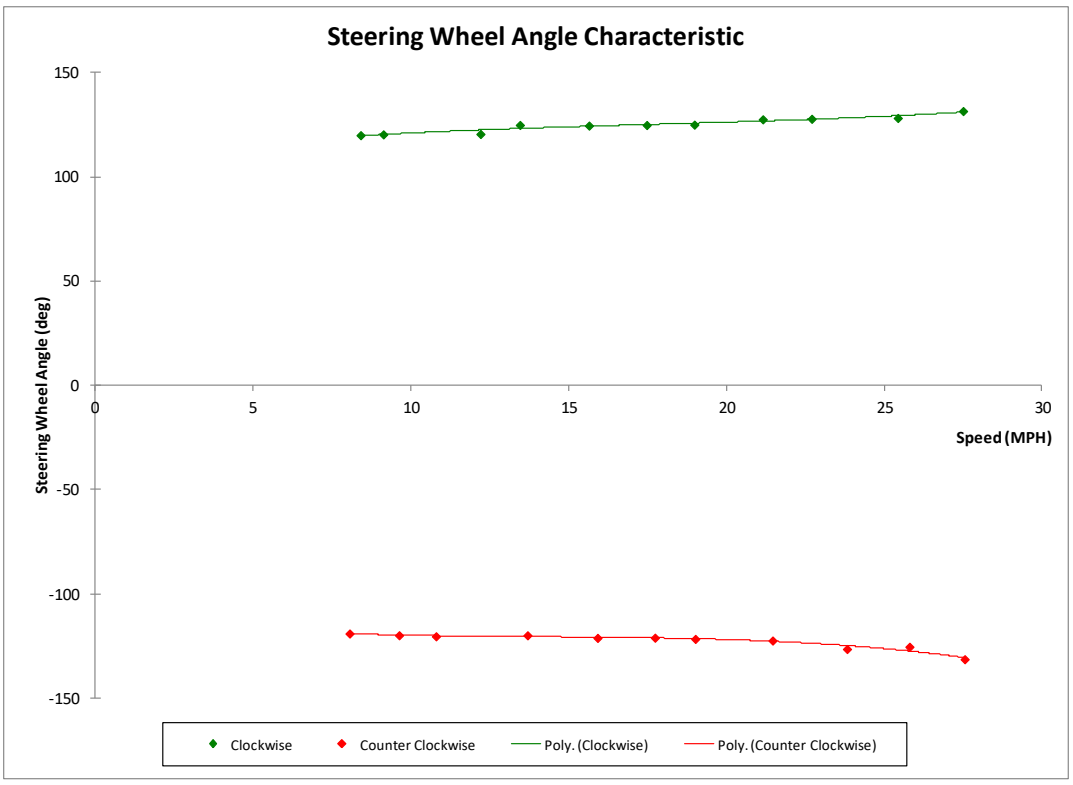

Figure 3.3.1.4-3: Relationship between steering wheel angle and speed of vehicle for steady-state turning

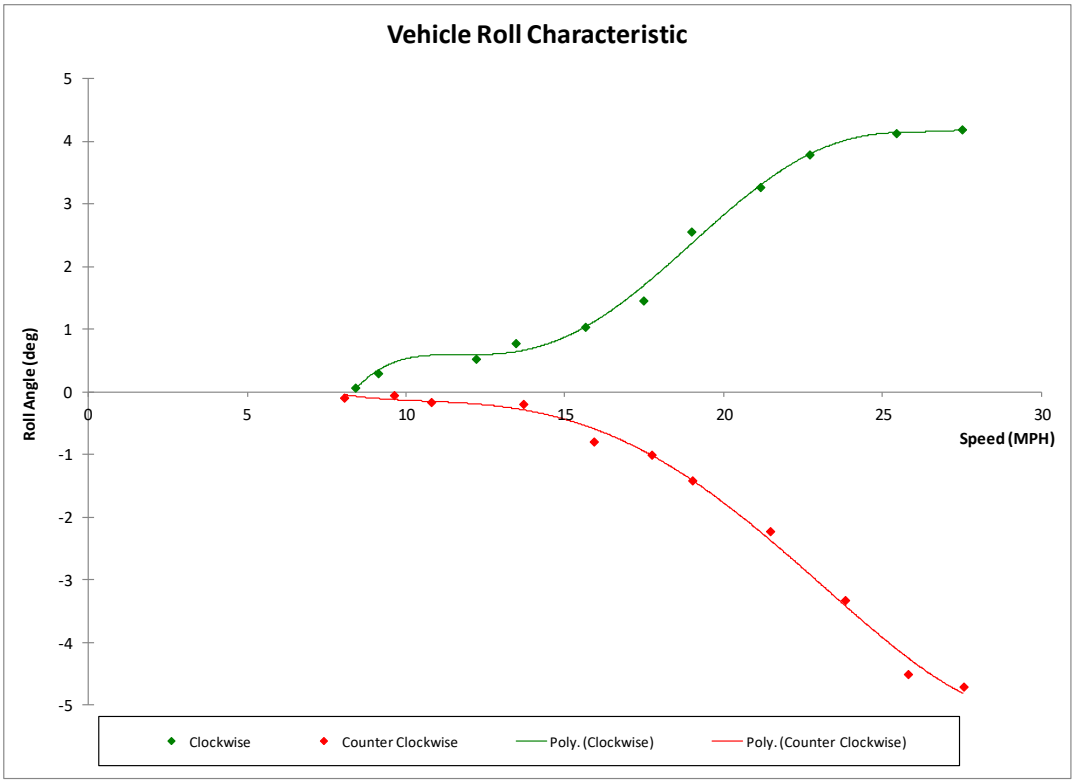

Figure 3.3.1.4-4: Relationship between roll angle and speed of vehicle for steady-state turning

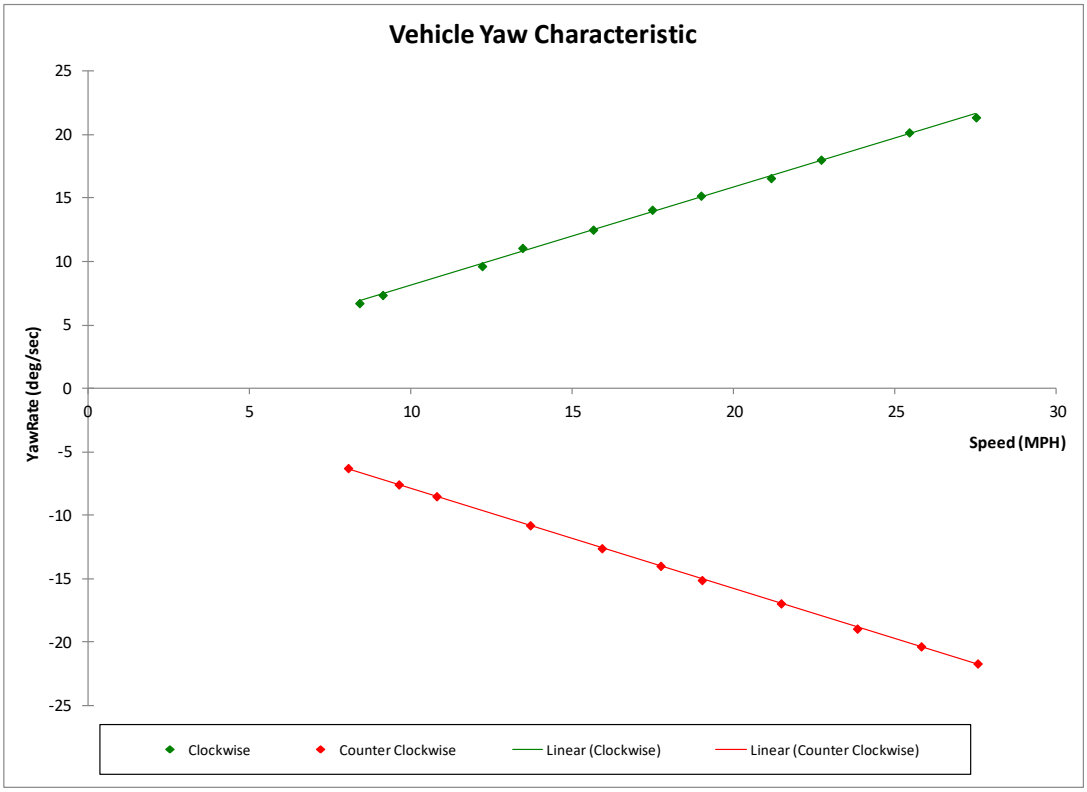

Figure 3.3.1.4-5: Relationship between yaw rate and speed of vehicle for steady-state turning

3.3.5 Gradeablility and Side Slope

The goal of this test was to determine the operating characteristics of the test item on longitudinal grades and side slopes and to evaluate the test item's service and parking brakes on the longitudinal grades and side slopes. The gradeability and side slope tests were conducted in accordance with IAW TOP 2-2-610 (Gradeability and Side Slope Performance).

To test the gradeability of the vehicle, the vehicle was maneuvered onto a 60% paved longitudinal grade. Once fully on the grade, the vehicle was stopped, the brakes applied, and the engine shut down to test the braking ability. When the braking test was done, the vehicle was started and attempted to climb the remained of the grade. The test was repeated with the vehicle moving backwards. This test and subtests were pass-fail, and the results are given in table 3.3.1.5-1.

To test the side-slope performance, the vehicle attempted to navigate a 30% side slope grade and to avoid a3 meter wide obstacle on the side-slope. Testing was repeated multiple times with both the left and right side of the vehicle facing up the slope. The results of the test are given in table 3.3.1.5-2.

Grade -%	Orientation	Climbing Ability	Descending Ability	Brake Holding Ability
60	Forward	Satisfactory	Satisfactory	Satisfactory
	Reverse	Satisfactory	Satisfactory	Satisfactory

Table 3.3.1.5-1: Longitudinal grade performance, FED-A at VCW.

Grade-%	Upslope Orientation	Obstacle Avoidance
30	Left Side	Satisfactory
	Right Side	Satisfactory

Table 3.3.1.5-2: Side slope performance, FED-A at VCW.

Figure 3.3.1.5-1: FED-A climbing 60% vertical paved longitudinal grade.

Figure 3.3.1.5-2: FED-A navigating side slope

3.3.6 Ride Quality

3.3.6.1 Half Rounds

The goal of this test was to determine the suspension capability of the test item while negotiating half-rounds and determine the speed of the vehicle that generates 2.5 g peak acceleration at the driver's seat. Testing was done in accordance with IAW TOP 1-1-014 (Ride Dynamics).

To test the vehicle on the half-rounds, the vehicle's tire pressure was adjusted to 35 psi. The vehicle was then driven over 4 inch, 8 inch, 10 inch, and 12 inch half rounds at increasing speeds until the vertical acceleration of the driver's seat exceeds 2.5 g's. The relationship between peak acceleration at the driver's seat for all half-round sizes and speeds is shown in figure 3.3.2.2-1. The interpolated speeds using a polynomial fit line at which 2.5 g's is reached is shown in figure 3.3.2.2.-2.

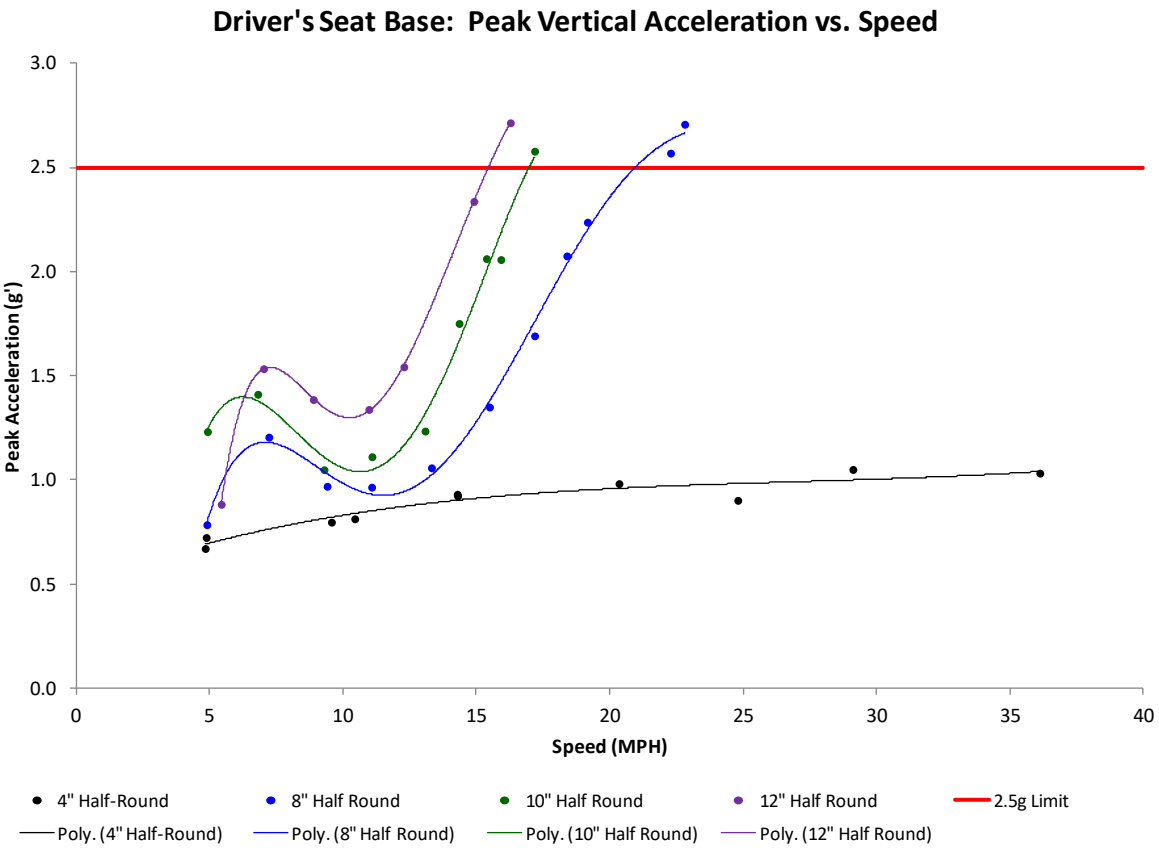

Figure 3.3.2.2-1: Relationship between peak acceleration and vehicle speed with 2.5 g limit line

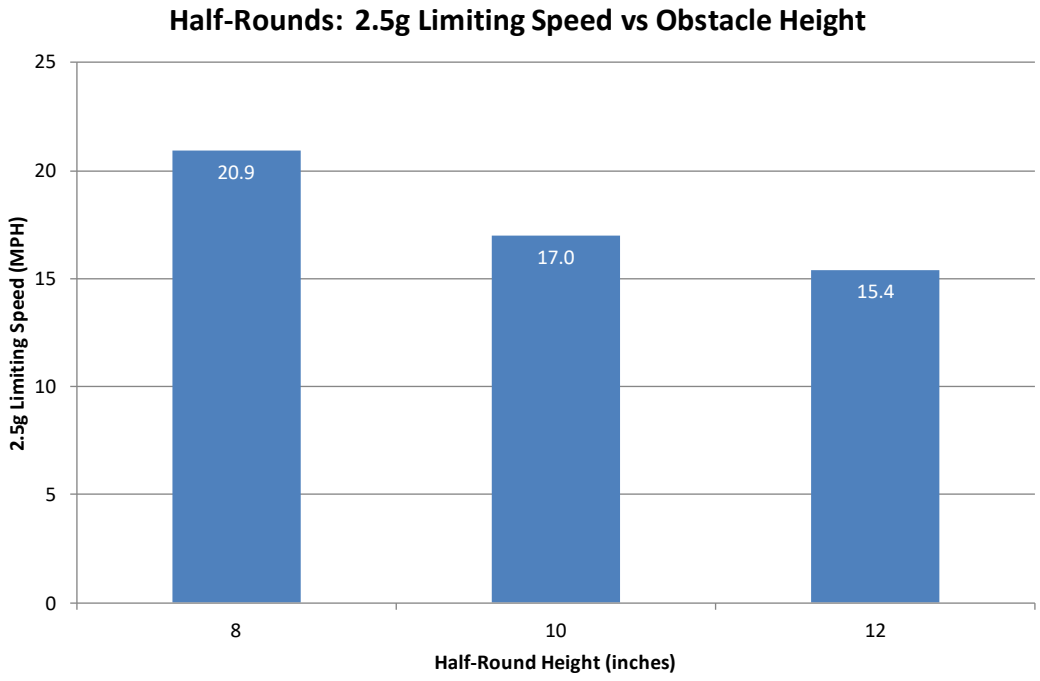

Figure 3.3.2.1-2: Interpolated limited speed for tall half-rounds

Figure 3.3.2.1-3: Tire deformation over half-round (High Speed Video of All Runs Is Available)

3.3.6.2 RMS Courses

The goal of this test was to determine the suspension capability of the test item while driving in undulating terrain and to determine the speed of the vehicle that generates 6W absorbed power at the driver's seat. RMS testing was done in accordance with IAW TOP 1-1-014 (Ride Dynamics).

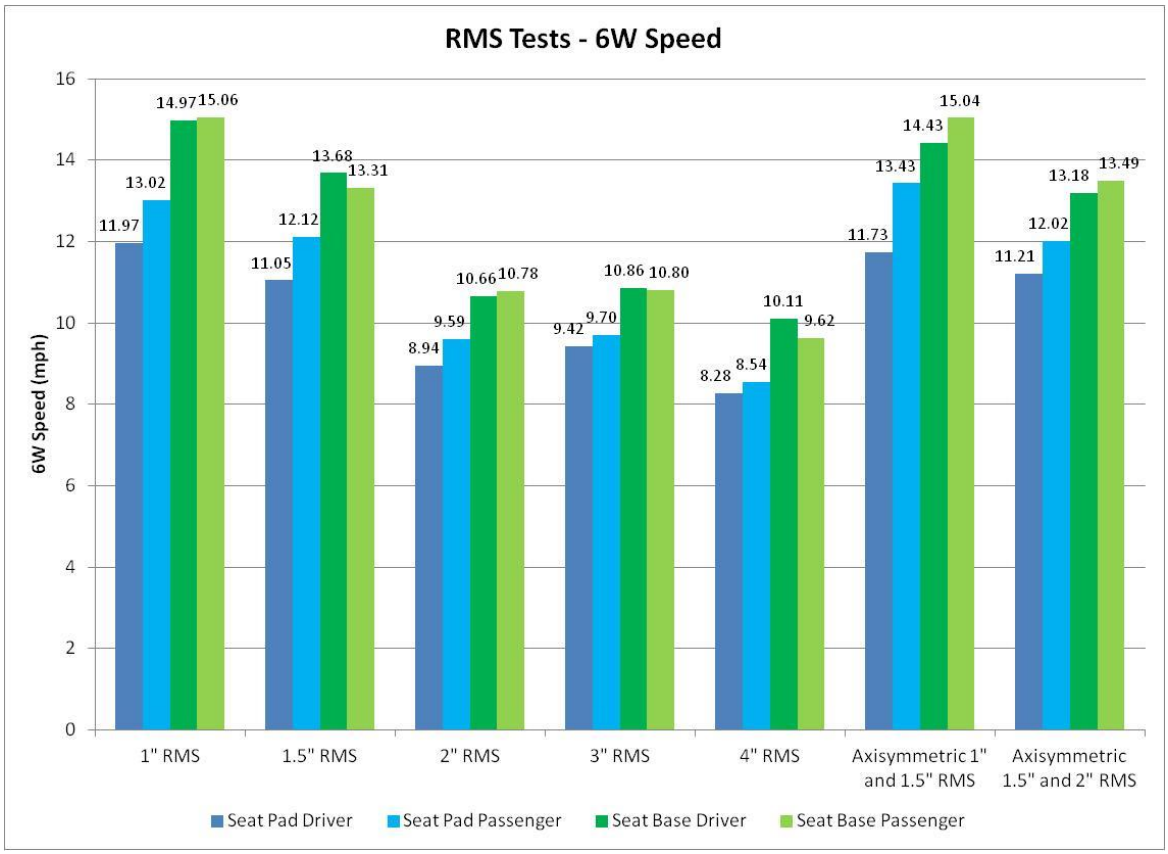

Figure 3.3.2.2-1: 6W speeds for each RMS course

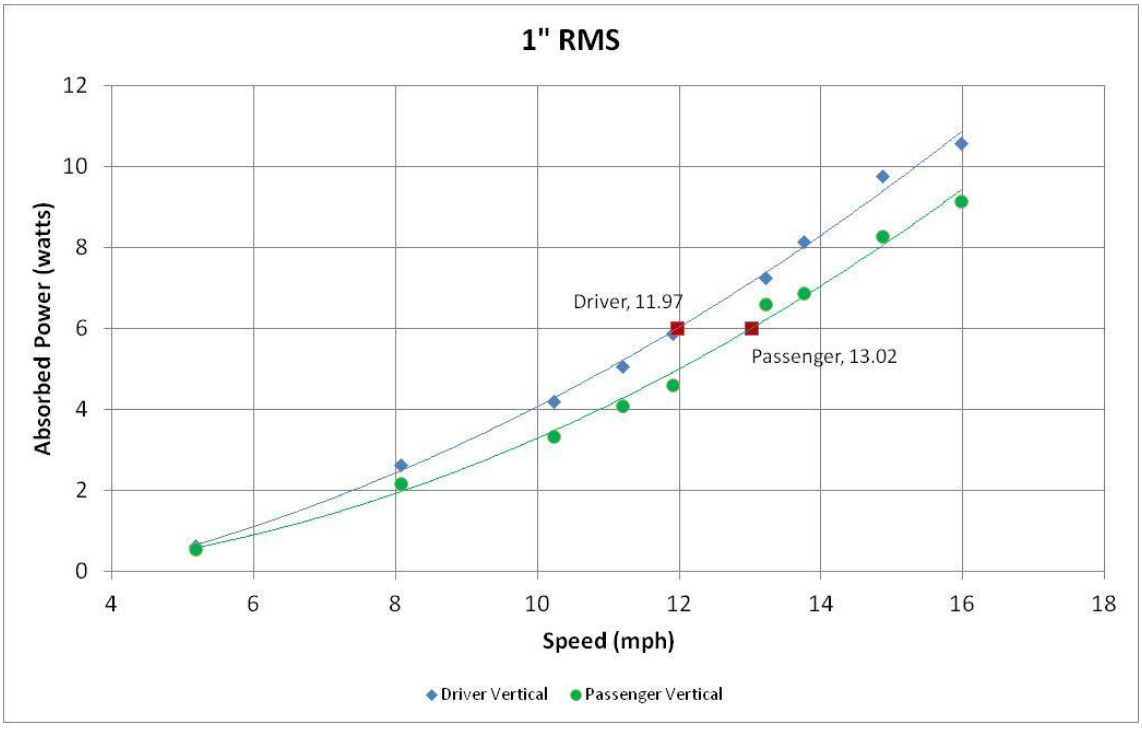

Figure 3.3.2.2-2: Representative plot of absorbed power at speeds with polynomial fit

3.3.7 Standard Obstacles

3.3.3.1 V-Ditch

The goal of this test was to determine the ability of the test item to negotiate V-ditch obstacles. TOP 2-2-611 (Standard Obstacles) was used as a general guide for testing.

The vehicle's tires were inflated to 35 psi, and the vehicle attempted to drive through a 35% V-ditch with a 25.5 foot span. Any contact of any part of the vehicle other than the tires with the V-ditch was noted. The test vehicle successfully navigated a 35% V-ditch with a 25.5 foot span.

Figure 3.3.3.1-1: Vehicle crossing a 35% V-ditch with 25.5 foot span

3.3.3.2 Vertical Steps

The goal of this test was to determine if the vehicle can negotiate vertical obstacles. TOP 2-2-611 (Standard Obstacles) was used as a general guide for testing.

To test vehicle handling over vertical steps, the vehicle's tire pressure was inflated to 35 psi. The vehicle's vehicles wheels were placed against a 12 inch vertical step, and vehicle was accelerated forward. If the vehicle successfully climbed the 12 inch step, testing was repeated with an 18 inch step. If successful, a final test with a 24 inch step was attempted. The vehicle climbed the 12 inch step, but failed to climb the 18 inch step.

Figure 3.3.3.2-1: Vehicle climbing 12 inch step

3.4 Trafficability

3.4.1 Soft Soil Gradability

The tire pressure was adjusted to 35 psi for the soft soil grade. The vehicle's differentials were in the locked setting and the gear box was set in low range. All gradeability and side slope testing were performed with fuel tank and lubricating oils at their respective full levels. All BII will be properly stored in their designated location.

The test item was evaluated on a variable-slope (0 to 30%) longitudinal sand grade by making a running approach to the designated grade at a predetermined speed of 5 mph. Once on the grade, throttle is applied and held to maintain a constant 5 mph speed until the vehicle ascends the grade or the tractive limit is reached. Testing will be repeated with the test item backing up the longitudinal grade.

Figure 3.4.1-1: Vehicle climbing Variable Grade Sand Slope

The test runs were conducted in both forward and reverse and were stopped once vehicle motion had essentially stopped. Figure 3.4.1.-2 shows the percent wheel slip verse vehicle pitch angle for forward motion on the grade.

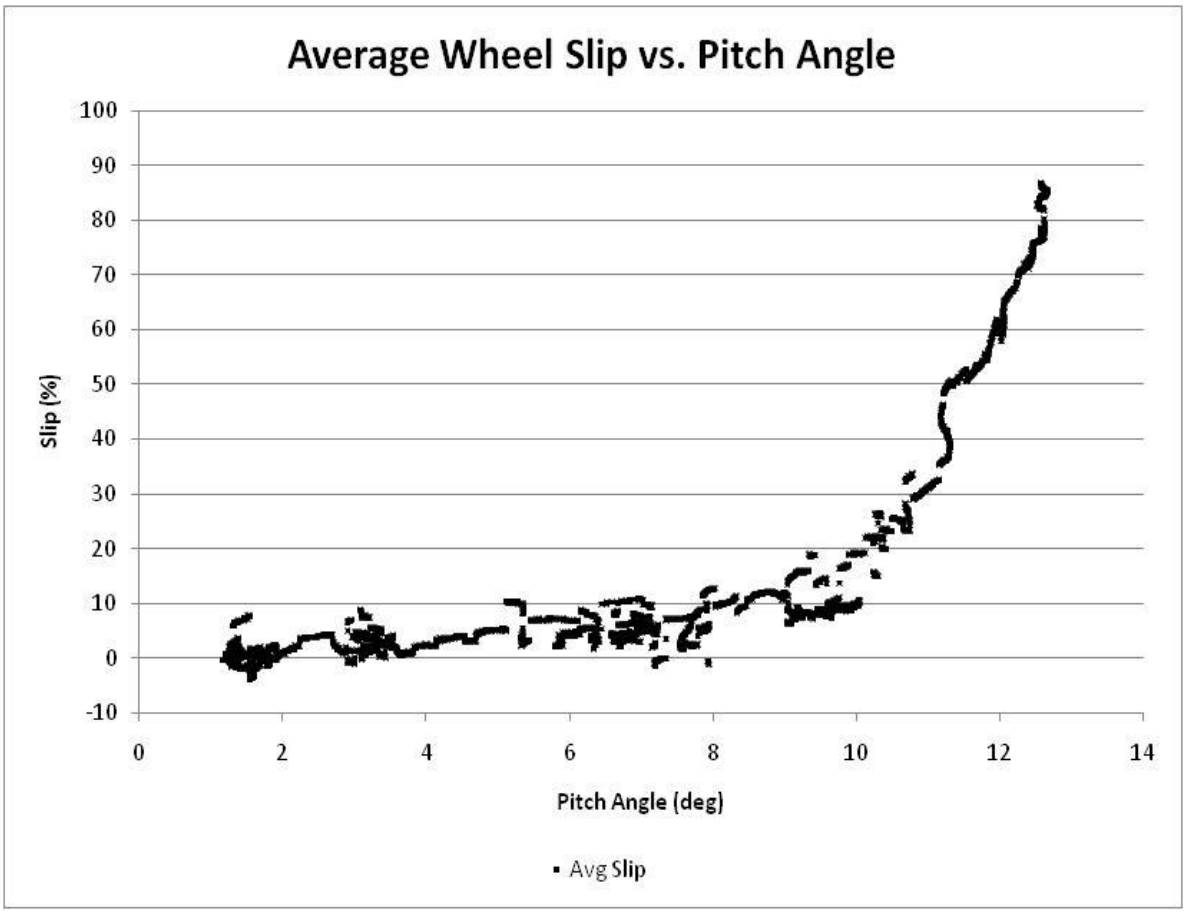

Figure 3.4.1-2 Average Wheel Slip vs. Vehicle Pitch Angel in Forward Direction on Sand Grade

Since the vehicle pitch is not a true measure of the actual grade attained, a terrestrial scan of the surface with the ruts created during the test runs was collected. The resulting point cloud was used to determine the grade of the undisturbed soil at the leading edge of the uphill tires for both the forward and reverse runs. Table 3.4.1-1 provides this derivation of the max grade attained. Figure 3.4.1-3 shows the point cloud on the grade with ruts and grade extraction lines.

Point Number	X (ft)	Y (ft)	Z (ft	Slope
FWD_GRADE1	105.08280	-22.14285	10.50176	18.5%
FWD_GRADE2	105.72176	-22.07695	10.61983	
REV_GRADE1	147.04204	-15.24309	20.13514	29.0%
REV_GRADE2	148.27748	-15.15287	20.49294	

Table 3.4.1-1 Sand Grade Derivation Data

Figure 3.4.1-3: Terrestrial LIDAR Scan of the Wheel Ruts Made During Sand Slope Testing

3.4.2 Draw Bar Pulls

The goal of this test was to determine the maximum tractive effort of the test item, and response of the system (drawbar pull vs. slip), for both coarse-grained sand and fine-grained soils. Testing was conducted using TOP 2-2-604, Drawbar Pull, as a guideline.

Prior to the start of testing a surface conditioning procedure was developed to establish the necessary steps to maintain consistent surfaces during testing. This procedure was utilized throughout draw bar testing as needed to insure a consistent surface. Tests were conducted on both coarse-grained sand and fine-grained soil surfaces. Fine grain soil tests were conducted under two moisture conditions: dry and wet. Soil characterizations (Bevameter, cone penetrometer, etc) were conducted on all test soils at the time of drawbar testing.

The FED-A tire pressure was adjusted to 35 psi and its differentials were in the locked setting for all drawbar pulls and the gear box was set in low range. The rolling distance of a single wheel revolution was computed from operation with the 35 psi tire pressure with zero slip. This distance was used for analyzing drawbar pull data to determine slip percentages from wheel speeds and vehicle speed over ground.

Drawbar pulls were conducted using both pull-to-stall and steady-state operating conditions. A description of each test procedure is as follows:

1) Pull-to-Stall Procedure

   The test vehicle proceeds (in the forward direction) towing the load vehicle at 5mph while approaching the test soil. The driver of the test vehicle modulates throttle input (up to 100%) attempting to maintain 5mph constant speed throughout the test. Once the test vehicle is completely within the test soil, the service brakes of the load vehicle are progressively applied until the test vehicle reaches 100% slip and forward progress is stalled. The test vehicle is slowed from 5mph to a complete stop in approximately 5 seconds. A minimum of three runs are made to demonstrate testing variation.

2) Steady-State Procedure

A load vehicle has its transmission placed in a specific gear range to provide resistance when it is towed by the test vehicle. The test vehicle proceeds (in the forward direction) towing the load vehicle at a constant 5mph through the entire length of the test soil. Due to the steady-state nature of the test, this procedure generates relatively constant speed, load and slip for greater than 30 seconds. The test is repeated using additional transmission ranges on the load vehicle to exercise new load and slip ranges. Five tests (with different gear ranges on the load vehicle) are run to cover a reasonable range of load and slips on the test vehicle.

Drawbar test data is presented plotting drawbar force (% of Vehicle GVW) versus average wheel slip (%). For the pull-to-stall procedure, a significant portion of the force measured by the drawbar load cell is generated to decelerate the mass of the vehicle from 5mph to stall. Using the mass and the deceleration profile of the vehicle, the drawbar force is corrected by subtracting this contribution. The same correction method is applicable to the steady-state procedure, though the effects are arguably negligible due to the inherently small variations in vehicle speed.

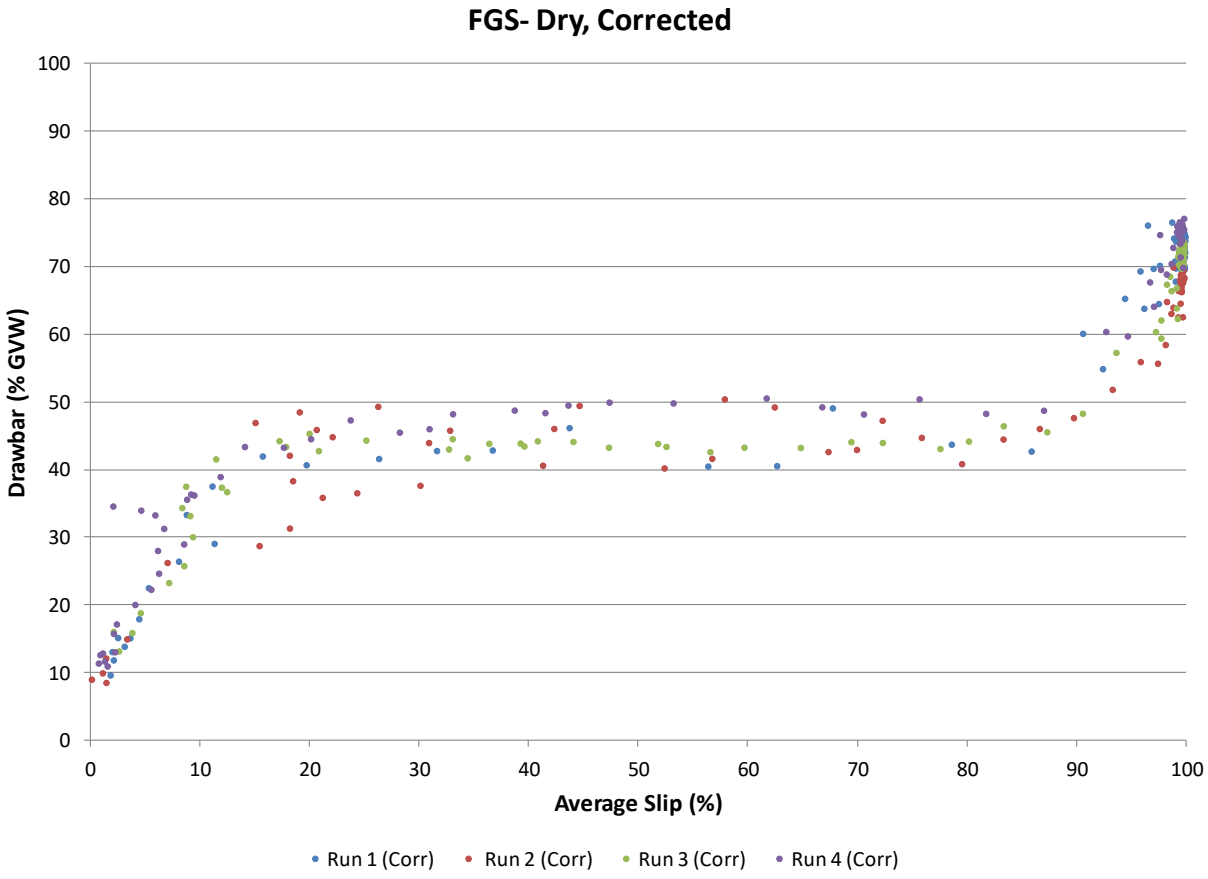

Figure 3.4.2-1 Corrected Drawbar Pull Results, Fine Grain Soil (Dry), Pull-to-Stall Procedure

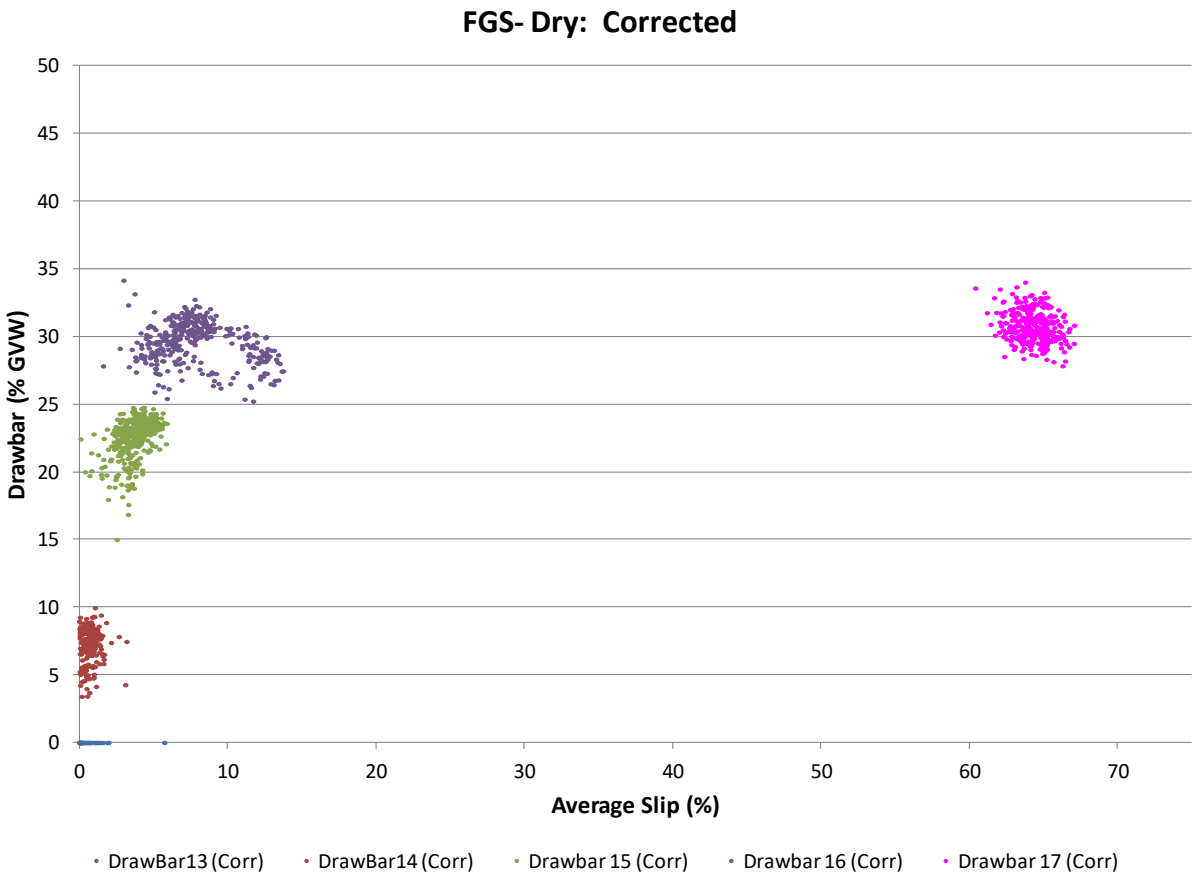

Figure 3.4.2-2 Corrected Drawbar Pull Results, Fine Grain Soil (Dry), Steady-State Procedure

3.5 Mobility Traverses

The goal of these tests was to obtain vehicle behavior information during a continuous traverse over composite terrain representative of a typical Mission Profile (MP) and to determine the capability of the test article to function properly over MP Representative Terrain without inhibiting operation.

Figure 3.5-1 provides an aerial image of the KRC test course and a plausible speed made good map of the same area. The issue that faced the effort to provide a verification between the physical testing and the virtual prediction of speed made good was the shear number of test that would have to be run to identify the maximum speed possible at any given terrain unit. Understand that a terrain unit size is highly dependent upon the terrain at any given location. The size is primarily the area in which all mobility input value are equal. In other words, a terrain unit is an area that would provide the same mobility prediction anywhere within that area. The size of a terrain unit for legacy NRMM is considerably larger than the vehicle but for the physics based models in NG-NRMM terrain units are conceivably the size of the vehicle terrain interaction area (i.e. tire patch) To physical determine the maximum speed possible for a given terrain unit, regardless of size, the vehicle would need to be run in every direction several times. The resulting damage to the terrain and the time required to collect the data makes physical determination of the speed made good map very difficult.

To address the issue of comparing the virtual predictions, the idea of conducting a continuous traverse at the maximum capacity of the vehicle and comparing the speeds attained to the speeds predicted.

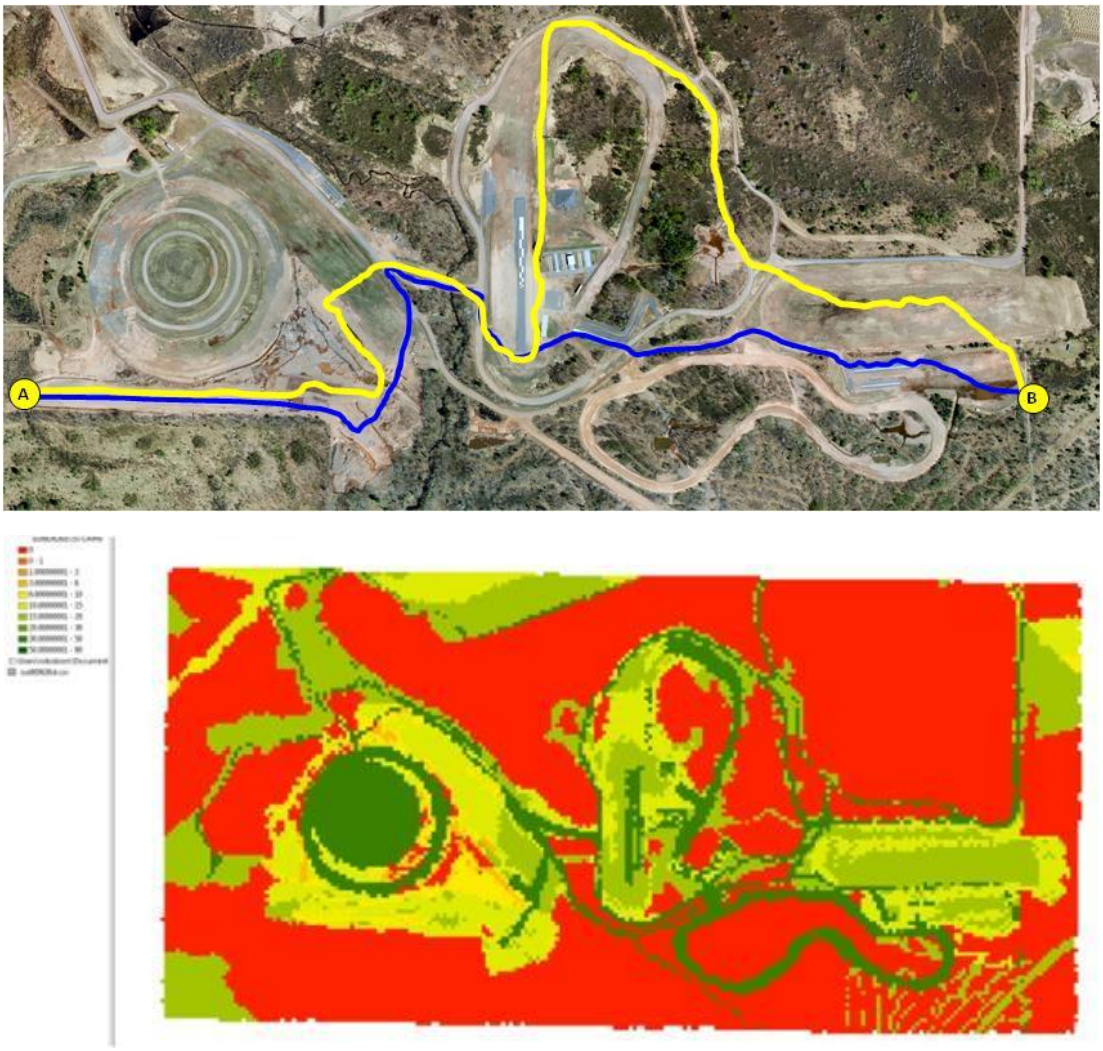

Figure 3.5-1 KRC Test Area with Example of a Speed Made Good Map for the Same Area

Two (2) mobility traverses comprised of engineered courses, natural terrain, and improved gravel roads were identified and well marked for driver visibility. Shown in Figure 3.5-2, the traverses intertwined so there was some terrain common to more than one traverse. With the exception of pavement, traverse composition was selected to contain a combination of terrain types that are representative of a typical mission profile (MP).

The composition of each traverse was selected with the thought that they would be completed as a continuous maneuver, not stopping unless the tractive limit of the vehicle is reached. With the exception of stopping at specified locations to change gear range and differential settings, each traverse was completed as a continuous maneuver. This continuous execution is much more representative of a real life event and is intended to augment the singular nature of the data collected for the individual performance evaluations. If the vehicle is unable to complete a portion of a traverse, it was extracted, examined for discrepancies, and if capable of continuing, repositioned to allow completion of the traverse.

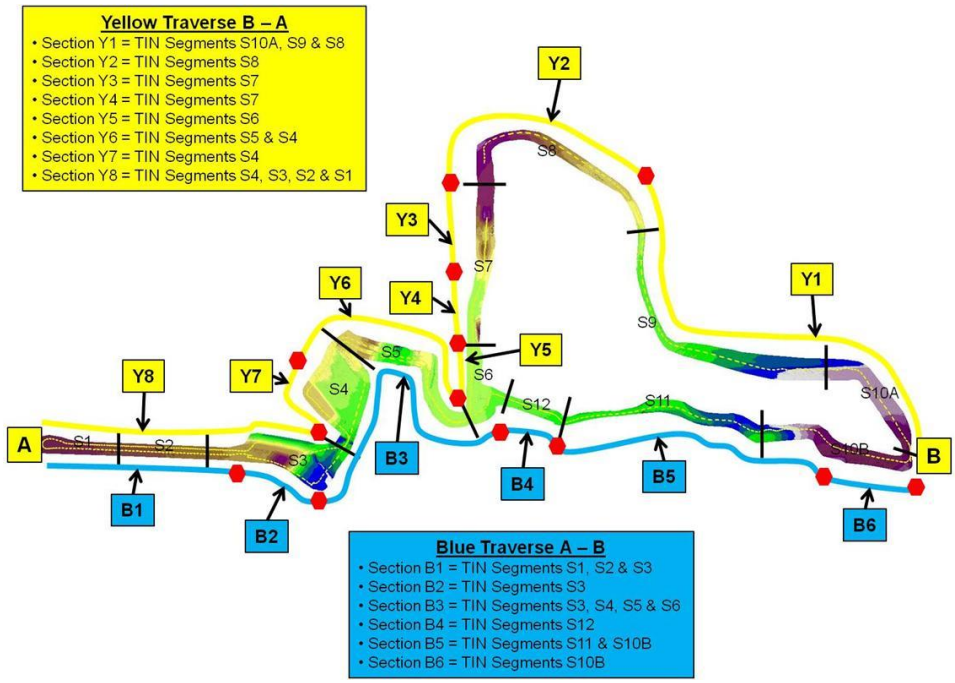

Figure 3.5-2 Mobility Traverses Used in the CDT with Corresponding Section Identifiers

A few portions utilized courses that were previously evaluated as a standalone maneuver that followed a standard test procedure. These courses were altered to highlight a specific maneuver of interest not typically performed during a standard performance test. For example, the driver conducted obstacle avoidance on side slope, executed a tight turn and a sinusoidal maneuver through the soft soil pits. These high fidelity maneuvers were well laid out and the driver was duly informed of the intended traverse prior to executing jury trials.

No portions of either traverse proved impassable for the vehicle.

Speed throughout a traverse was not constant. The vehicle slowed to negotiate certain portions of each traverse. Some portions allowed high speed transit. For the most part, vehicle speed and transition between terrain segments was at the discretion of the driver. The driver was well informed of each traverse and methodology established during a jury ride procedure performed prior to actual testing. Safety for personnel and the vehicle was paramount. The general objective was to safely complete each traverse in as short a time as possible but be safe.

Prior to the start of testing, a surface conditioning procedure was developed to establish the necessary steps to maintain a consistent surface throughout testing.

All data channels were recorded for each of 3 runs for both traverses but vehicle speed was used for comparison to the virtual predictions. Figure 5.3-3 provides an example of the speed consistency attained for section Y8.

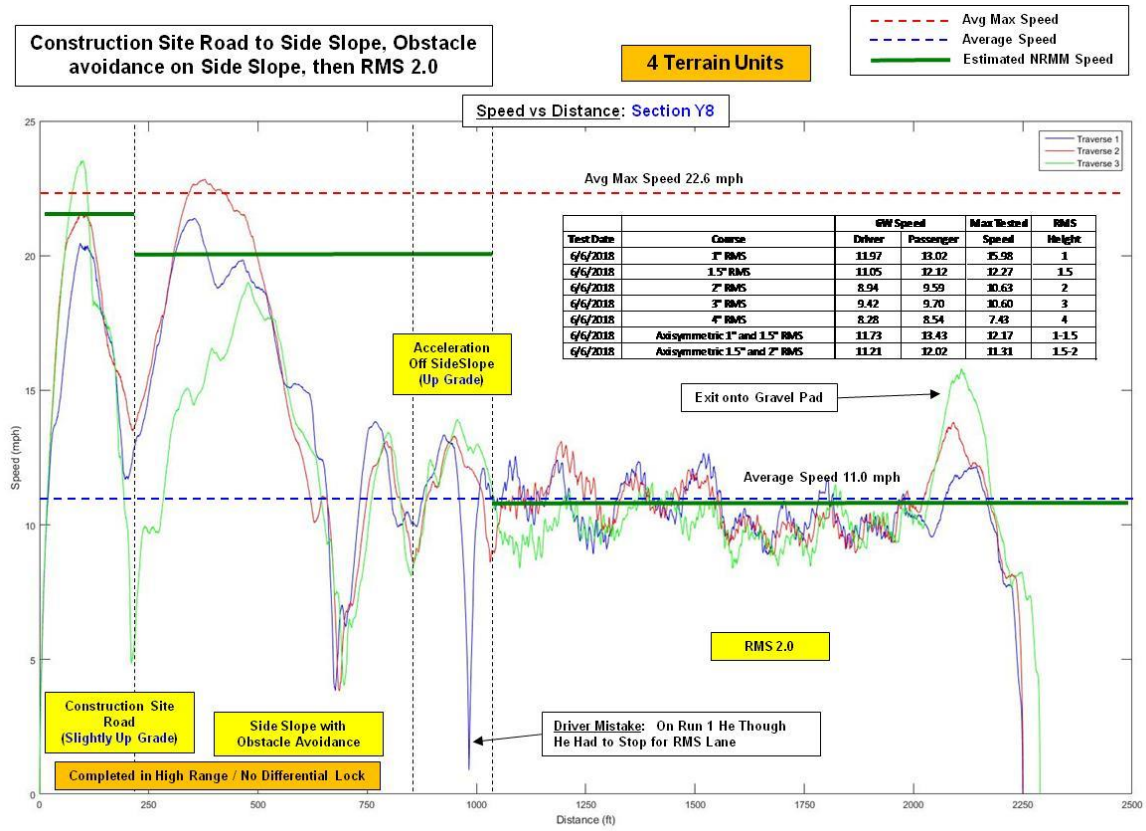

Figure 5.3-3 Speed Results for each Test Run over Section Y8

Chapter 4 CDT Event

The Cooperative Demonstration of Technology (CDT) was an event held over three days at the MTU/KRC test facility (figure 4). A total of 161 persons representing 14 different nations registered to attend the CDT. The goal of the CDT was to be a critical peer review of the Next Generation NATO Reference Mobility Model (NG-NRMM), a product of the NG-NRMM AVT-248 and AVT-308 committee's multiple years of work dedicated to the task as well as a showcase of the physical testing methods involved in collecting data for the project.

Figure 4-1. NATO CDT event in Houghton, MI, USA.

The presentations given to familiarize the attendees with the NG-NRMM and its capabilities were:

1. History, Motivation, and Goals for NG-NRMM

2. NATO Task Group and CDT Objective

3. NG-NRMM Virtual and Physical Demonstration Plan

4. Thrust 1- Geospatial Terrain and Mobility Mapping

5. Thrust 2 - Simple Terramechanics Model & Data

6. Thrust 3 - Complex Terramechanics Model & Data

7. NG-NRMM Virtual Demonstration

8. Thrust 5 - Uncertainty & Stochastic Mobility Maps

9. Thrust 6 - NG-NRMM Verification and Validation

10. NG-NRMM Standard

11. Thrust 7 - Gaps and Operational Readiness

12. CDT Results and Vision for the Future

The NG-NRMM Virtual Demonstration was an "end-to-end software demo" that showcased how the NG-NRMM adopted new technologies, modeling techniques, and computational tools to provide a superior physics-based simulation of any vehicle design in complex environments, terrain, and scenarios compared to the previous NRMM version. GIS Data inputs, terrain and soil data, terramechanics, mobility event studies, uncertainty quantification, mobility maps, and the latest modeling and simulation technology were integrated together into a set of tools and methodologies used for vehicle mobility prediction that allow for improvements as new data and methods become available in the future. The software developers produced results including charts, graphs, visuals, and other material as updates on the progress of the NG-NRMM software that they shared in the following presentations:

13. MSC - Military Vehicle Simulation with Adams: Mobility and Beyond

14. CSIR - South African Mobility Prediction Software MOBSIM

15. CML - Real-Time Vehicle Simulation using Vortex Studio

16. VSDC - Wheeled Vehicle Mobility Prediction using NWVPM

17. AU - ROAMS, a Fast Running Mobility Simulator Utilizing GeoTIFF Terrain Maps

18. ASA - DIS/A Complex Terramechanics Software Tool for Predicting Vehicle Mobility

All of these presentations were held in a specialized presentation space in an outdoor tent set up by KRC staff that included a 9 x 12 foot main screen in the front and center of the room with five additional 55-inch TV screens mirroring the main screen. Speakers were elevated at the podium with a clear view to a dedicated 55-inch TV used as a video prompter. Audience members were encouraged to participate in the presentations, which resulted in lively discussion. Audience members also took advantage of breaks between presentations and evening programming for networking opportunities.

The tent complex had one other room housing both food and static exhibits of various vehicles. This exhibit room was deliberately sectioned off from the presentation room to keep noise levels down from socializing and networking by attendees during presentations. The static displays included nine vehicles displaying small, medium, and large variants of both wheeled and tracked vehicles and some additional robotic vehicles, including:

- M1 Abrams
- AAV
- M113
- RG 33L Panther
- RG31 Mk5
- FED-A
- 6 wheel skid steer variant of the Lockheed Martin SMSS
- Tracked Howe and Howe Punisher SMET Variant
- Polaris MRZR

Other activities at the CDT were meant to keep attendees active, engaged, and as close as possible to the testing. Activities included two types of ride-alongs, a soil data collection demonstration, driving simulators in the exhibit area, a large driving simulator brought by MSC located in the main KRC building, and two walk-around demonstrations meant to showcase the vehicle testing performed at the KRC test course. These demonstrations highlighted the RMS, Obstacle Avoidance on a Side Slope, Sand Grade, and a 90 Degree Turn in the Fine Grain Soil Pit tests that were used to collect data used in the NG-NRMM model refinement. These four tests were demonstrated twice, once with a wheeled FED-A and once with a tracked M113 A2/A3 Armored Personnel Carrier (figure 5).

Figure 4-2. NATO CDT vehicle/course demonstrations.

Many logistical challenges were met and solved by the KRC staff. Attendees registered through the NATO Science and Technology (STO) website, but event communication was handled through an MTU website. This allowed the KRC staff to update the website with up-to-date information about housing at local hotels, transportation arrangements between those hotels and the KRC facility, flight arrangements, and meal accommodations. Lodging for over 400 people was arranged in local Houghton hotels. The presentation tent was built to accommodate to seat up to 200 people, hold 11 total exhibits, and have space for tables of food to be served. Shuttle services were also necessary to take all attendees out about 1.5 miles into the test course to get to the main event location. A fleet of five twelve-passenger vans ran

continuously throughout the day to carry people to and from demonstration areas and the main event area. Finally, KRC staff provided security to prevent unwanted access into secured KRC areas.

Feedback from participant surveys, particularly from five of the major presenters, revealed a unanimous agreement that the CDT was a success and that the event logistics were well handled by KRC. All events on the agenda, as tight as it was, ran as scheduled and all unforeseen occurrences were well handled and the agenda adjusted accordingly. The demonstrations of technology were greatly appreciated and provided valuable first-hand experience to those who participated, especially to those who had never seen a military vehicle or had not experienced riding in off-road vehicles.

Appendix A
Laboratory Soil Test Results
KRC Soils

Coarse Pit – SP/SM (Poorly Graded Sand/Silty Sand)

Fine Pit – ML (Silt LL<50% Low PL)

Stability – SW/SM (Well Graded Sand/Silty Sand)

Rink Natural – SM (Silty Sand)

2NS – SP (Poorly Graded Sand)

AVT-248 and AVT-308
CDT

June 2018

Sample Locations

The soil variation at KRC as related to AVT -248 and AVT-308 CDT testing was determined to be described my 5 soil variations. Those 5 soil types were tested in the laboratory using a number of standard soil mechanics tests. The overview of those tests is contained in this report. All test results and data are contained separately in a number of file folders broken down by test type. The following map shows the sampling location of these soils. The overall terrain data set for AVT-248 and AVT-308 contains a further breakdown of where these 5 soils are present within the operational window of CDT testing.

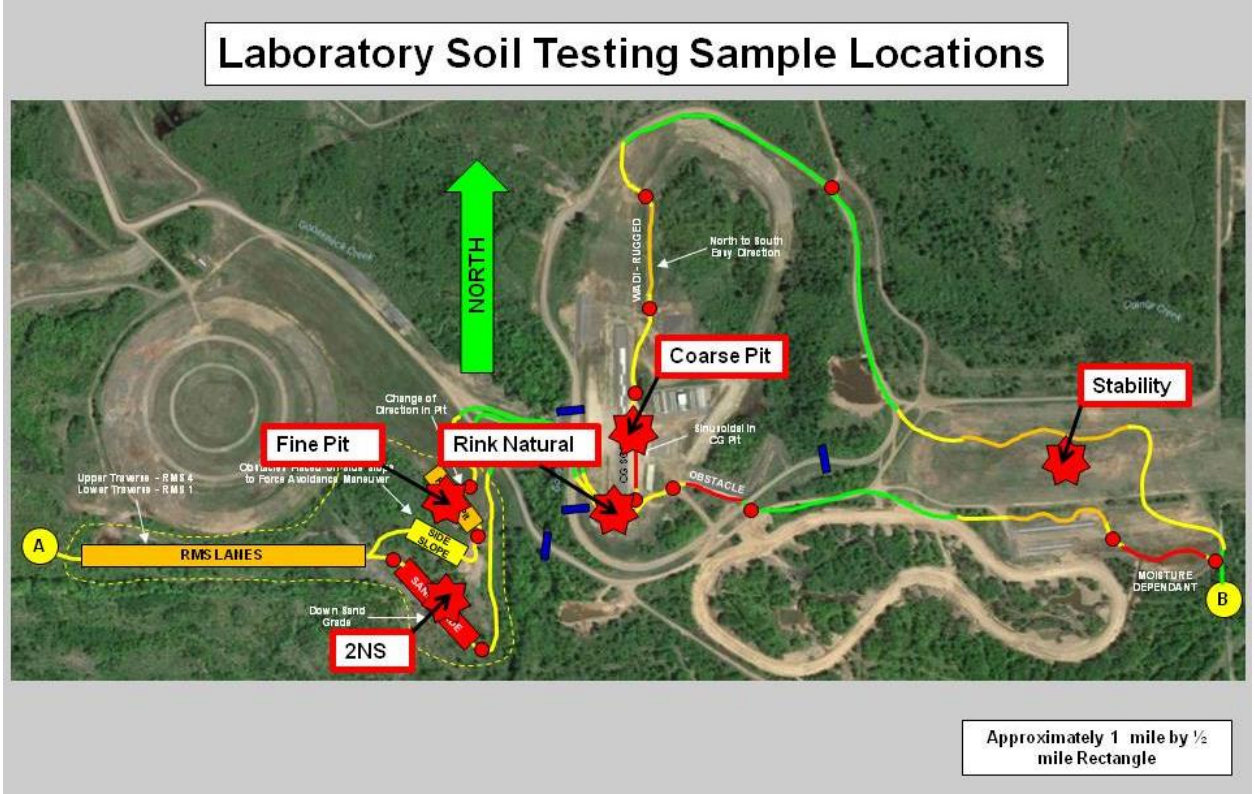

Coarse Pit

Visual – ASTM D2488

Brown-gray, Medium sand with some fines.

Moisture Content at Time of Sample Collection – ASTM D2216

3.7%

Grain Size Analysis: Sieve – ASTM D6913 & Hydrometer - ASTM D7928

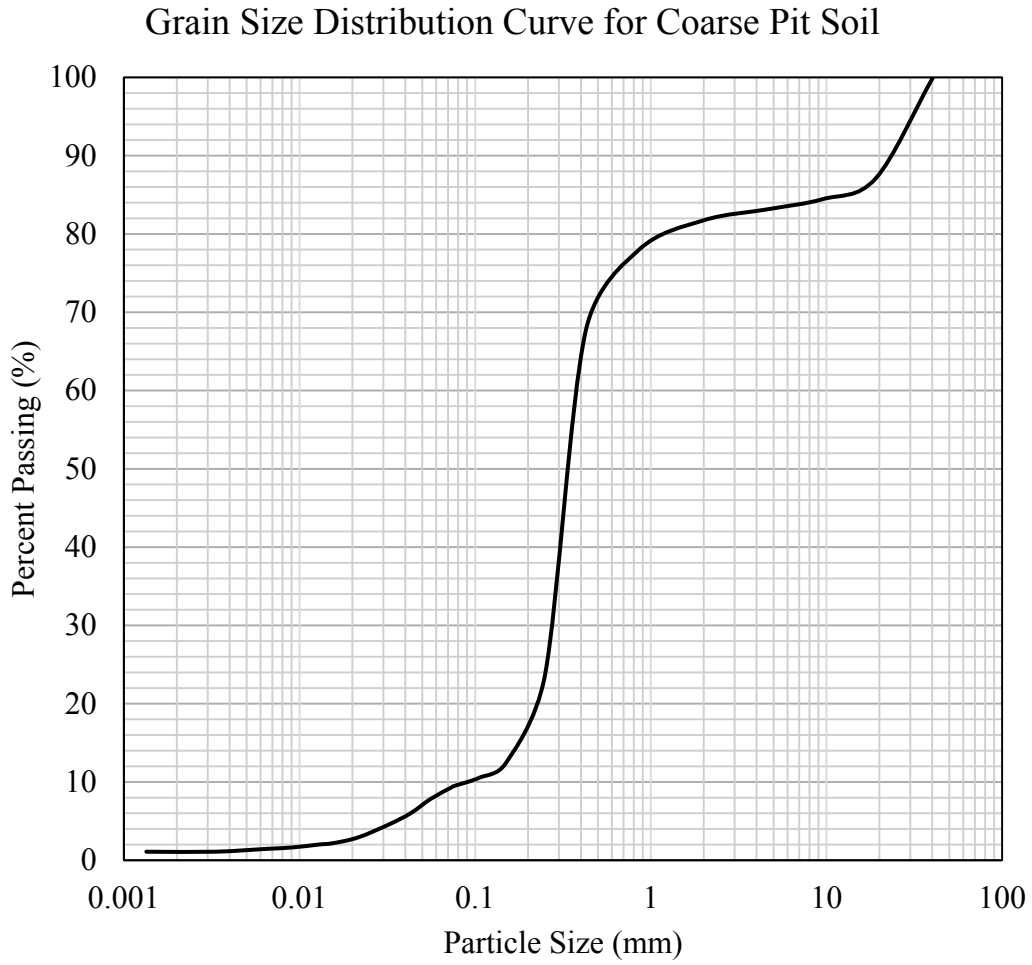

Atterberg Limits – ASTM D4318

NP

ASTM USCS Classification

D10	D30	D60	Cu	Cc	w% Gravel	w% Sand	W% Fine	USCS
0.085	0.27	0.38	4.5	2.3	16.8073	73.73772	9.454973	**Sp-SM** Poorly Graded Sand With Silt and Gravel

Specific Gravity – ASTM D854 and Relative Density ASTM D4254 and D4253

Specific Gravity-Water Displacement method (ASTM D854)				
Weight of dry soil (g)	Weight of bottle+water (g)	Weight of bottle+water+soil (g)	Gs (water)	Specific Gravity
160.4	670.8	770.5	0.99	2.62

Maximum Void ratio (Minimum density/loose state) ASTM D4254					
Weight of Mold (g)	Weight of Mold + Soli (g)	Weight of Soli (g)	Density kg/m^3	Density of Particles (kg/m^3)	e
4221.6	5698.3	1476.7	1564.47	2616	0.67

Minimum Void ratio (Maximum density/Dense state) ASTM D4253					
Weight of Mold (g)	Weight of Mold + Soli (g)	Weight of Soli (g)	Density kg/m^3	Density of Particles (kg/m^3)	e
4221.6	5919.8	1698.2	1799.141	2616	0.45

Standard Proctor – ASTM D698

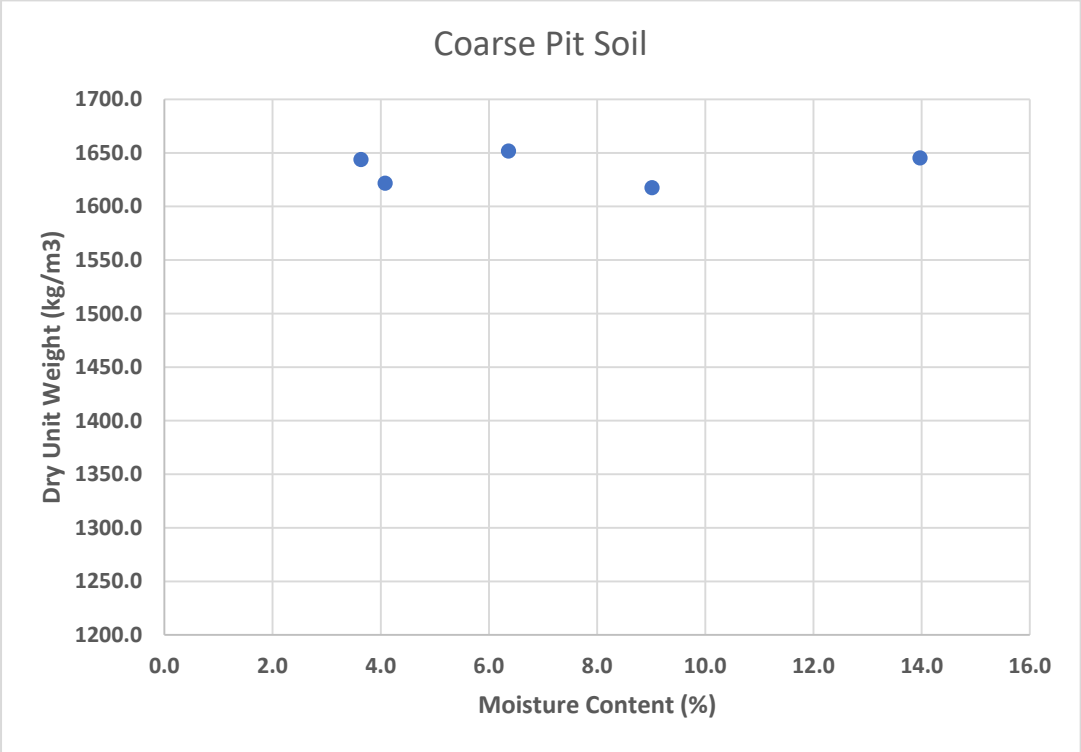

No optimum moisture content can be determined for this sand.

Total Organics – ASTM D2974

0% organic content

Direct Shear – ASTM D3080

Moist Unit Weight (Kg/m^3)	Dry Unit Weight (Kg/m^3)	Moisture Content (%)	Phi (degrees)	Comments
1633.66	1633.66	0	33.7	
1694.10	1633.66	3.7	36.5	Natural Moisture Content
1739.85	1633.66	6.5	30.0	
1862.37	1633.66	14	31.6	

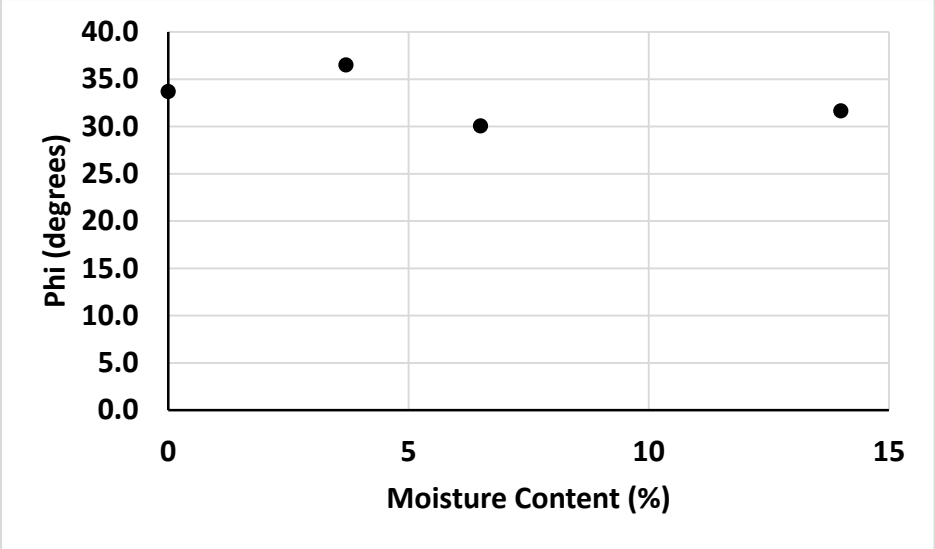

Triaxial Test (drained) – ASTM D7181

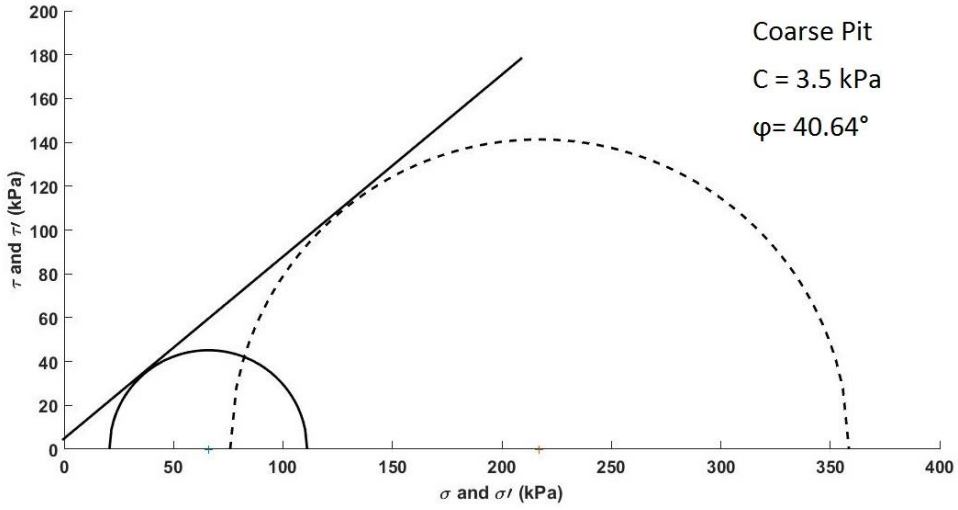

Compressibility in Pressure Cell - ASTM D7181

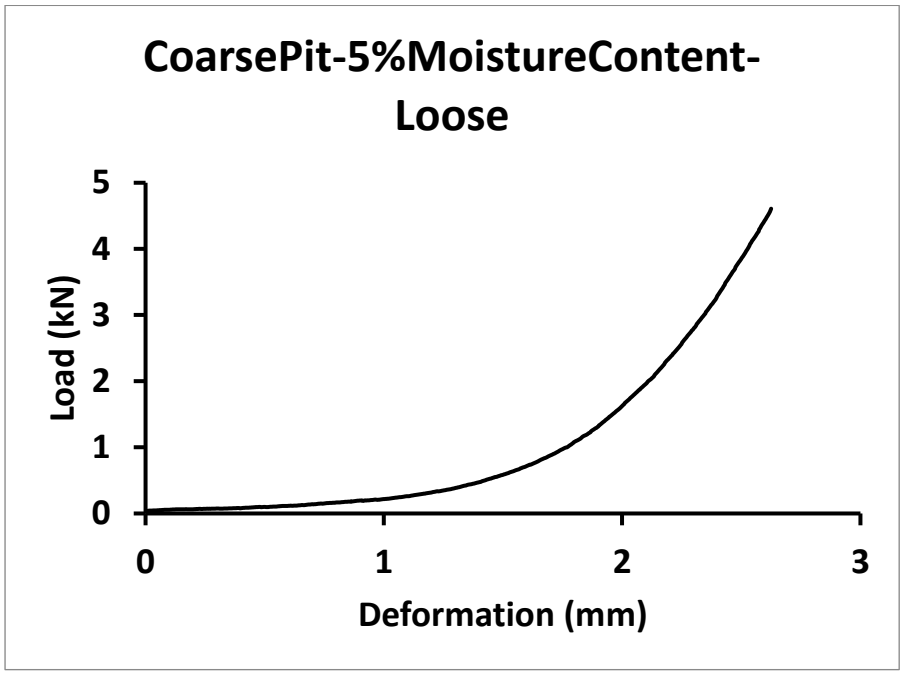

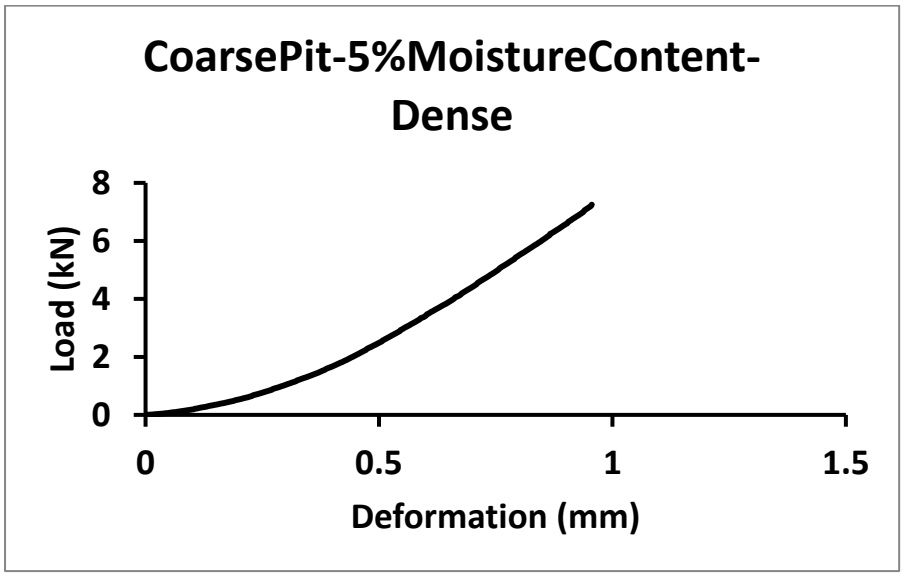

Fine Pit

Visual – ASTM D2488

Brown-gray, Fine sand with fines.

Moisture Content at Time of Sample Collection – ASTM D2216

18.55%

Grain Size Analysis: Sieve – ASTM D6913 & Hydrometer - ASTM D7928

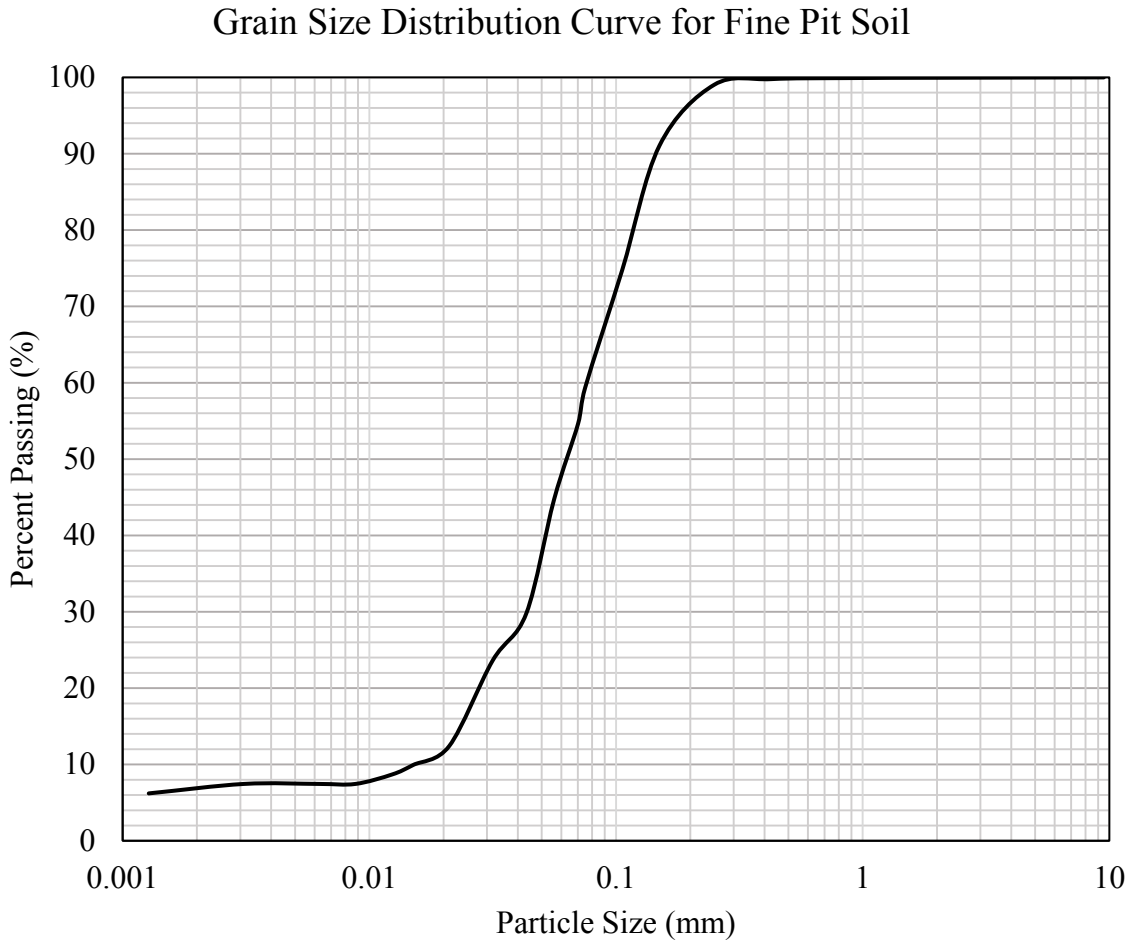

Atterberg Limits – ASTM D4318

NP

ASTM USCS Classification

ML Sandy Silt

Specific Gravity – ASTM D854 and Relative Density ASTM D4254 and D4253

Specific Gravity-Water Displacement method (ASTM D854)				
Weight of dry soil (g)	Weight of bottle+water (g)	Weight of bottle+water+soil (g)	Gs (water)	Specific Gravity
148.2	670.9	762.1	0.99	2.574

Maximum Void ratio (Minimum density/loose state) ASTM D4254					
Weight of Mold (g)	Weight of Mold + Soli (g)	Weight of Soli (g)	Density kg/m^3	Density of Particles (kg/m^3)	e
4222.5	5496.7	1274.2	1349.93845	2574	0.9

Note: This soil is technically a Fine grain soil which means the relative density is not defined for this soil. But it is almost 50% fine 50% coarse we conducted the test on the soil

Minimum Void ratio (Maximum density/Dense state) ASTM D4253					
Weight of Mold (g)	Weight of Mold + Soli (g)	Weight of Soli (g)	Density kg/m^3	Density of Particles (kg/m^3)	e
4222.5	5758.4	1535.9	1627.194	2574	0.58

Standard Proctor – ASTM D698

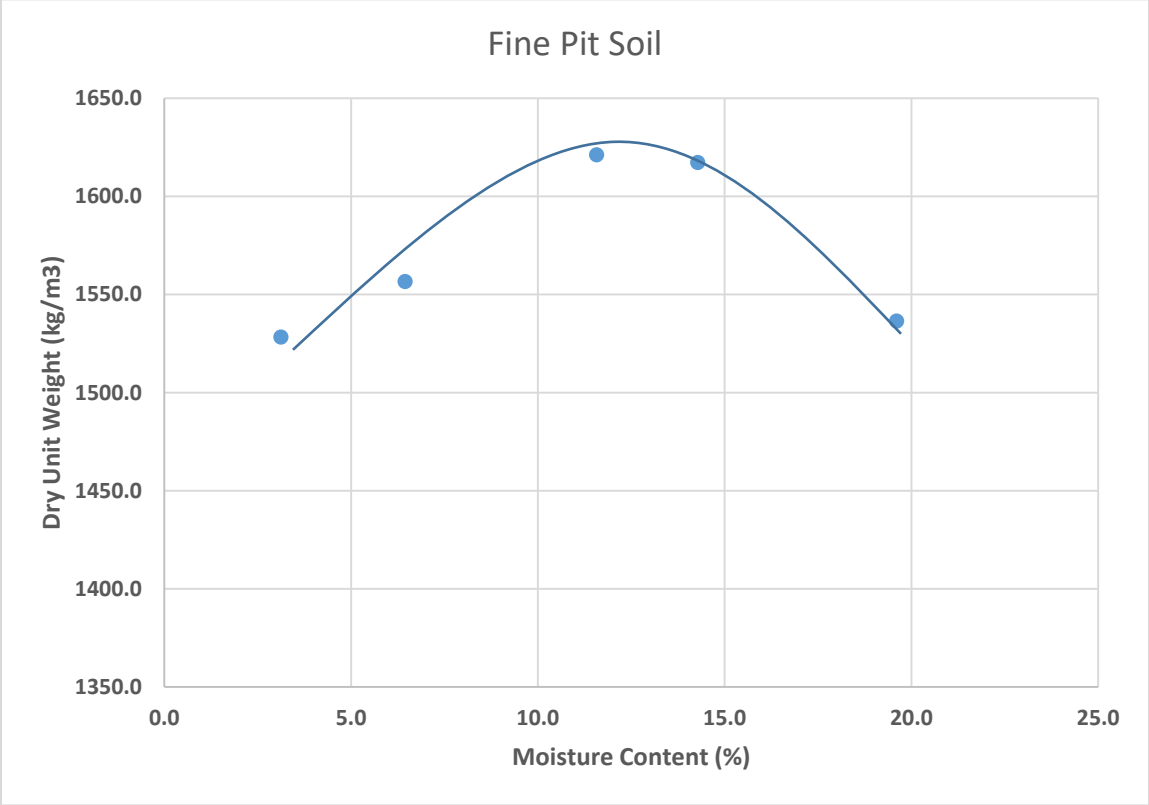

Optimum moisture content: 12.5%
Maximum Dry Unit Weight: 1628 Kg/m^3

Total Organics – ASTM D2974

0.3 % organic content

Direct Shear – ASTM D3080

Moist Unit Weight (Kg/m^3)	Dry Unit Weight (Kg/m^3)	Moisture Content (%)	Phi (degrees)	Comments
1507.94	1507.94	0	34.8	
1553.18	1507.94	3	27.2	
1605.96	1507.94	6.5	33.8	
1787.66	1507.94	18.55	44.9	Natural Moisture Content

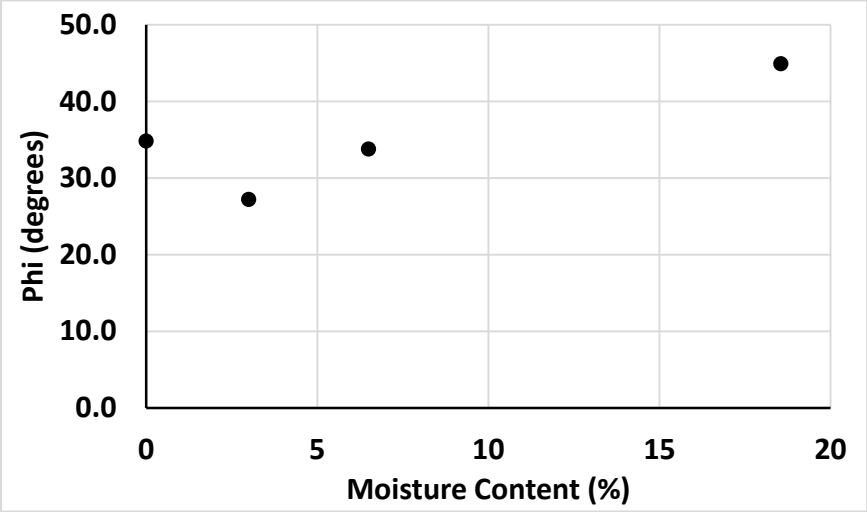

Triaxial Test (drained) – ASTM D7181

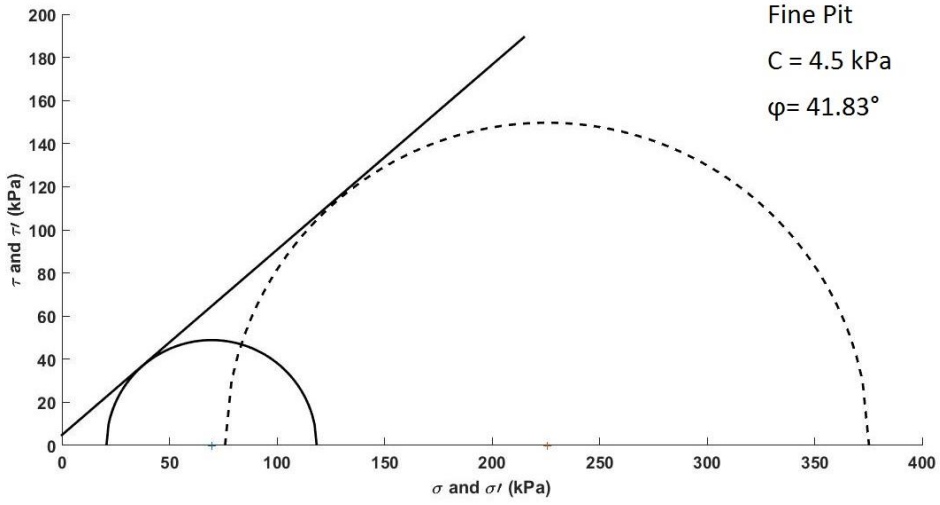

Compressibility in Pressure Cell - ASTM D7181

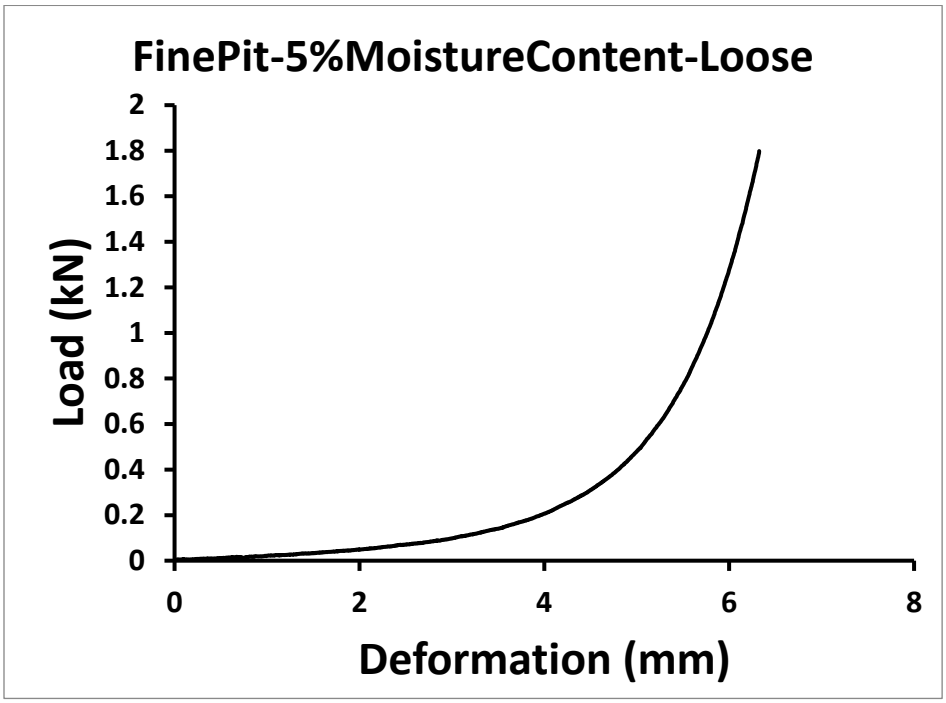

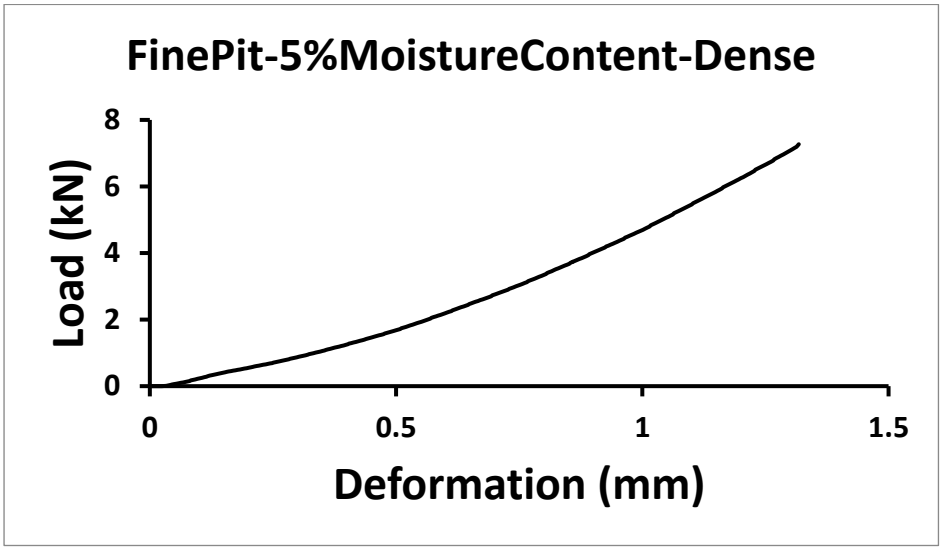

Stability

Visual – ASTM D2488

Brown, Silty Sand with gravel.

Moisture Content at Time of Sample Collection – ASTM D2216

18.8%

Grain Size Analysis: Sieve – ASTM D6913 & Hydrometer - ASTM D7928

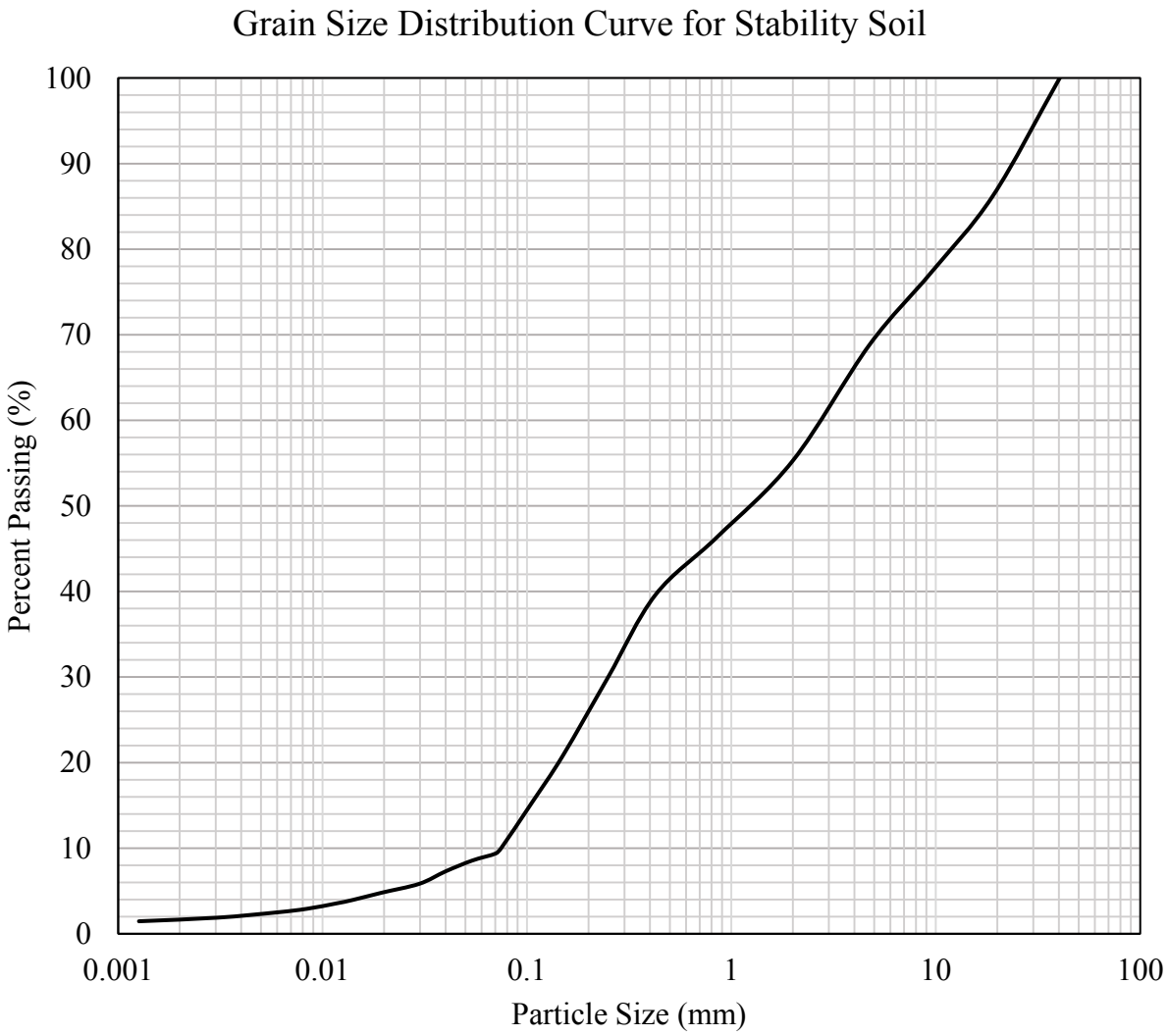

Atterberg Limits – ASTM D4318

NP

ASTM USCS Classification

D10	D30	D60	Cu	Cc	w% Gravel	w% Sand	W% Fine	USCS

0.075	0.25	2.65	35.3	0.3	31.1	58.8	10.0	**SW-SM** Well Graded Sand With Silt and

Specific Gravity – ASTM D854 and Relative Density ASTM D4254 and D4253

Specific Gravity-Water Displacement method (ASTM D854)				
Weight of dry soil (g)	Weight of bottle+water (g)	Weight of bottle+water+soil (g)	Gs (water)	Specific Gravity
154.4	670.9	762.7	0.99	2.4417891

Maximum Void ratio (Minimum density/loose state) ASTM D4254					
Weight of Mold (g)	Weight of Mold + Soli (g)	Weight of Soli (g)	Density kg/m^3	Density of Particles (kg/m^3)	e
4206.4	5572.1	1365.7	1446.87721	2444	0.69

Minimum Void ratio (Maximum density/Dense state) ASTM D4253					
Weight of Mold (g)	Weight of Mold + Soli (g)	Weight of Soli (g)	Density kg/m^3	Density of Particles (kg/m^3)	e
4206.4	5825.5	1619.1	1715.339	2444	0.42

Standard Proctor – ASTM D698

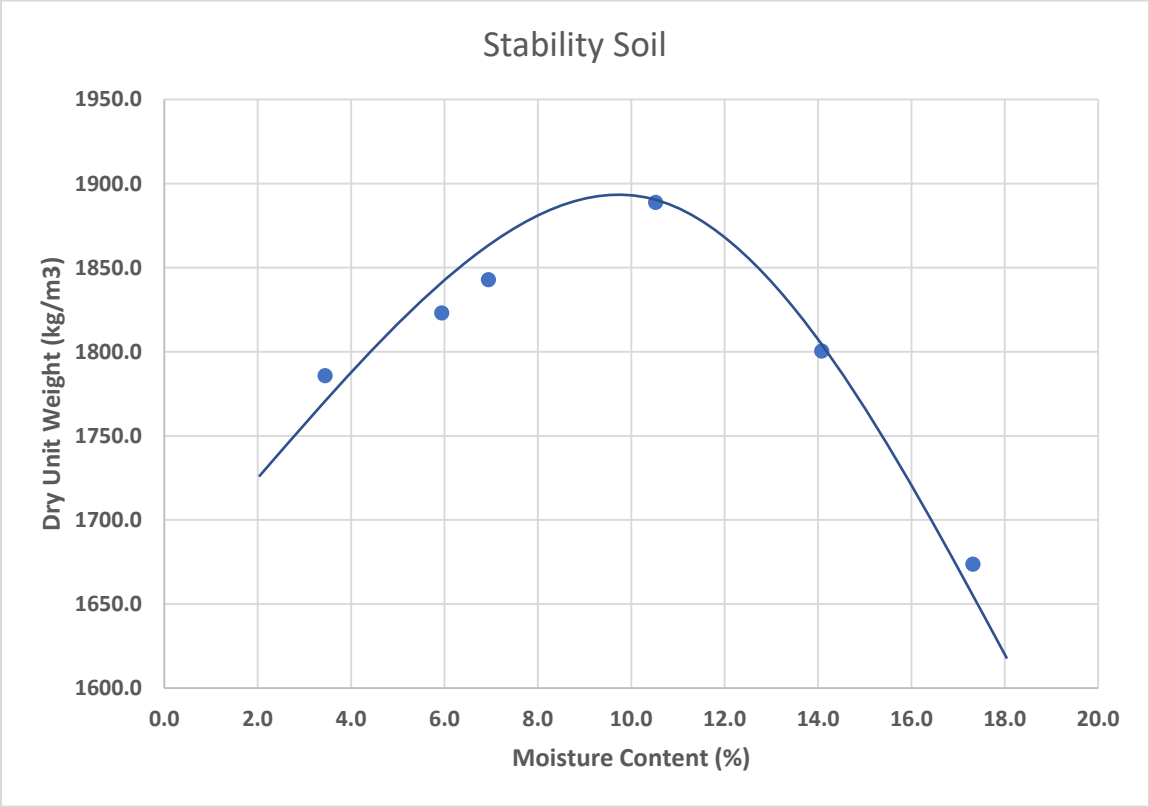

Optimum moisture content: 9.5%
Maximum Dry Unit Weight: 1890 Kg/m^3

Total Organics – ASTM D2974

2.5 % Organic Content

Direct Shear – ASTM D3080

Moist Unit Weight (Kg/m^3)	Dry Unit Weight (Kg/m^3)	Moisture Content (%)	Phi (degrees)	Comments
1604.41	1604.41	0	35.8	
1652.54	1604.41	3	30.9	
1708.69	1604.41	6.5	36.5	
1906.04	1604.41	18.8	23.5	Natural Moisture Content

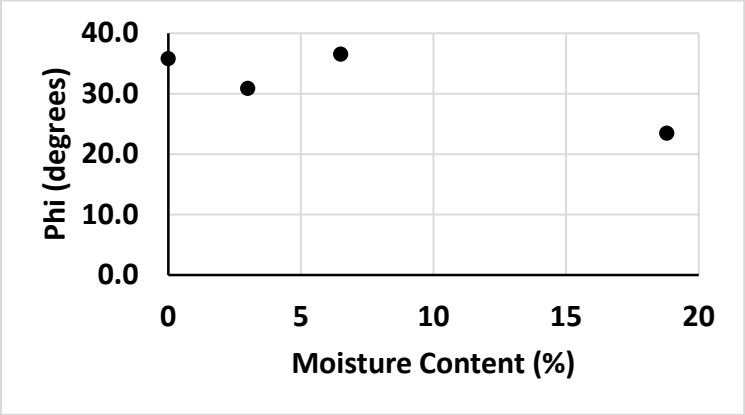

Triaxial Test (drained) – ASTM D7181

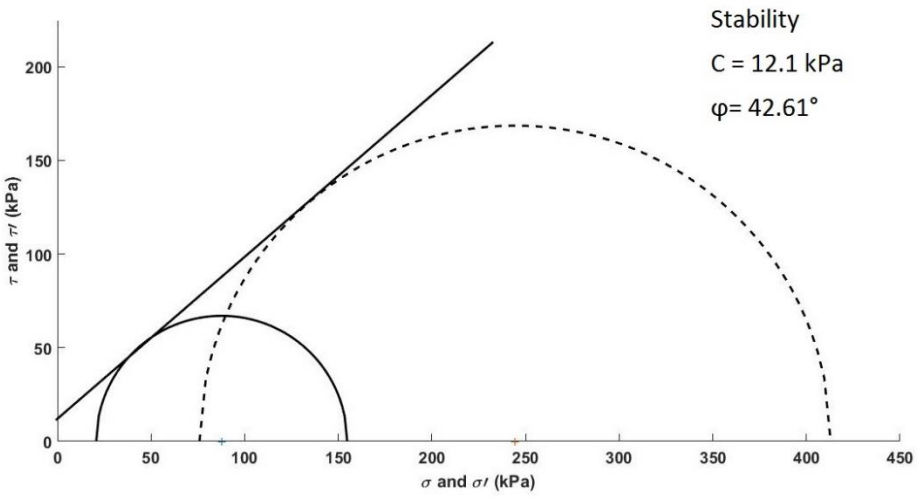

Compressibility in Pressure Cell - ASTM D7181

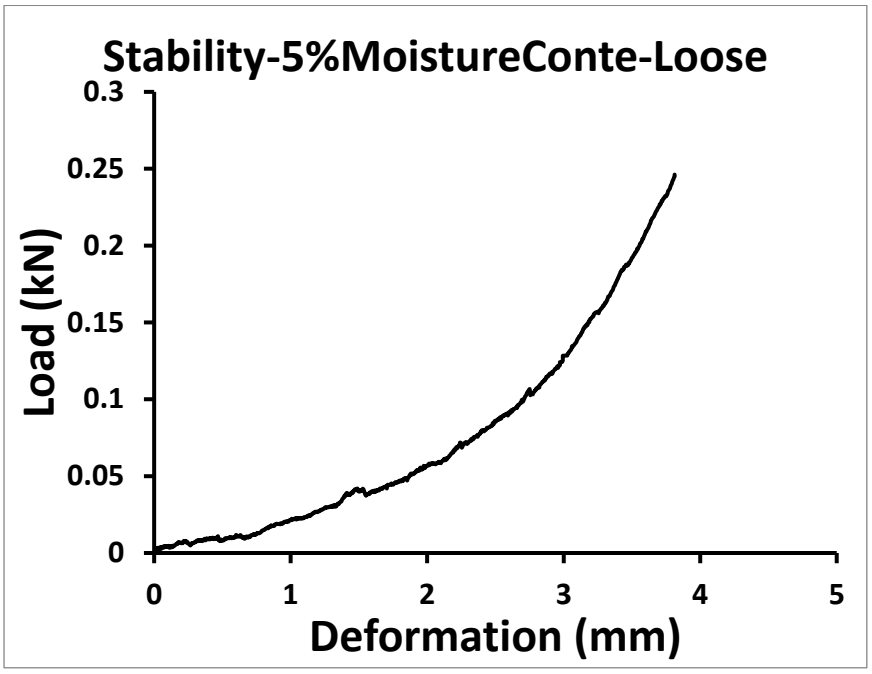

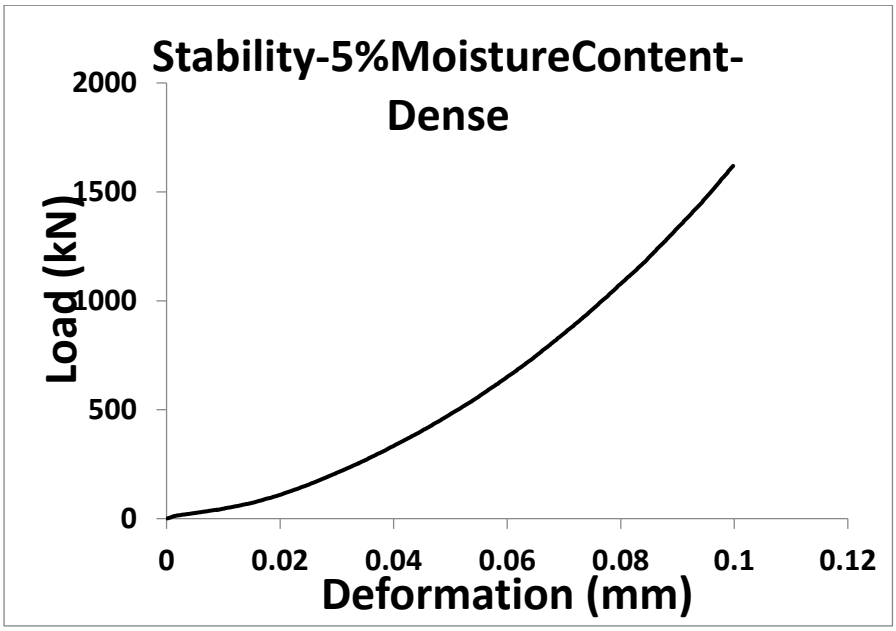

Rink Natural

Visual – ASTM D2488

Brown, Silty Sand with gravel.

Moisture Content at Time of Sample Collection – ASTM D2216

15%

Grain Size Analysis: Sieve – ASTM D6913 & Hydrometer - ASTM D7928

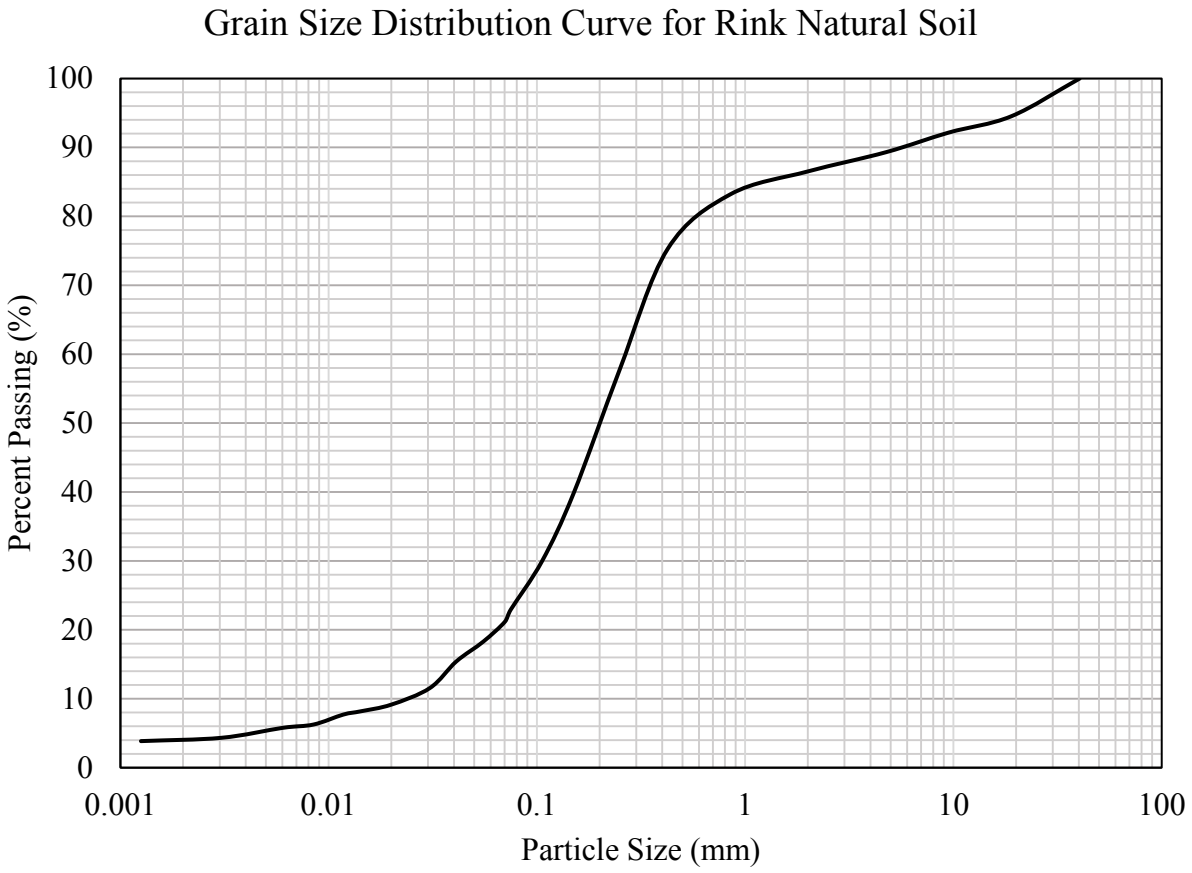

Atterberg Limits – ASTM D4318

NP

ASTM USCS Classification

D10	D30	D60	Cu	Cc	w% Gravel	w% Sand	W% Fine	USCS
0.015	0.12	0.25	16.7	3.8	10.7	66.4	23.0	**SM** Silty Sand

Specific Gravity – ASTM D854 and Relative Density ASTM D4254 and D4253

Specific Gravity-Water Displacement method (ASTM D854)				
Weight of dry soil (g)	Weight of bottle+water (g)	Weight of bottle+water+soil (g)	Gs (water)	Specific Gravity
154.7	670.7	763.3	0.99	2.4662319

Maximum Void ratio (Minimum density/loose state) ASTM D4254					
Weight of Mold (g)	Weight of Mold + Soli (g)	Weight of Soli (g)	Density kg/m^3	Density of Particles (kg/m^3)	e
4193.6	5558.7	1365.1	1446.241546	2466	0.7

Minimum Void ratio (Maximum density/Dense state) ASTM D4253					
Weight of Mold (g)	Weight of Mold + Soli (g)	Weight of Soli (g)	Density kg/m^3	Density of Particles (kg/m^3)	e
4193.6	5827.1	1633.5	1730.595	2466	0.42

Standard Proctor – ASTM D698

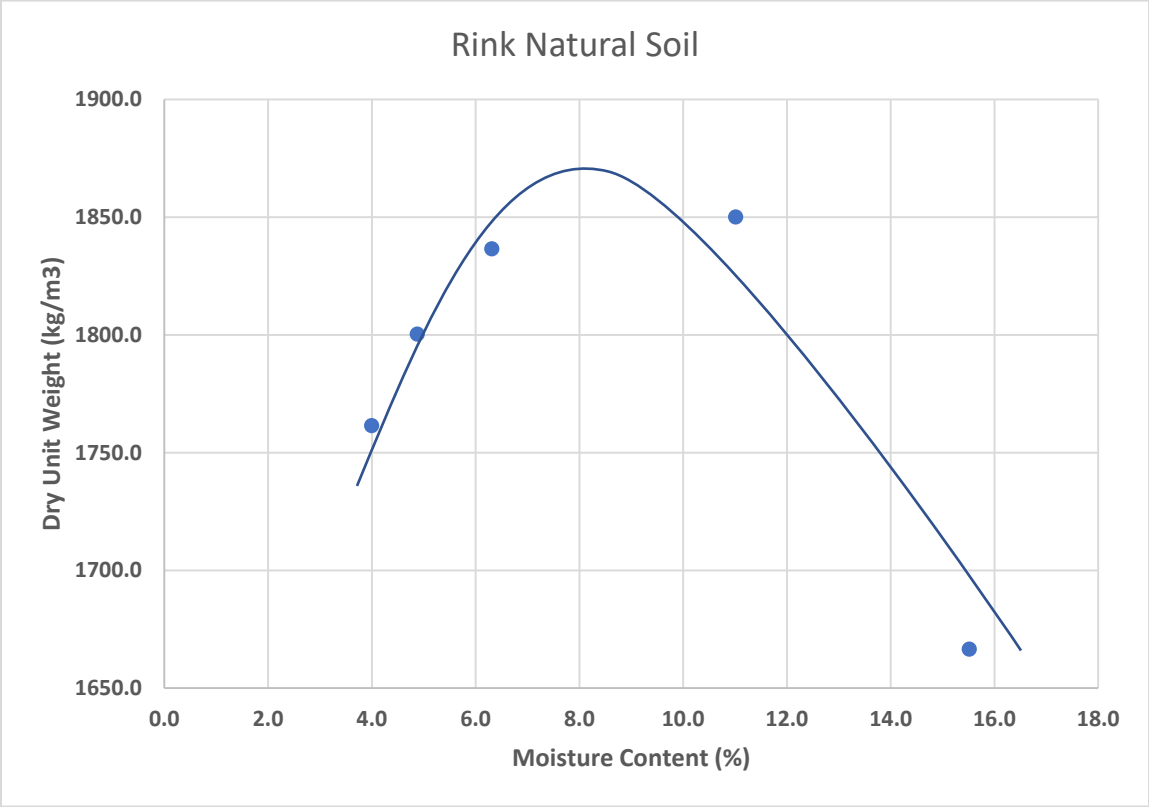

Optimum moisture content: 8%
Maximum Dry Unit Weight: 1870 Kg/m^3

Total Organics – ASTM D2974

1.5 % Organic Content

Direct Shear – ASTM D3080

Moist Unit Weight (Kg/m^3)	Dry Unit Weight (Kg/m^3)	Moisture Content (%)	Phi (degrees)	Comments
1604.41	1604.41	0	44.1	
1652.54	1604.41	3	41.3	
1708.69	1604.41	6.5	43.9	
1845.07	1604.41	15	35.1	Natural Moisture Content

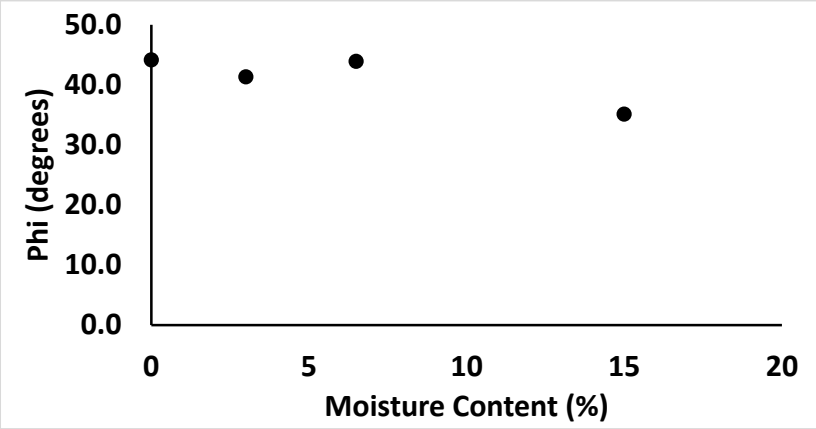

Triaxial Test (drained) – ASTM D7181

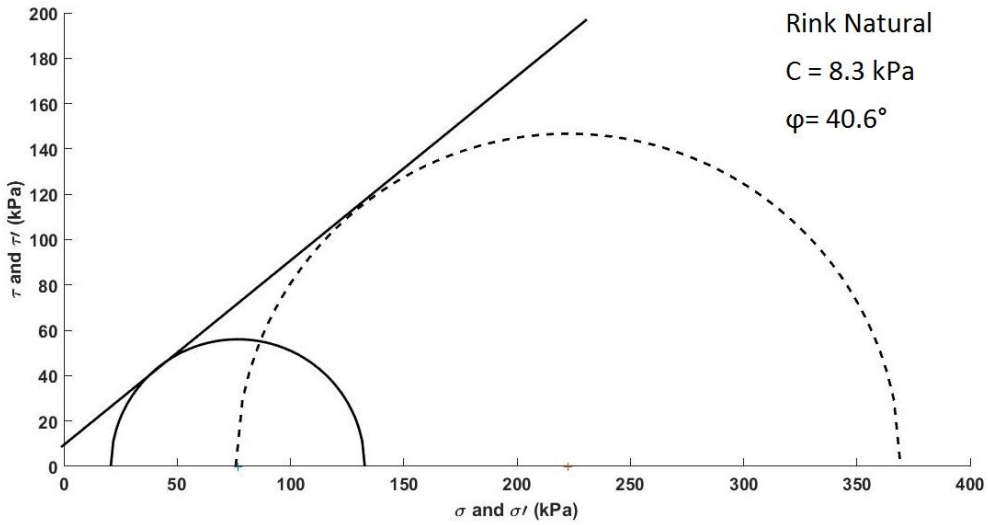

Compressibility in Pressure Cell - ASTM D7181

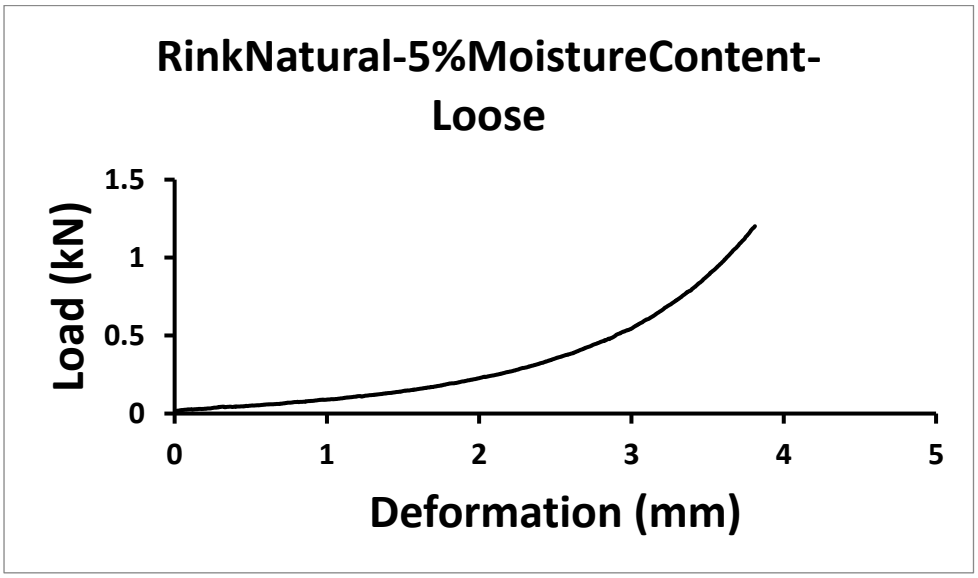

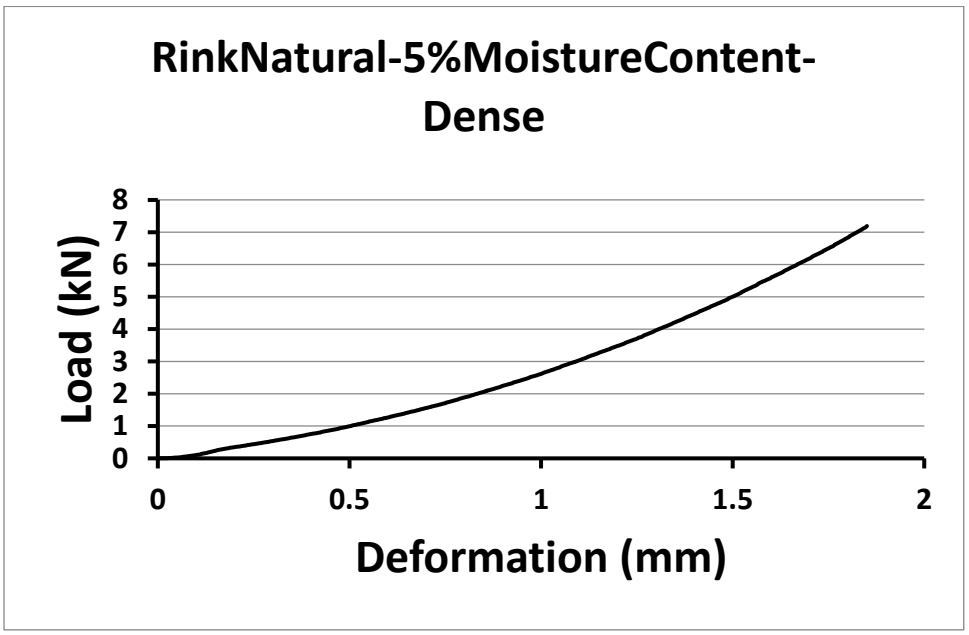

2NS Sand

This soil type is found in the “Coarse Grained Soil Pit” and the “Variable Hill Climb” areas. GPS

Visual – ASTM D2488

Brown-gray, coarse sand with some medium sand and trace fines.

Moisture Content at Time of Sample Collection – ASTM D2216

Table 1. Moisture Content of Blizzard 2NS, Tested 1/29/18, by RMB and AJM, ASTM D2216			
Mass (g)	**Trial #1**	**Trial #2**	**Trial #3**
Drying Dish	31.24	30.61	38.14
Dish + Moist Soil	112.93	106.49	122.97
Moist Soil	81.69	75.88	84.83
Dish + Dry Soil	112.03	105.65	122.01
Dry Soil	80.79	75.04	83.87
Water Content	0.90	0.84	0.96
Water Content (%)	**1.11**	**1.12**	**1.14**
Avg. Water Content (%)	**1.13**		

Grain Size Analysis: Sieve – ASTM D6913 & Hydrometer - ASTM D7928

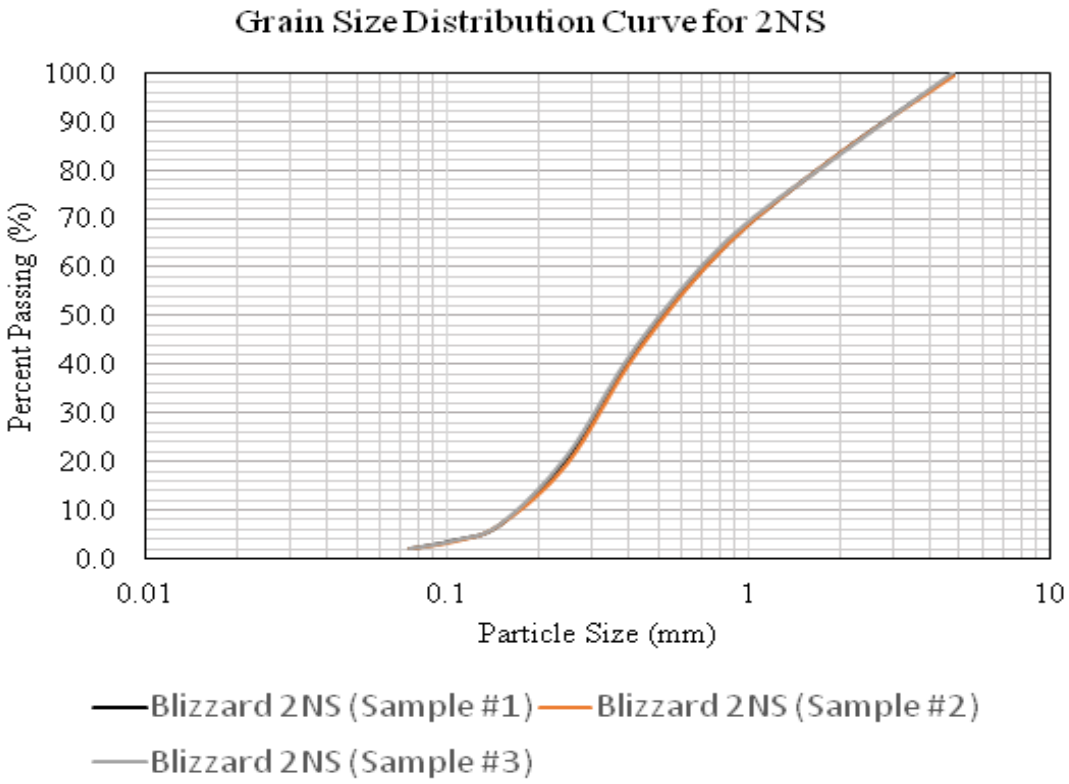

Atterberg Limits – ASTM D4318

NP

ASTM USCS Classification

C_u = 4.0 C_c = 0.7

ASTM USCS Classification: Poorly-Graded Sand (SP)

Specific Gravity and Density – ASTM D5550

Table 11. Density of Blizzard 2NS using Helium Pycnometer, Tested 2/16/18, by RMB		
Blizzard 2NS	**Mass (g)**	**Density (g/cm^3)**
Sample #1	145.8	2.7201
Sample #2	139.4	2.7189
Sample #3	138.8	2.7283
Average		2.7224

Table 13. Minimum Void Ratio / Maximum Density of Blizzard 2NS, Tested 3/2/18 by RMB and AJM, ASTM D4253, G_s = 2.72g/cm^3, $V_{mold} = V_T$ = 943.9cm^3			
Mass (g)	**Sample #1**	**Sample #2**	**Sample #3**
Proctor Mold	4218.1	4218.1	4218.1
Proctor Mold + Dense Soil	6078.8	6068.5	6086.9
Dense Soil	1860.7	1850.4	1868.8
Volume Solids (cm^3)	684.1	680.3	687.1
Volume Voids (cm^3)	259.8	263.6	256.8
e_{max}	0.38	0.39	0.37
Average e_{max}	0.38		

Table 14. Maximum Void Ratio / Minimum Density of Blizzard 2NS, Tested 3/2/18 by RMB and AJM, ASTM D4253, G_s = 2.72g/cm^3, $V_{mold} = V_T$ = 943.9cm^3			
Mass (g)	**Sample #1**	**Sample #2**	**Sample #3**
Proctor Mold	4218.1	4218.1	4218.1
Proctor Mold + Loose Soil	5756.9	5781.8	5781.8
Loose Soil	1538.8	1563.7	1563.7
Volume Solids (cm^3)	565.7	574.9	574.9
Volume Voids (cm^3)	378.2	369.0	369.0
e_{min}	0.67	0.64	0.64
Average e_{min}	0.65		

Standard Proctor – ASTM D698

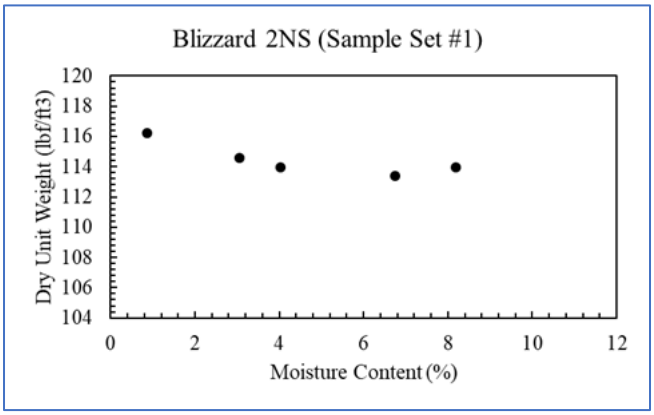

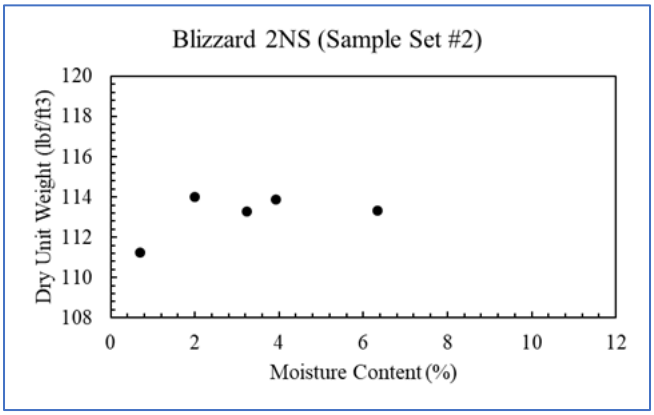

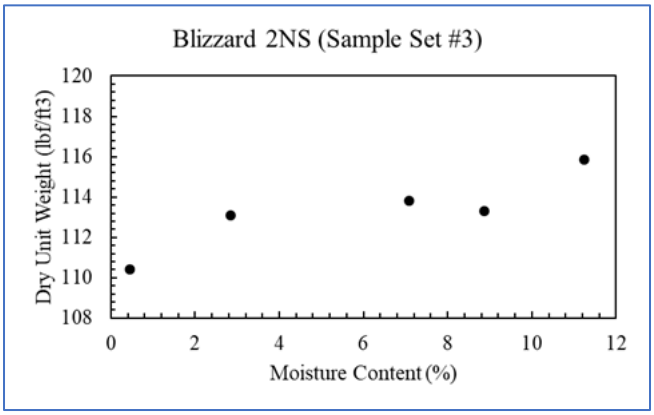

No optimum moisture content can be determined for this sand.

Total Organics – ASTM D2974

0% organic content

Direct Shear – ASTM D3080

Moist Unit Weight (Kg/m^3)	Dry Unit Weight (Kg/m^3)	Moisture Content (%)	Phi (degrees)	Comments
1604.41	1604.41	0	41.9	
1652.54	1604.41	3	33.8	
1708.69	1604.41	6.5	38.1	Natural Moisture Content
1780.89	1604.41	11	34.3	

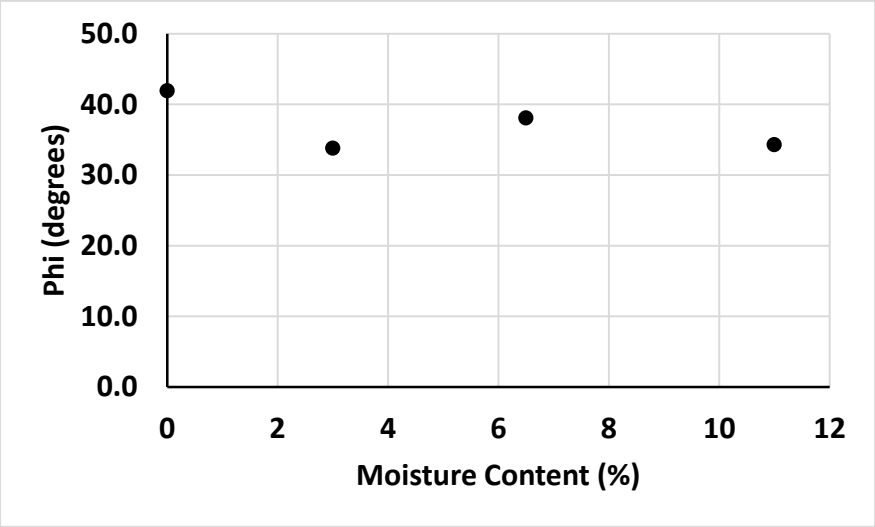

Triaxial Test (drained) – ASTM D7181

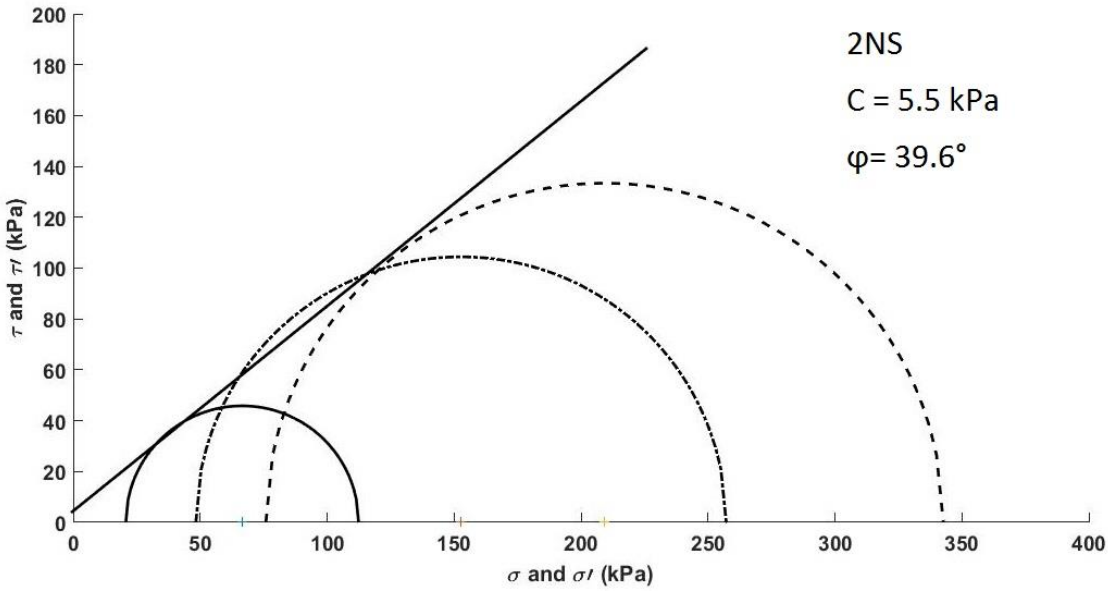

Compressibility in Pressure Cell - ASTM D7181